Higgs physics as a probe of electroweak baryogenesis

Eibun Senaha (NCU)

@Kavli IPMU, May 27, 2015.

Outline

- Introduction
  - Review of electroweak baryogenesis (EWBG)
- Real singlet-extended SM (rSM)
  - Electroweak phase transition (EWPT) & sphaleron decoupling condition
  - Impact on the hhh coupling
- Summary

Higgs and cosmology

❐ Higgs boson was discovered.

ATLAS+CMS combined Higgs mass [PRL114,191803 (2015)]

$$m_H = 125.09 \pm 0.24 \text{ GeV}$$
$$= 125.09 \pm 0.21(\text{stat.}) \pm 0.11(\text{syst.}) \text{ GeV}$$

❐ What is the implications of Higgs physics for cosmology?

- cosmic baryon asymmetry $\Leftrightarrow$ EW baryogenesis
- dark matter $\Leftrightarrow$ inert Higgs, Higgs portal etc.
- inflation $\Leftrightarrow$ Higgs inflation
- etc

We discuss EW baryogenesis in light of recent LHC data.

Higgs and cosmology

❐ Higgs boson was discovered.

ATLAS+CMS combined Higgs mass [PRL114,191803 (2015)]

$$m_H = 125.09 \pm 0.24 \text{ GeV}$$
$$= 125.09 \pm 0.21(\text{stat.}) \pm 0.11(\text{syst.}) \text{ GeV}$$

❐ What is the implications of Higgs physics for cosmology?

- cosmic baryon asymmetry $\Leftrightarrow$ EW baryogenesis
- dark matter $\Leftrightarrow$ inert Higgs, Higgs portal etc.
- inflation $\Leftrightarrow$ Higgs inflation
- etc

We discuss EW baryogenesis in light of recent LHC data.

Baryon Asymmetry of the Universe (BAU)

❒ Our Universe is baryon-asymmetric.

$$\eta_{\rm CMB} = \frac{n_B}{n_\gamma} = (6.047 \pm 0.074) \times 10^{-10},$$
$$\eta_{\rm BBN} = \frac{n_B}{n_\gamma} = (5.7 - 6.7) \times 10^{-10} \ (95\% \ {\rm CL}).$$

[PDG2014]

❒ Sakharov criteria ('67)

(1) Baryon number (B) violation
(2) C and CP violation
(3) Out of equilibrium

BAU must arise

- After inflation
- Before Big-Bang Nucleosynthesis (T≃O(1) MeV).

Many possibilities

[Shaposhnikov, J.Phys.Conf.Ser.171:012005,2009.]

1. GUT baryogenesis. 2. GUT baryogenesis after preheating. 3. Baryogenesis from primordial black holes. 4. String scale baryogenesis. 5. Affleck-Dine (AD) baryogenesis. 6. Hybridized AD baryogenesis. 7. No-scale AD baryogenesis. 8. Single field baryogenesis. 9. Electroweak (EW) baryogenesis. 10. Local EW baryogenesis. 11. Non-local EW baryogenesis. 12. EW baryogenesis at preheating. 13. SUSY EW baryogenesis. 14. String mediated EW baryogenesis. 15. Baryogenesis via leptogenesis. 16. Inflationary baryogenesis. 17. Resonant leptogenesis. 18. Spontaneous baryogenesis. 19. Coherent baryogenesis. 20. Gravitational baryogenesis. 21. Defect mediated baryogenesis. 22. Baryogenesis from long cosmic strings. 23. Baryogenesis from short cosmic strings. 24. Baryogenesis from collapsing loops. 25. Baryogenesis through collapse of vortons. 26. Baryogenesis through axion domain walls. 27. Baryogenesis through QCD domain walls. 28. Baryogenesis through unstable domain walls. 29. Baryogenesis from classical force. 30. Baryogenesis from electrogenesis. 31. B-ball baryogenesis. 32. Baryogenesis from CPT breaking. 33. Baryogenesis through quantum gravity. 34. Baryogenesis via neutrino oscillations. 35. Monopole baryogenesis. 36. Axino induced baryogenesis. 37. Gravitino induced baryogenesis. 38. Radion induced baryogenesis. 39. Baryogenesis in large extra dimensions. 40. Baryogenesis by brane collision. 41. Baryogenesis via density fluctuations. 42. Baryogenesis from hadronic jets. 43. Thermal leptogenesis. 44. Nonthermal leptogenesis.

Many possibilities

[Shaposhnikov, J.Phys.Conf.Ser.171:012005,2009.]

1. GUT baryogenesis. 2. GUT baryogenesis after preheating. 3. Baryogenesis from primordial black holes. 4. String scale baryogenesis. 5. Affleck-Dine (AD) baryogenesis. 6. Hybridized AD baryogenesis. 7. No-scale AD baryogenesis. 8. Single field baryogenesis. 9. Electroweak (EW) baryogenesis. 10. Local EW baryogenesis. 11. Non-local EW baryogenesis. 12. EW baryogenesis at preheating. 13. SUSY EW baryogenesis. 14. String mediated EW baryogenesis. 15. Baryogenesis via leptogenesis. 16. Inflationary baryogenesis. 17. Resonant leptogenesis. 18. Spontaneous baryogenesis. 19. Coherent baryogenesis. 20. Gravitational baryogenesis. 21. Defect mediated baryogenesis. 22. Baryogenesis from long cosmic strings. 23. Baryogenesis from short cosmic strings. 24. Baryogenesis from collapsing loops. 25. Baryogenesis through collapse of vortons. 26. Baryogenesis through axion domain walls. 27. Baryogenesis through QCD domain walls. 28. Baryogenesis through unstable domain walls. 29. Baryogenesis from classical force. 30. Baryogenesis from electrogenesis. 31. B-ball baryogenesis. 32. Baryogenesis from CPT breaking. 33. Baryogenesis through quantum gravity. 34. Baryogenesis via neutrino oscillations. 35. Monopole baryogenesis. 36. Axino induced baryogenesis. 37. Gravitino induced baryogenesis. 38. Radion induced baryogenesis. 39. Baryogenesis in large extra dimensions. 40. Baryogenesis by brane collision. 41. Baryogenesis via density fluctuations. 42. Baryogenesis from hadronic jets. 43. Thermal leptogenesis. 44. Nonthermal leptogenesis.

Many possibilities

[Shaposhnikov, J.Phys.Conf.Ser.171:012005,2009.]

1. GUT baryogenesis. 2. GUT baryogenesis after preheating. 3. Baryogenesis from primordial black holes. 4. String scale baryogenesis. 5. Affleck-Dine (AD) baryogenesis. 6. Hybridized AD baryogenesis. 7. No-scale AD baryogenesis. 8. Single field baryogenesis. 9. Electroweak (EW) baryogenesis. 10. Local EW baryogenesis. 11. Non-local EW baryogenesis. 12. EW baryogenesis at preheating. 13. SUSY EW baryogenesis. 14. String mediated EW baryogenesis. 15. Baryogenesis via leptogenesis. 16. Inflationary baryogenesis. 17. Resonant leptogenesis. 18. Spontaneous baryogenesis. 19. Coherent baryogenesis. 20. Gravitational baryogenesis. 21. Defect mediated baryogenesis. 22. Baryogenesis from long cosmic strings. 23. Baryogenesis from short cosmic strings. 24. Baryogenesis from collapsing loops. 25. Baryogenesis through collapse of vortons. 26. Baryogenesis through axion domain walls. 27. Baryogenesis through QCD domain walls. 28. Baryogenesis through unstable domain walls. 29. Baryogenesis from classical force. 30. Baryogenesis from electrogenesis. 31. B-ball baryogenesis. 32. Baryogenesis from CPT breaking. 33. Baryogenesis through quantum gravity. 34. Baryogenesis via neutrino oscillations. 35. Monopole baryogenesis. 36. Axino induced baryogenesis. 37. Gravitino induced baryogenesis. 38. Radion induced baryogenesis. 39. Baryogenesis in large extra dimensions. 40. Baryogenesis by brane collision. 41. Baryogenesis via density fluctuations. 42. Baryogenesis from hadronic jets. 43. Thermal leptogenesis. 44. Nonthermal leptogenesis.

- Electroweak baryogenesis (EWBG) $\leftrightarrow$ Higgs physics.

  1st scenario that we can verify or falsify with experimental data.

Electroweak baryogenesis

[Kuzmin, Rubakov, Shaposhnikov, PLB155,36 ('85)]

Sakharov's criteria

- B violation: anomalous process $0 \leftrightarrow \sum_{i=1,2,3} (3q_L^i + l_L^i)$ (LH fermions)
- C violation: chiral gauge interaction
- CP violation: CKM matrix and other complex phases in the beyond the SM
- Out of equilibrium: 1st-order EW phase transition (EWPT) with expanding bubble walls

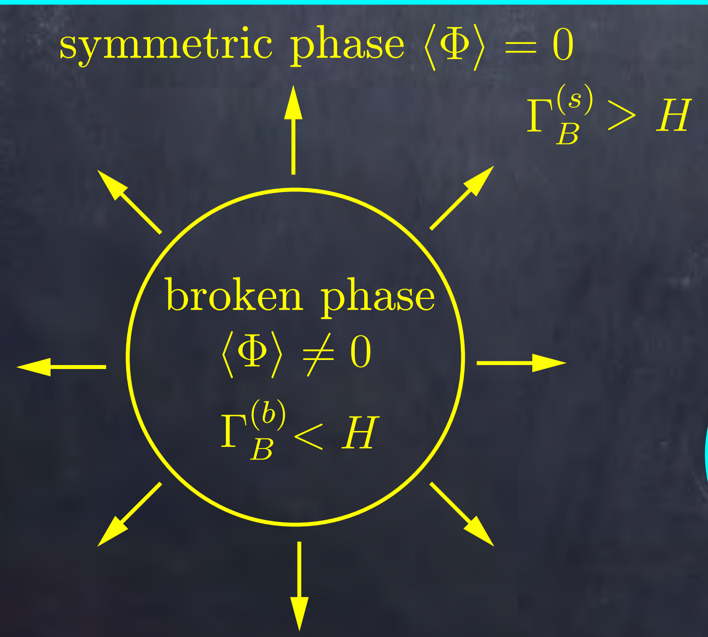

average bubble radius $\mathcal{O}(10^{-6})$ m

[Carrington, Kapusta, PRD47, ('93) 5304]

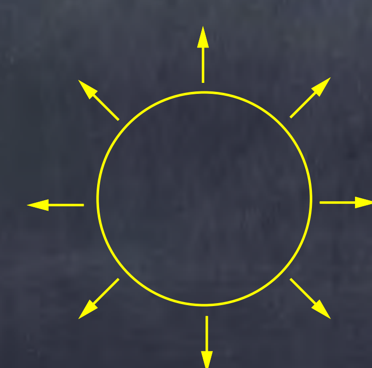

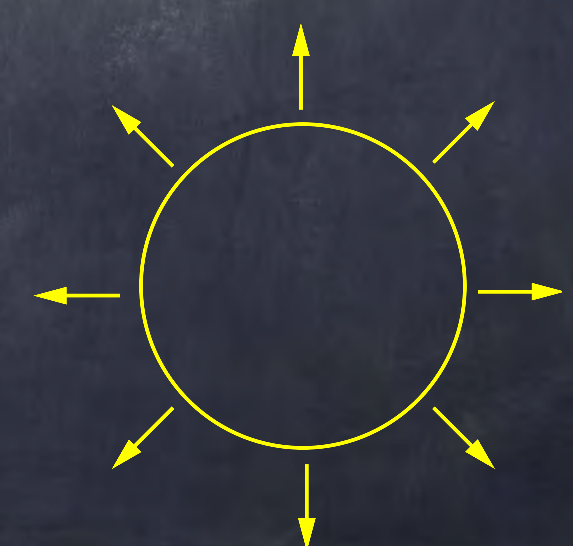

❒ BAU can arise by the growing bubbles.

EW Baryogenesis mechanism

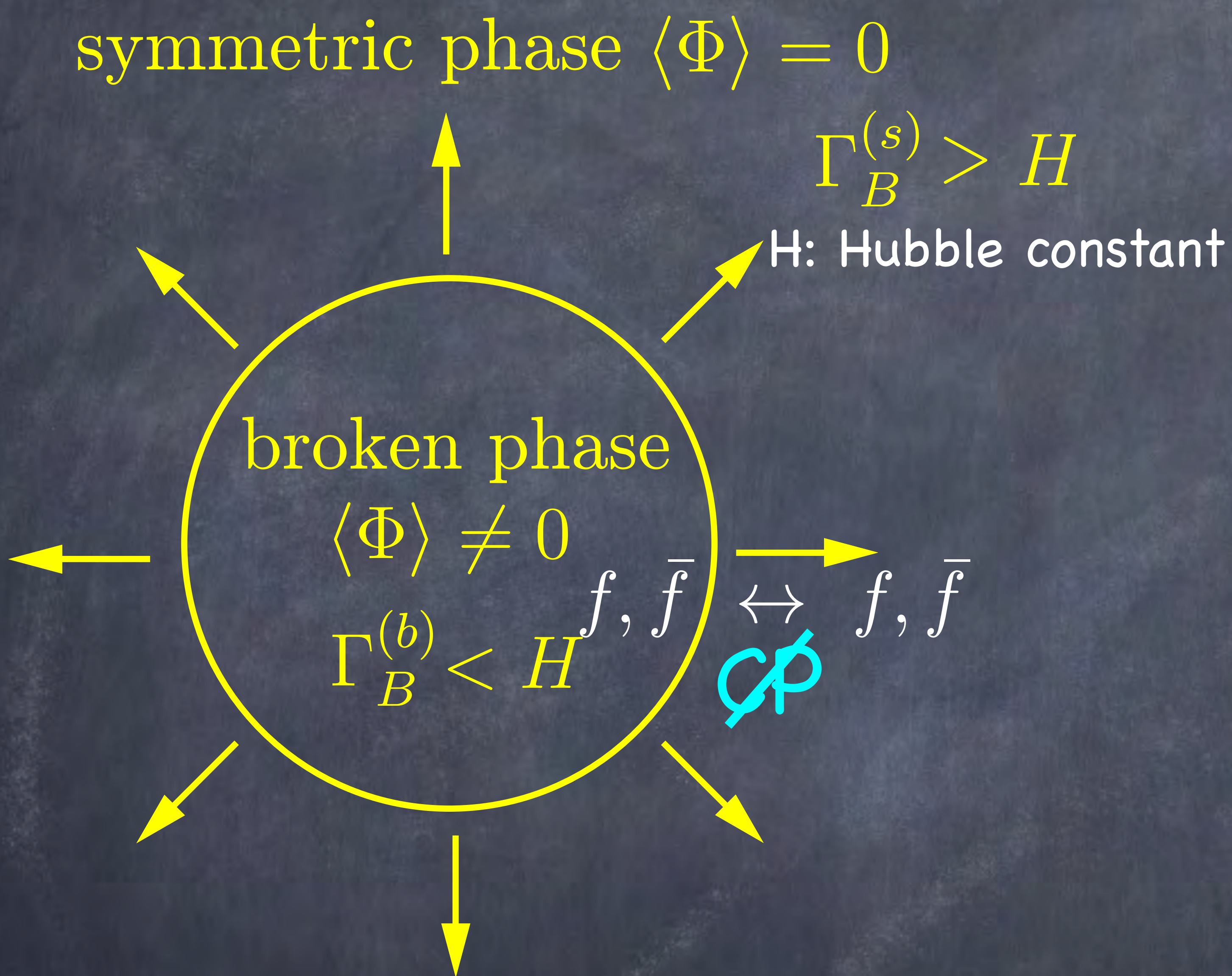

EW Baryogenesis mechanism

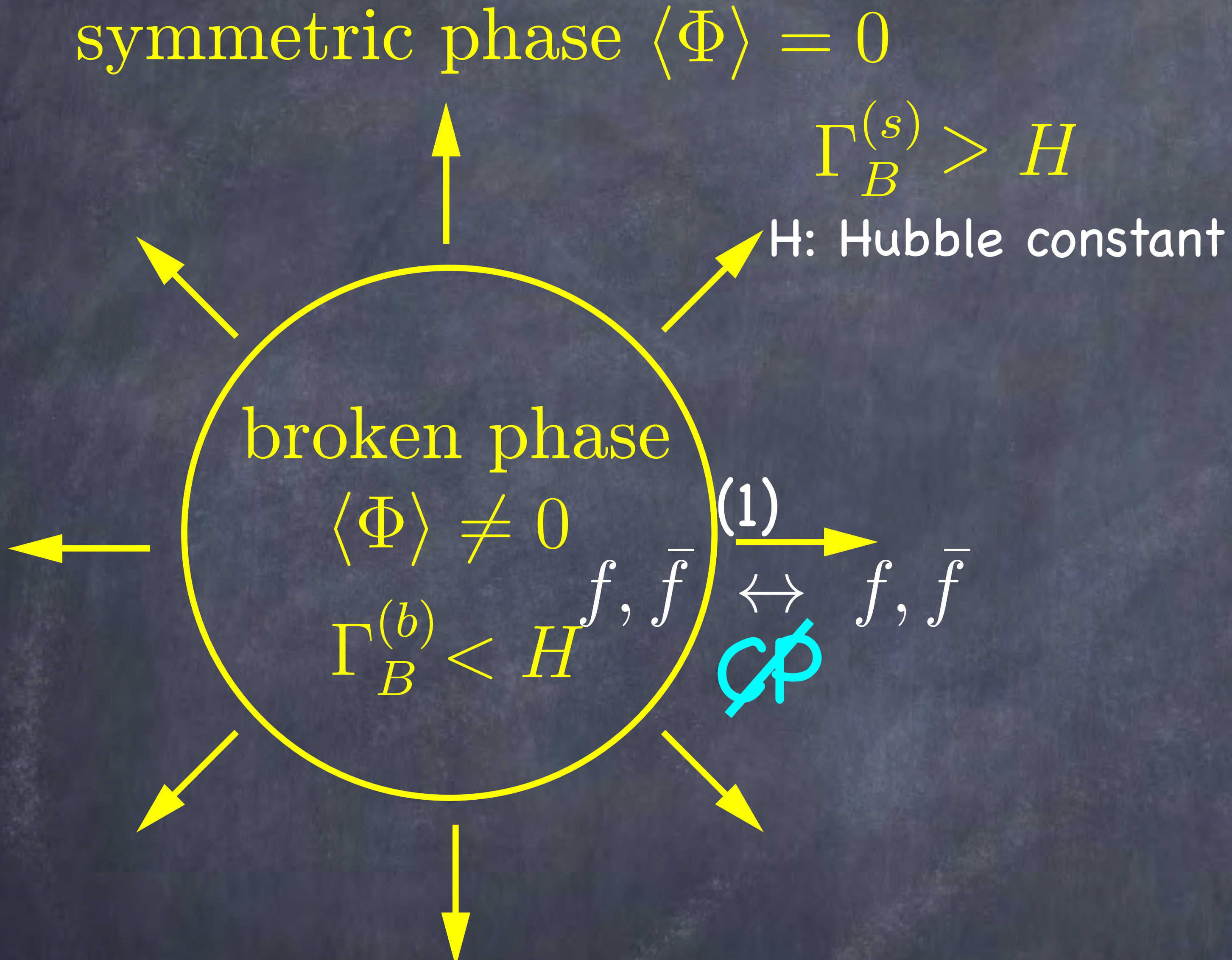

(1) Asymmetries arise ($\because$ CPV) but no BAU. $n_B = \underbrace{n_b^L - n_{\bar{b}}^L}_{\neq 0} + \underbrace{n_b^R - n_{\bar{b}}^R}_{\neq 0} = 0$

EW Baryogenesis mechanism

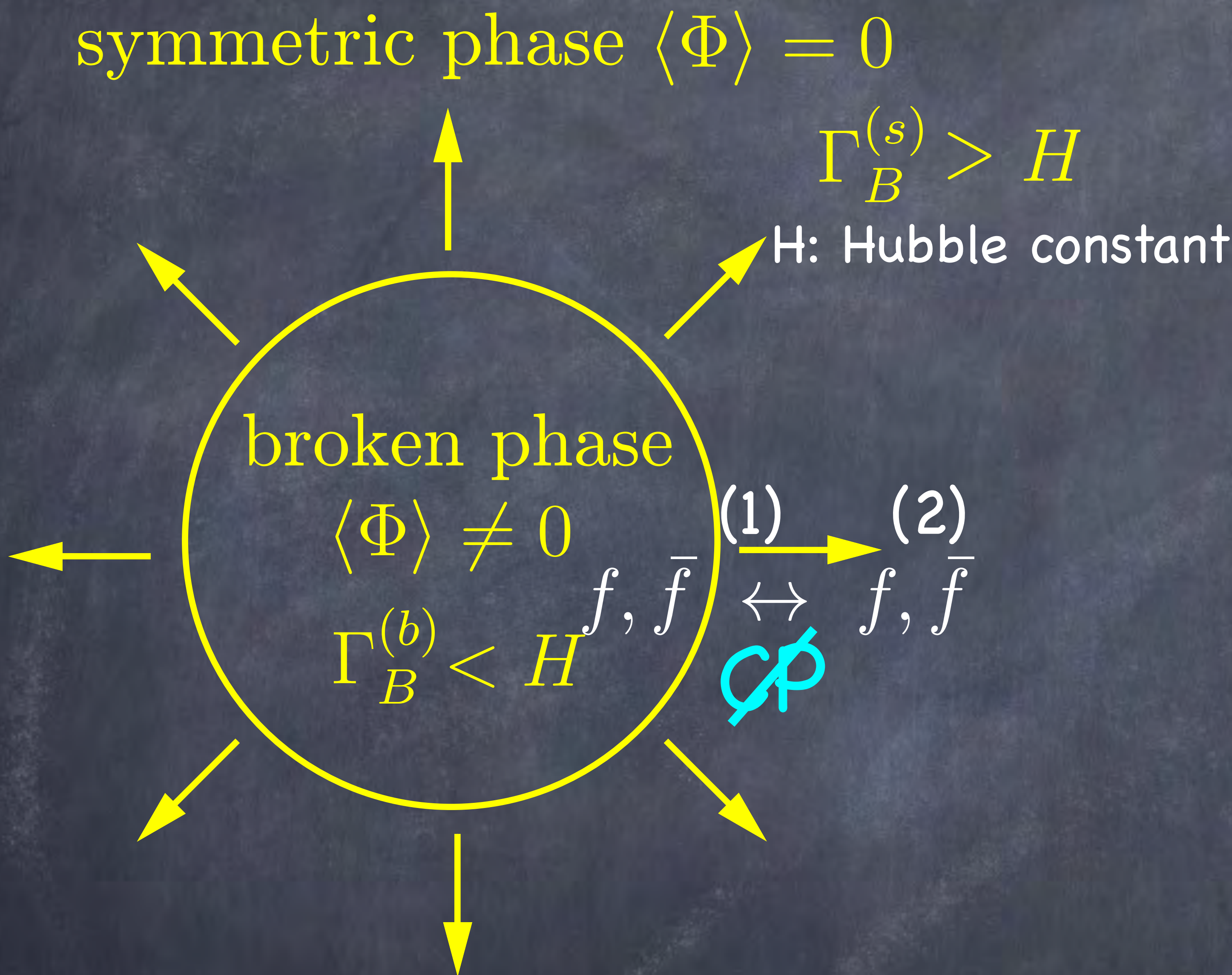

(1) Asymmetries arise (∵ CPV) but no BAU.

$$n_B = \underbrace{n_b^L - n_{\bar{b}}^L}_{\neq 0} + \underbrace{n_b^R - n_{\bar{b}}^R}_{\neq 0} = 0$$

(2) LH part changes (∵ sphaleron) -> BAU

$$n_B = \underbrace{n_b^L - n_{\bar{b}}^L}_{\text{changed}} + n_b^R - n_{\bar{b}}^R \to n_B \neq 0$$

EW Baryogenesis mechanism

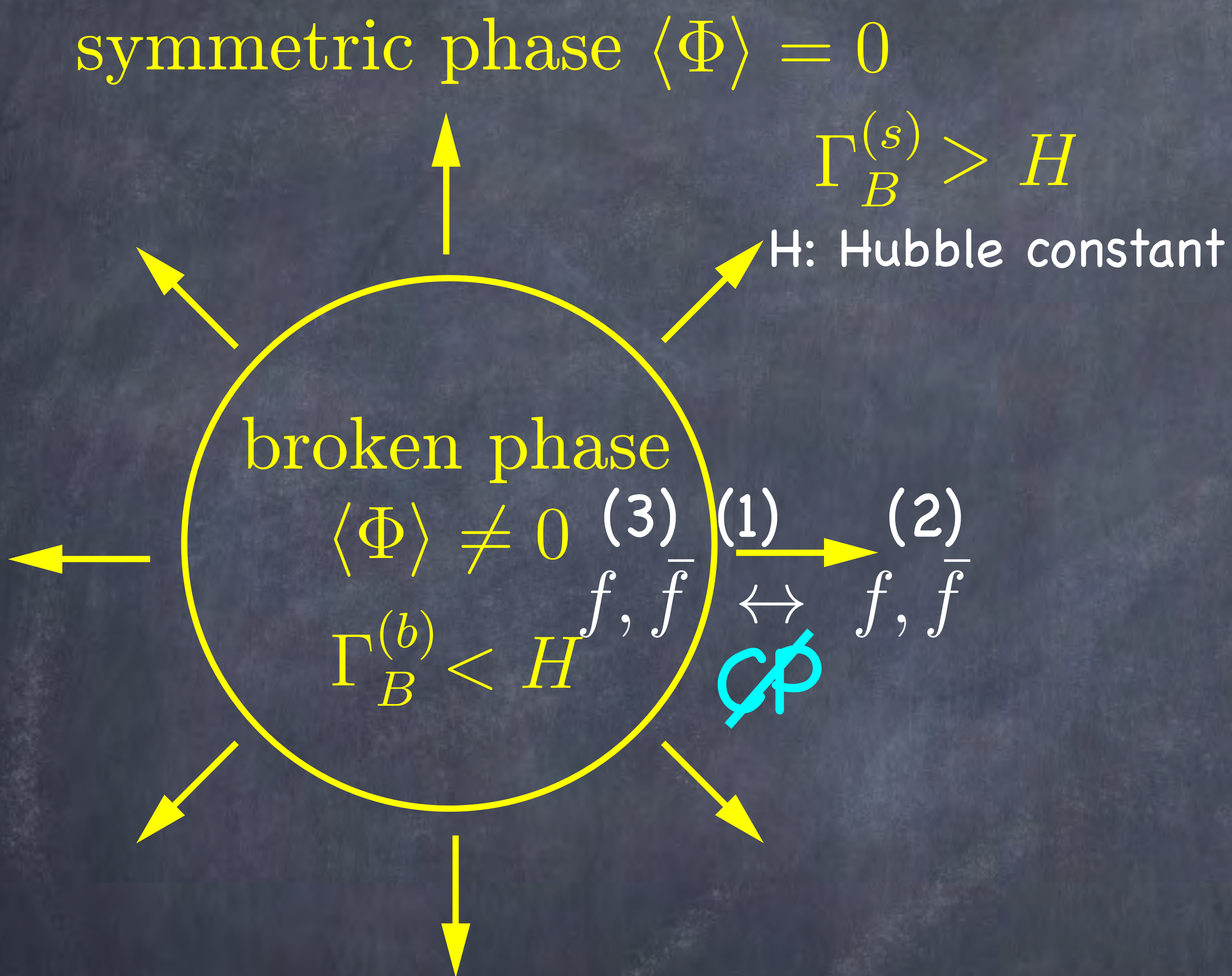

(1) Asymmetries arise ($\because$ CPV) but no BAU.

$$n_B = \underbrace{n_b^L - n_{\bar{b}}^L}_{\neq 0} + \underbrace{n_b^R - n_{\bar{b}}^R}_{\neq 0} = 0$$

(2) LH part changes ($\because$ sphaleron) -> BAU

$$n_B = \underbrace{n_b^L - n_{\bar{b}}^L}_{\text{changed}} + n_b^R - n_{\bar{b}}^R \to n_B \neq 0$$

(3) If $\boxed{\Gamma_B^{(b)} < H}$ the BAU can survive.

EW Baryogenesis mechanism

How do we test this scenario?

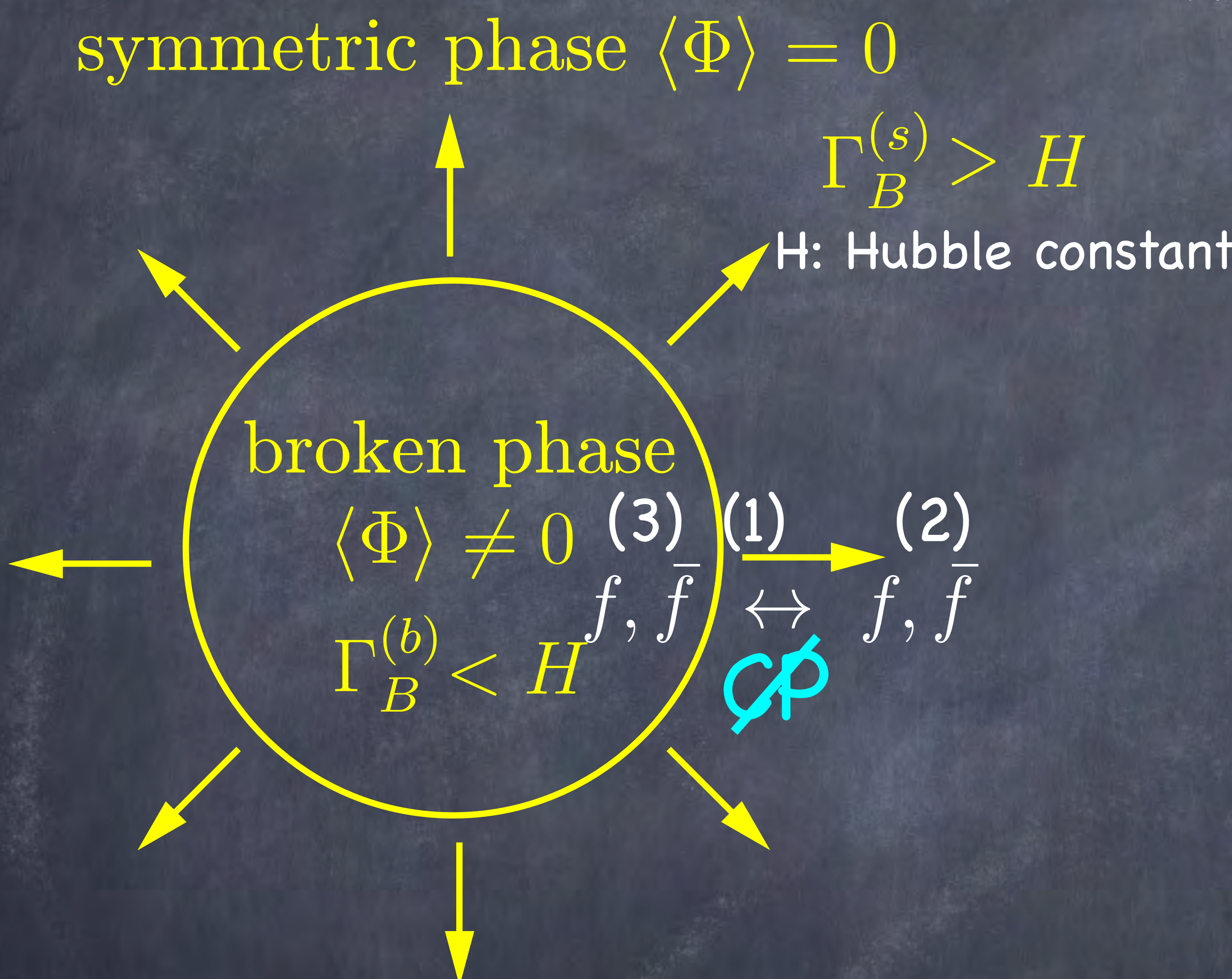

(1) Asymmetries arise (∵ CPV) but no BAU. $n_B = \underbrace{n_b^L - n_{\bar{b}}^L}_{\neq 0} + \underbrace{n_b^R - n_{\bar{b}}^R}_{\neq 0} = 0$

(2) LH part changes (∵ sphaleron) -> BAU $n_B = \underbrace{n_b^L - n_{\bar{b}}^L}_{\text{changed}} + n_b^R - n_{\bar{b}}^R \to n_B \neq 0$

(3) If $\boxed{\Gamma_B^{(b)} < H}$ the BAU can survive.

EW Baryogenesis mechanism

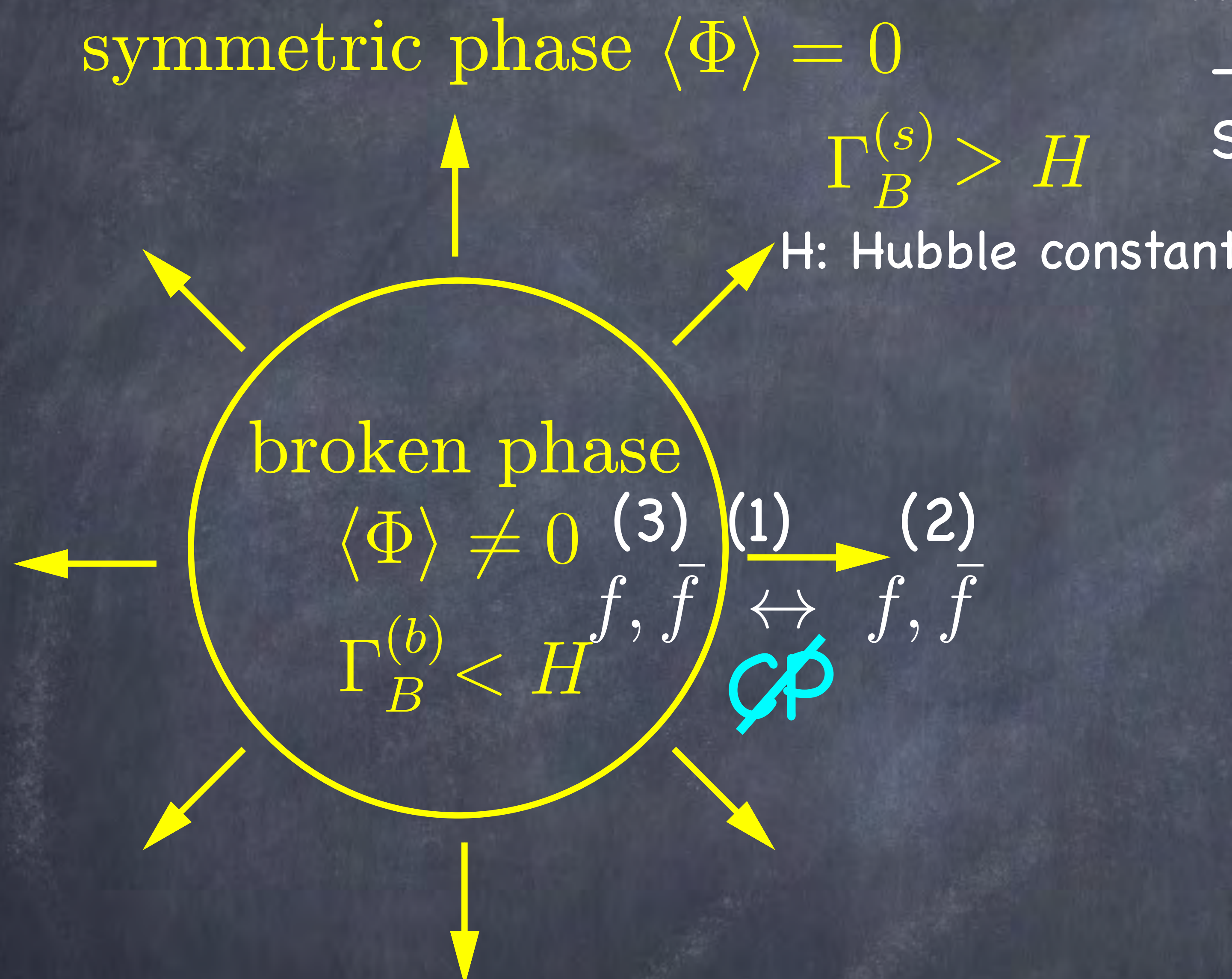

How do we test this scenario?

-> cannot redo EWPT in lab. exp.

So, test Sakharov'criteria instead.

(1) Asymmetries arise ($\because$ CPV) but no BAU.

$$n_B = \underbrace{n_b^L - n_{\bar{b}}^L}_{\neq 0} + \underbrace{n_b^R - n_{\bar{b}}^R}_{\neq 0} = 0$$

(2) LH part changes ($\because$ sphaleron) -> BAU

$$n_B = \underbrace{n_b^L - n_{\bar{b}}^L}_{\text{changed}} + n_b^R - n_{\bar{b}}^R \to n_B \neq 0$$

(3) If $\boxed{\Gamma_B^{(b)} < H}$ the BAU can survive.

EW Baryogenesis mechanism

How do we test this scenario?

-> cannot redo EWPT in lab. exp.

So, test Sakharov'criteria instead.

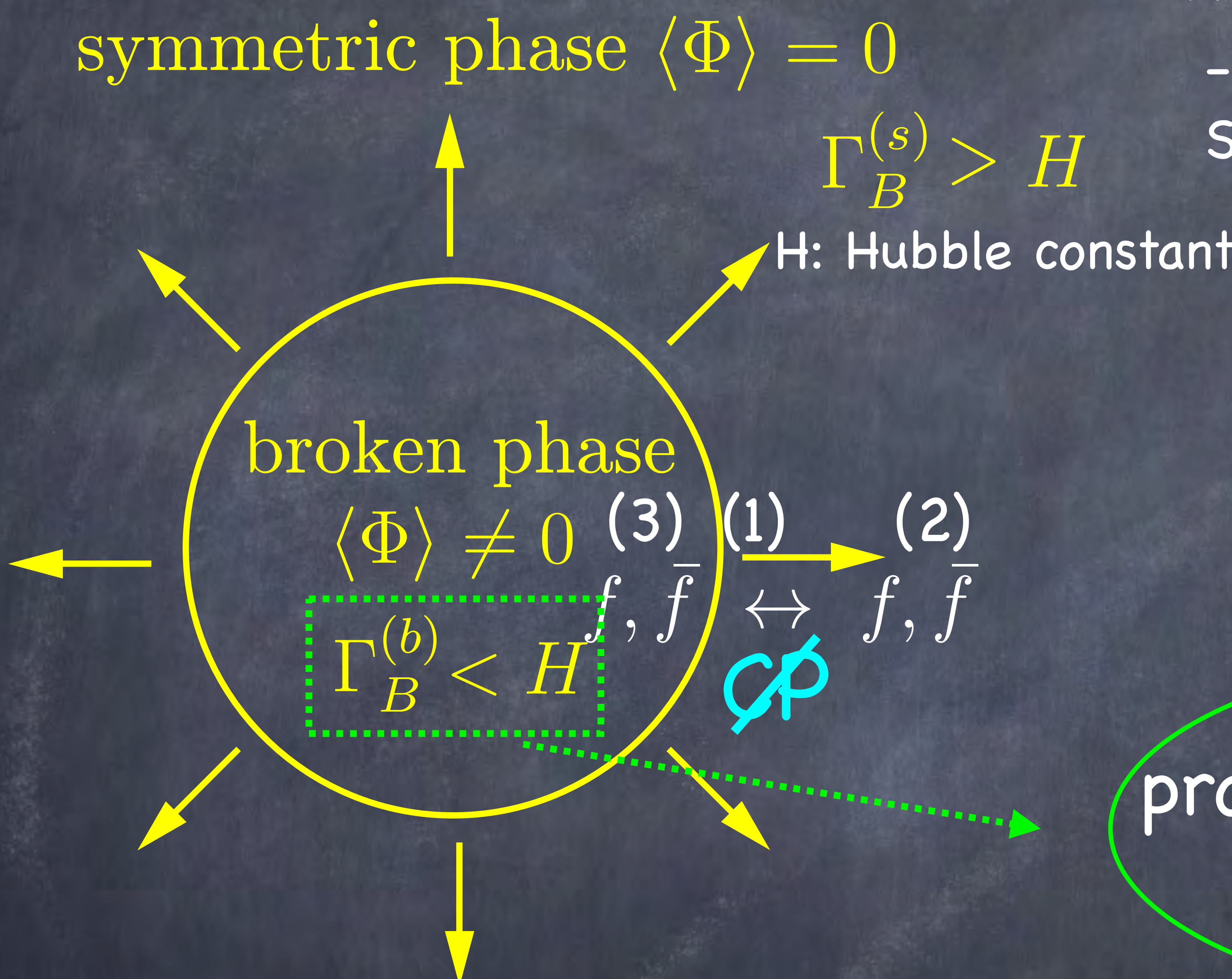

probe by collider physics

Higgs physics etc

(1) Asymmetries arise ($\because$ CPV) but no BAU.

$$n_B = \underbrace{n_b^L - n_{\bar{b}}^L}_{\neq 0} + \underbrace{n_b^R - n_{\bar{b}}^R}_{\neq 0} = 0$$

(2) LH part changes ($\because$ sphaleron) -> BAU

$$n_B = \underbrace{n_b^L - n_{\bar{b}}^L}_{\text{changed}} + n_b^R - n_{\bar{b}}^R \to n_B \neq 0$$

(3) If $\boxed{\Gamma_B^{(b)} < H}$ the BAU can survive.

EW Baryogenesis mechanism

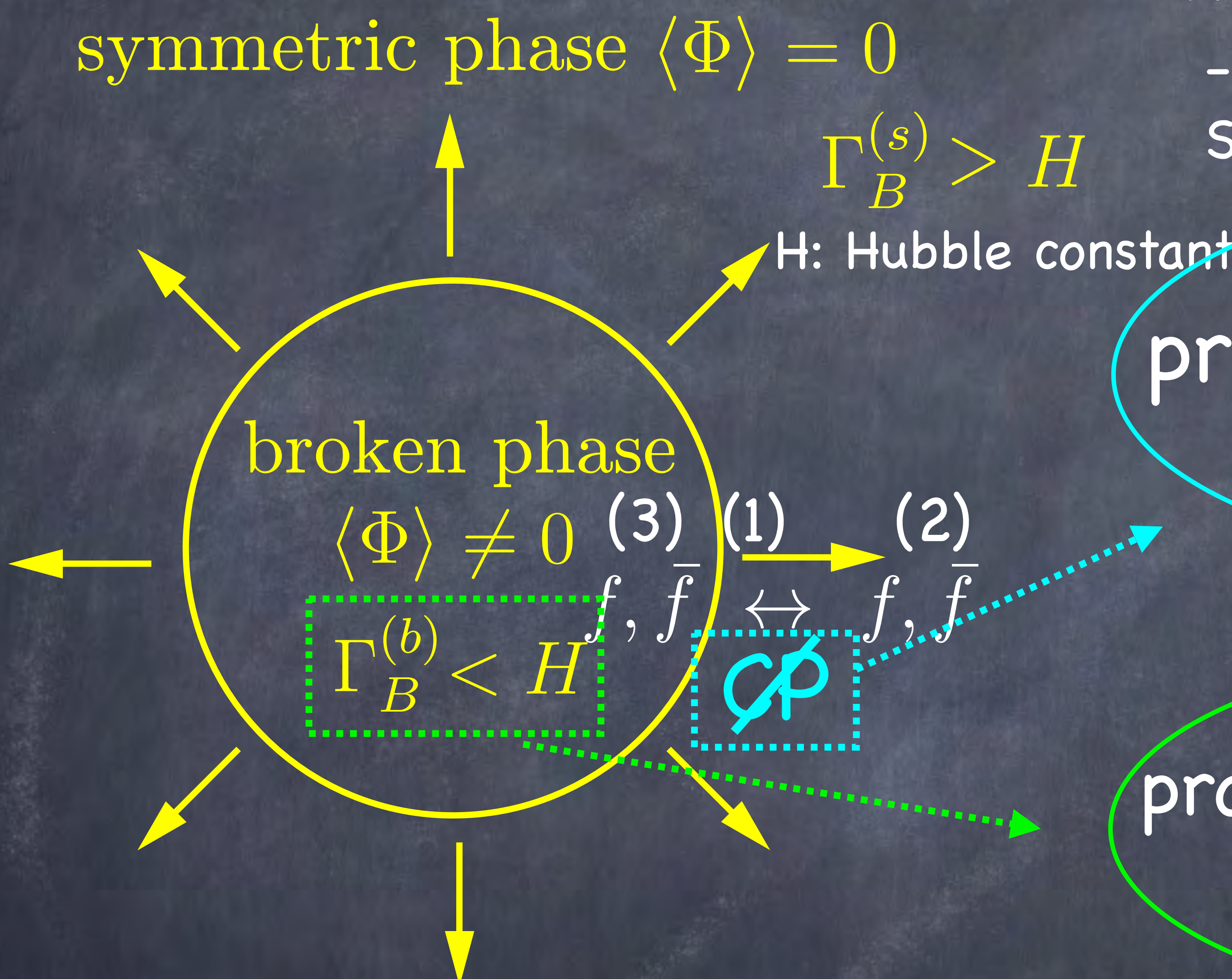

How do we test this scenario?

-> cannot redo EWPT in lab. exp.

So, test Sakharov'criteria instead.

probe by CPV physics

EDMs, B decays etc

probe by collider physics

Higgs physics etc

(1) Asymmetries arise (∵ CPV) but no BAU.

$$n_B = \underbrace{n_b^L - n_{\bar{b}}^L}_{\neq 0} + \underbrace{n_b^R - n_{\bar{b}}^R}_{\neq 0} = 0$$

(2) LH part changes (∵ sphaleron) -> BAU

$$n_B = \underbrace{n_b^L - n_{\bar{b}}^L}_{\text{changed}} + n_b^R - n_{\bar{b}}^R \to n_B \neq 0$$

(3) If $\boxed{\Gamma_B^{(b)} < H}$ the BAU can survive.

EW Baryogenesis mechanism

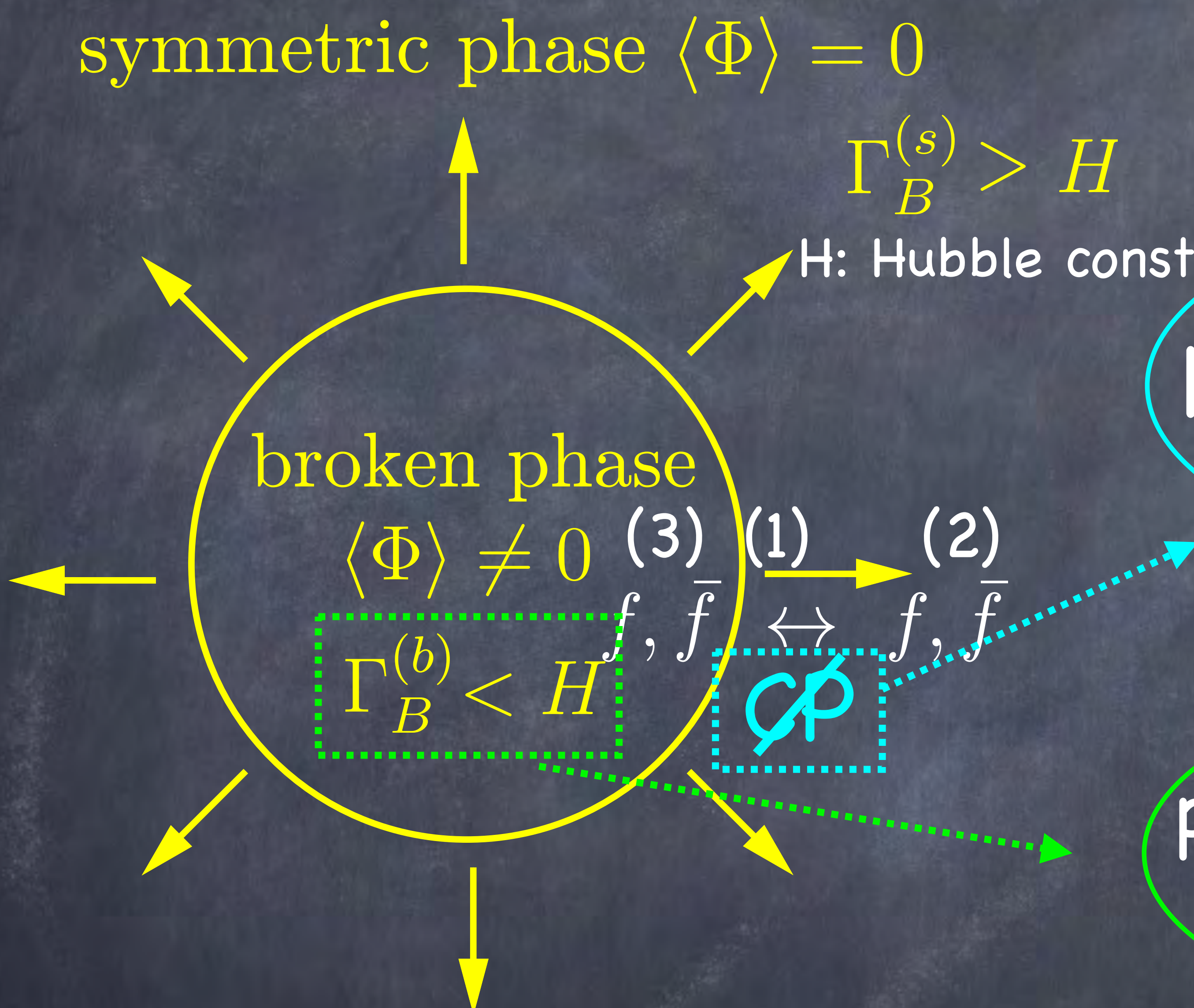

How do we test this scenario?

-> cannot redo EWPT in lab. exp.

So, test Sakharov'criteria instead.

probe by CPV physics

EDMs, B decays etc

Relevant particles are light (<1TeV)

probe by collider physics

Higgs physics etc

(1) Asymmetries arise (∵ CPV) but no BAU.

$$n_B = \underbrace{n_b^L - n_{\bar{b}}^L}_{\neq 0} + \underbrace{n_b^R - n_{\bar{b}}^R}_{\neq 0} = 0$$

(2) LH part changes (∵ sphaleron) -> BAU

$$n_B = \underbrace{n_b^L - n_{\bar{b}}^L}_{\text{changed}} + n_b^R - n_{\bar{b}}^R \to n_B \neq 0$$

(3) If $\boxed{\Gamma_B^{(b)} < H}$ the BAU can survive.

$$\Gamma_B^{(b)} < H$$

B-changing rate in the broken phase is

$$\boxed{\Gamma_B^{(b)}(T) \simeq (\text{prefactor})e^{-E_{\rm sph}/T}}$$

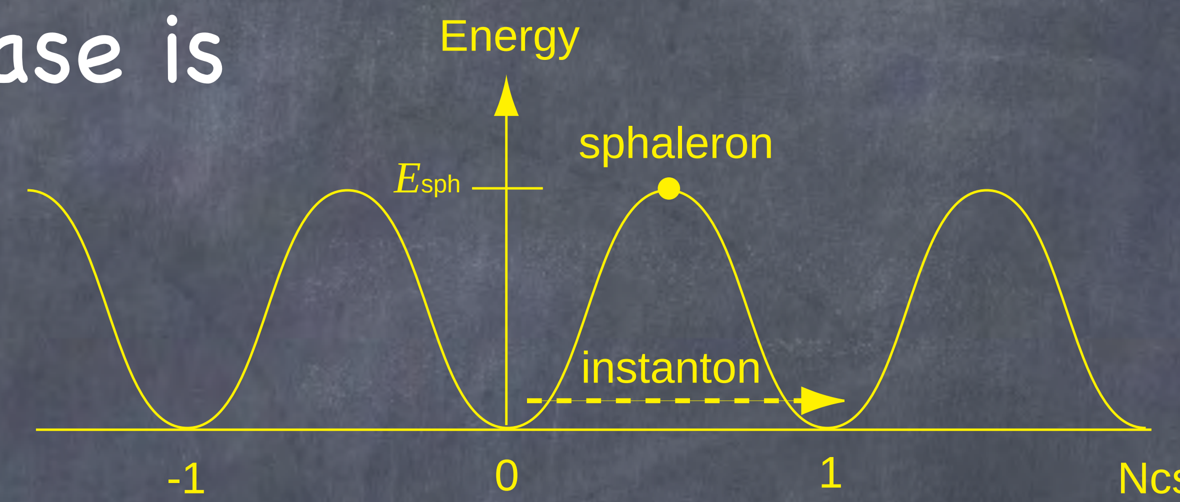

$E_{\rm sph}$ is proportional to the Higgs VEV

$$\boxed{E_{\rm sph} \propto v(T)}$$

what we need is

large Higgs VEV after the EWPT

EWPT has to be "**strong**" 1st order!!

$$\Gamma_B^{(b)}(T_C) < H(T_C) \quad \Longrightarrow \quad \boxed{\frac{v_C}{T_C} \gtrsim 1}$$

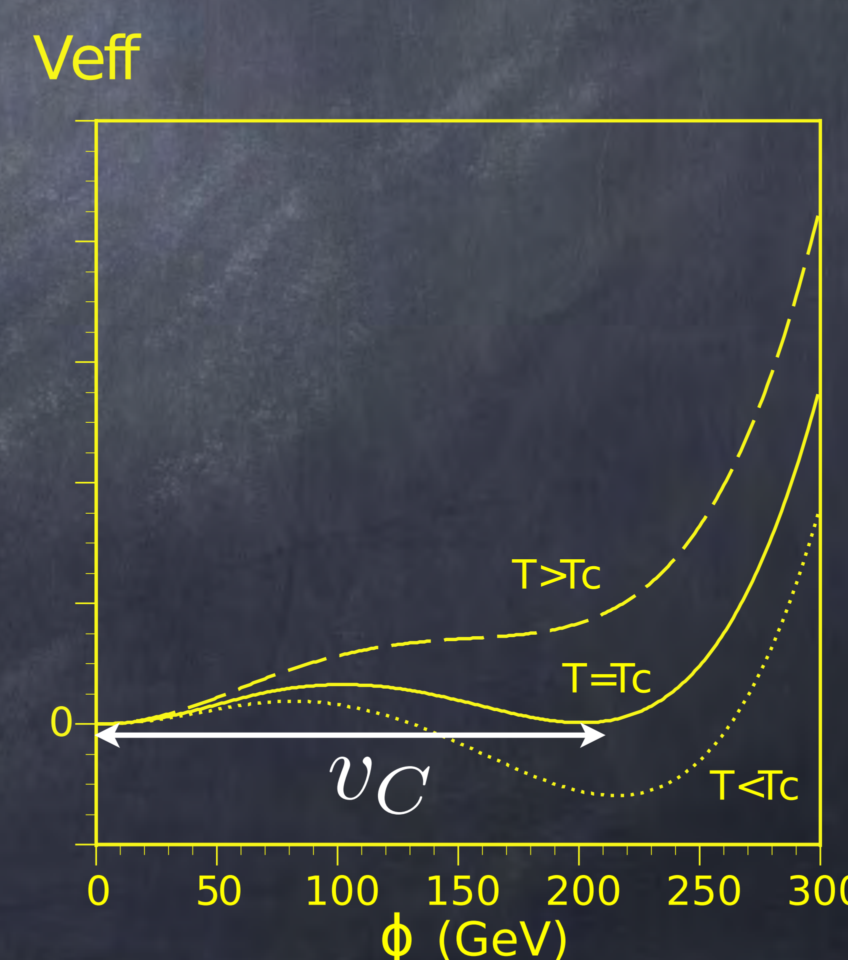

$$\Gamma_B^{(b)} < H$$

B-changing rate in the broken phase is

$$\boxed{\Gamma_B^{(b)}(T) \simeq (\text{prefactor})e^{-E_{\text{sph}}/T}}$$

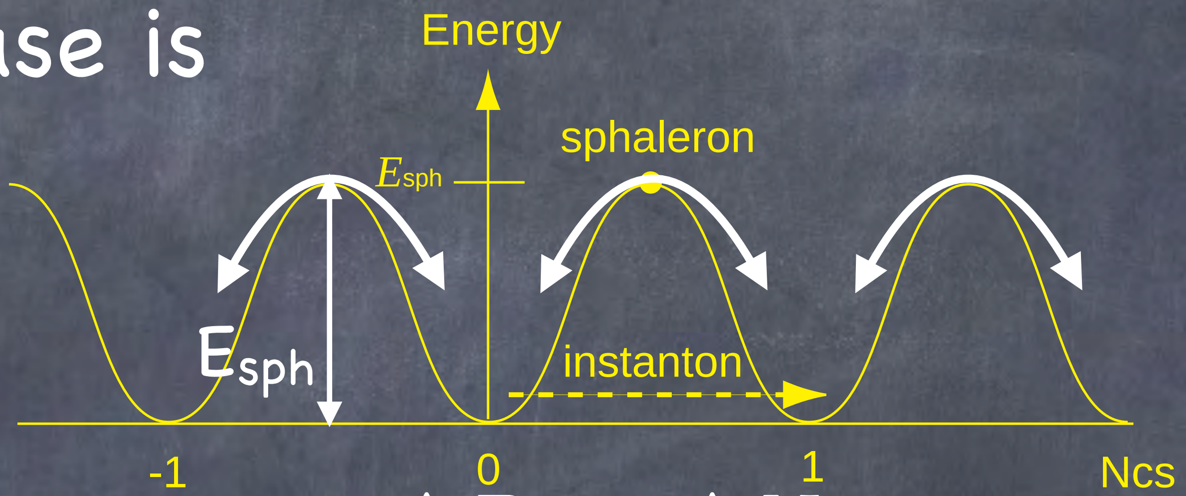

$$\Delta B = 3\Delta N_{\text{CS}}$$

Esph is proportional to the Higgs VEV

$$\boxed{E_{\text{sph}} \propto v(T)}$$

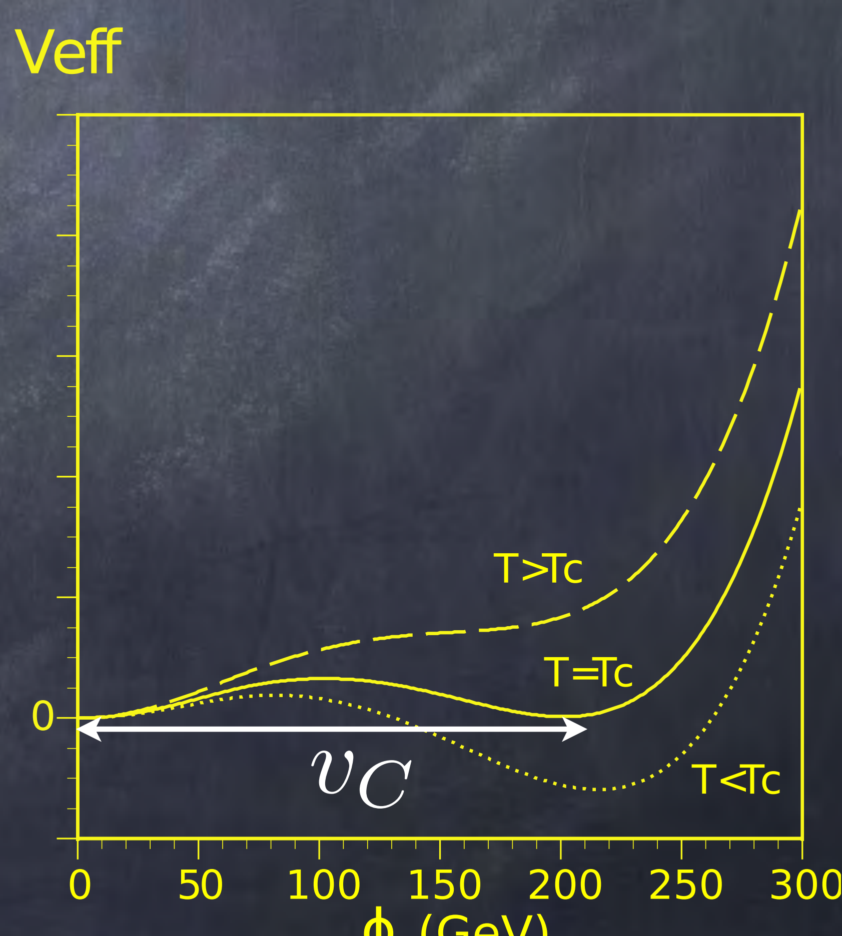

what we need is

large Higgs VEV after the EWPT

→ EWPT has to be "**strong**" 1st order!!

$$\Gamma_B^{(b)}(T_C) < H(T_C) \quad \longrightarrow \quad \boxed{\frac{v_C}{T_C} \gtrsim 1}$$

How do we get 1st-order EWPT?

1st(2nd) order PT = discontinuities in 1st(2nd) derivatives of free energy

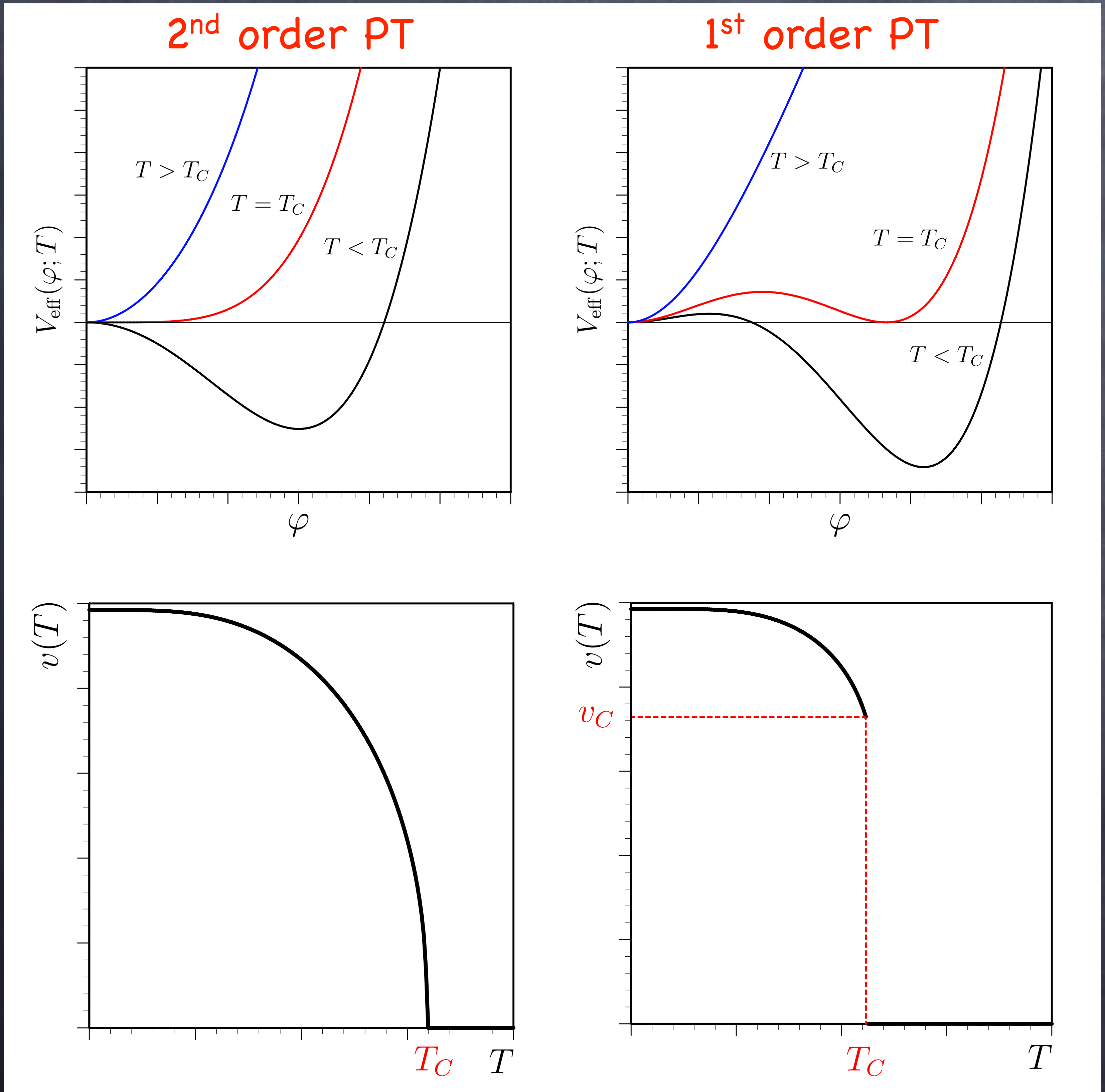

How do we get 1st-order EWPT?

1st(2nd) order PT = discontinuities in 1st(2nd) derivatives of free energy

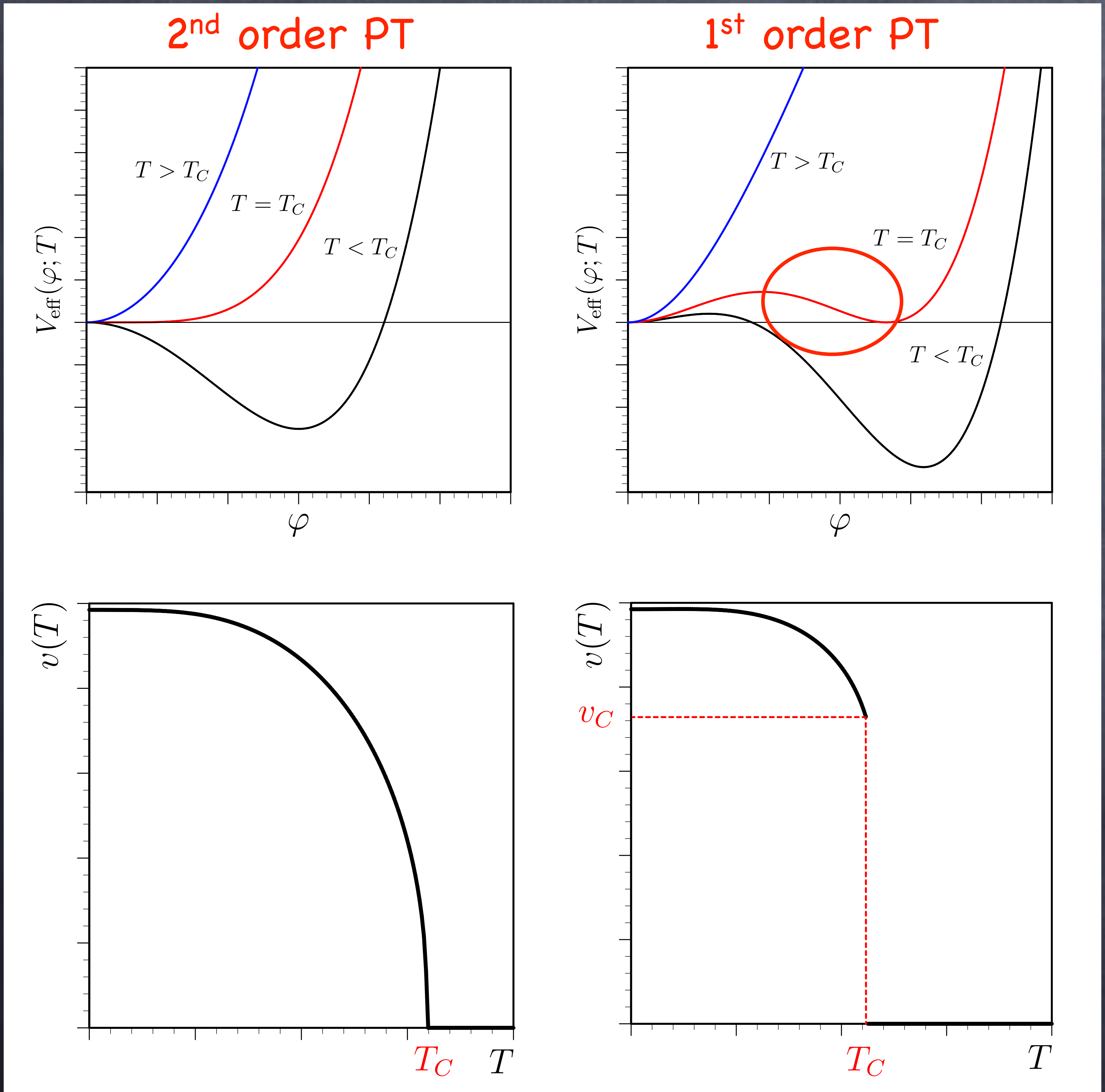

1st-order PT

$\Downarrow$

Negative contributions in V_{eff}.

How do we get 1^{st}-order EWPT?

1st(2nd) order PT = discontinuities in 1st(2nd) derivatives of free energy

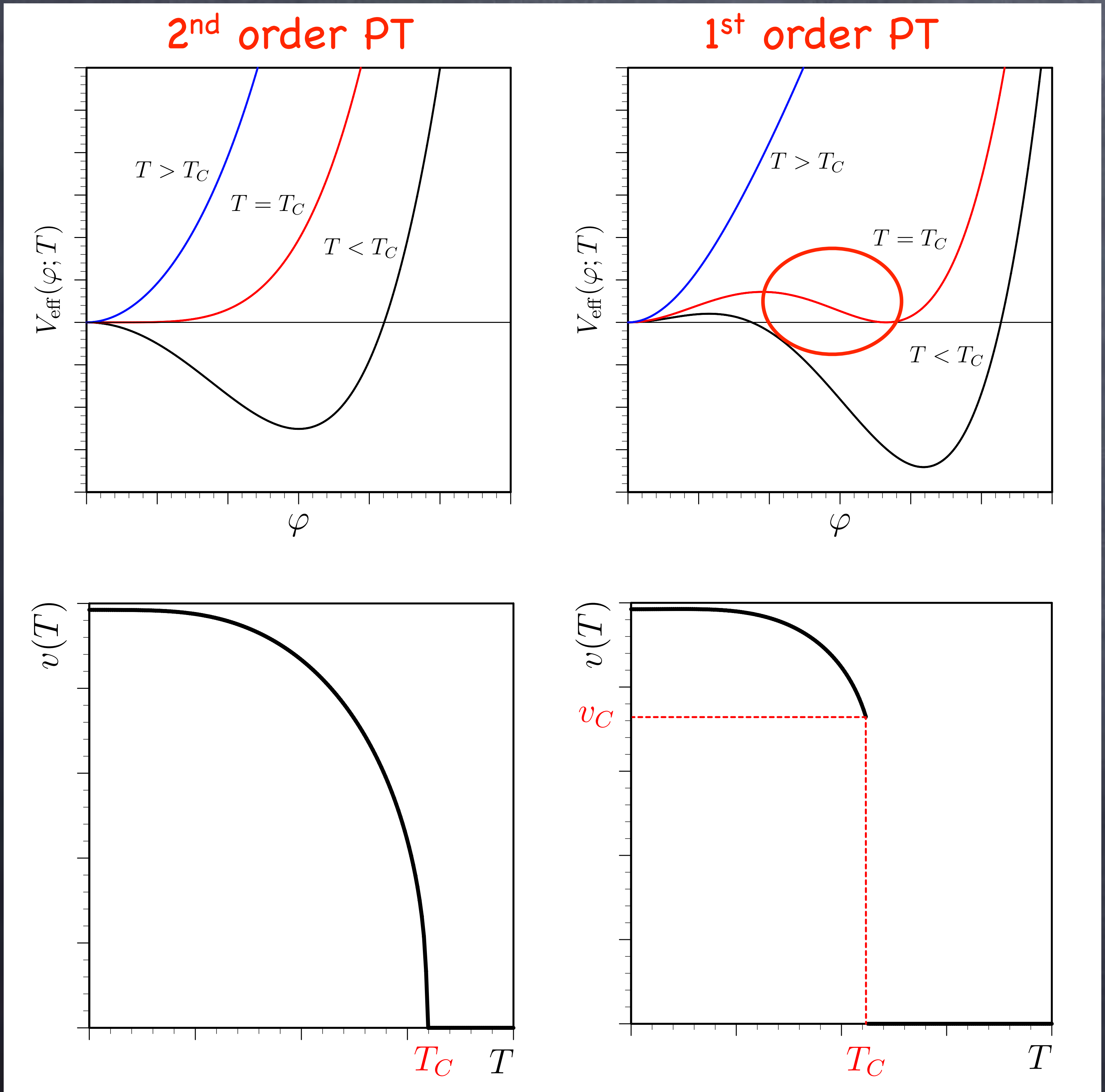

1^{st}-order PT

$\Downarrow$

Negative contributions in V_{eff}.

From where?

Origins of the negative contributions in $V_{eff.}$

2 representative cases.

Origins of the negative contributions in $V_{eff.}$

2 representative cases.

1. Thermal loop driven case e.g. SM, MSSM. ∋ doublet Higgs

thermal boson loop

$$V_1^{(\mathrm{boson})}(\varphi;T) \ni -\frac{T(m^2(\varphi))^{3/2}}{12\pi}$$

$$\underset{m^2=g^2\varphi^2}{=} -\frac{Tg^3|\varphi|^3}{12\pi}$$

Origins of the negative contributions in $V_{eff.}$

2 representative cases.

---

1. Thermal loop driven case e.g. SM, MSSM. ∋ doublet Higgs

thermal boson loop

$$V_1^{(\mathrm{boson})}(\varphi;T) \ni -\frac{T(m^2(\varphi))^{3/2}}{12\pi}$$

$$\underset{m^2=g^2\varphi^2}{=} -\frac{Tg^3|\varphi|^3}{12\pi}$$

[N.B.] If $m^2(\varphi) = g^2\varphi^2 + M^2 \simeq M^2$, no $|\varphi|^3$ term!!

Origins of the negative contributions in $V_{eff.}$

2 representative cases.

---

1. Thermal loop driven case

e.g. SM, MSSM. ∋ doublet Higgs

thermal boson loop

$$V_1^{(\text{boson})}(\varphi;T) \ni -\frac{T(m^2(\varphi))^{3/2}}{12\pi} \underset{m^2=g^2\varphi^2}{=} -\frac{Tg^3|\varphi|^3}{12\pi}$$

Typical signals

Deviations of hgg and/or hγγ and/or hhh couplings

[N.B.] If $m^2(\varphi) = g^2\varphi^2 + M^2 \simeq M^2$, no $|\varphi|^3$ term!!

Origins of the negative contributions in $V_{eff.}$

2 representative cases.

---

1. Thermal loop driven case

e.g. SM, MSSM. ∋ doublet Higgs

thermal boson loop

$$V_1^{(\mathrm{boson})}(\varphi;T) \ni -\frac{T(m^2(\varphi))^{3/2}}{12\pi} \underset{m^2=g^2\varphi^2}{=} -\frac{Tg^3|\varphi|^3}{12\pi}$$

Typical signals

Deviations of hgg and/or hγγ and/or hhh couplings

[N.B.] If $m^2(\varphi) = g^2\varphi^2 + M^2 \simeq M^2$, no $|\varphi|^3$ term!!

---

2. Tree driven case

e.g. rSM, NMSSM. ∋ singlet Higgs

$$\begin{aligned} V_0 &\ni \mu_{HS}\varphi_H^2\varphi_S + \mu_S\varphi_S^3 \\ &\ni M(\mu_{HS}, \mu_S)(\varphi_H^2 + \varphi_S^2)^{3/2} \end{aligned}$$

Origins of the negative contributions in $V_{eff.}$

2 representative cases.

1. Thermal loop driven case
e.g. SM, MSSM. ∋ doublet Higgs

thermal boson loop

$$V_1^{(\text{boson})}(\varphi;T) \ni -\frac{T(m^2(\varphi))^{3/2}}{12\pi} \underset{m^2=g^2\varphi^2}{=} -\frac{Tg^3|\varphi|^3}{12\pi}$$

Typical signals

Deviations of hgg and/or hγγ and/or hhh couplings

[N.B.] If $m^2(\varphi) = g^2\varphi^2 + M^2 \simeq M^2$, no $|\varphi|^3$ term!!

2. Tree driven case
e.g. rSM, NMSSM. ∋ singlet Higgs

$$V_0 \ni \mu_{HS}\varphi_H^2\varphi_S + \mu_S\varphi_S^3$$
$$\ni \boxed{M(\mu_{HS},\mu_S)}(\varphi_H^2+\varphi_S^2)^{3/2}$$

can be negative!

Origins of the negative contributions in $V_{eff.}$

2 representative cases.

1. Thermal loop driven case

e.g. SM, MSSM. ∋ doublet Higgs

thermal boson loop

$$V_1^{(\mathrm{boson})}(\varphi;T) \ni -\frac{T(m^2(\varphi))^{3/2}}{12\pi}$$

$$\underset{m^2=g^2\varphi^2}{=} -\frac{Tg^3|\varphi|^3}{12\pi}$$

Typical signals

Deviations of hgg and/or hγγ and/or hhh couplings

[N.B.] If $m^2(\varphi) = g^2\varphi^2 + M^2 \simeq M^2$, no $|\varphi|^3$ term!!

2. Tree driven case

e.g. rSM, NMSSM. ∋ singlet Higgs

$$V_0 \ni \mu_{HS}\varphi_H^2\varphi_S + \mu_S\varphi_S^3$$

$$\ni \boxed{M(\mu_{HS}, \mu_S)}(\varphi_H^2 + \varphi_S^2)^{3/2}$$

can be negative!

Typical signals

Deviations of HVV and/or Hff and/or hhh couplings.

Current status of EWBG

Current status of EWBG

- SM EWBG was excluded.

  ∵ No 1st-order PT for m_h=125 GeV.

[Kajantie at al, PRL77,2887 ('96); Rummukainen et al, NPB532,283 ('98); Csikor et al, PRL82, 21 ('99); Aoki et al, PRD60,013001 ('99). Laine et al, NPB73,180('99)]

Current status of EWBG

- SM EWBG was excluded.

$\because$ No 1st-order PT for m_h=125 GeV. $\frac{v_C}{T_C} \gtrsim 1$ not satisfied

[Kajantie at al, PRL77,2887 ('96); Rummukainen et al, NPB532,283 ('98); Csikor et al, PRL82, 21 ('99); Aoki et al, PRD60,013001 ('99). Laine et al, NPB73,180('99)]

Current status of EWBG

- SM EWBG was excluded.

∵ No 1st-order PT for m_h=125 GeV. $\frac{v_C}{T_C} \gtrsim 1$ not satisfied

[Kajantie at al, PRL77,2887 ('96); Rummukainen et al, NPB532,283 ('98); Csikor et al, PRL82, 21 ('99); Aoki et al, PRD60,013001 ('99). Laine et al, NPB73,180('99)]

- MSSM EWBG was excluded.

∵ light stop scenario is inconsistent with LHC data

[D. Curtin, P. Jaiswall, P. Meade., JHEP08(2012)005; T. Cohen, D. E. Morrissey, A. Pierce, PRD86, 013009 (2012); K. Krizka, A. Kumar, D. E. Morrissey, PRD87, 095016 (2013)]

Current status of EWBG

- SM EWBG was excluded.

∵ No 1st-order PT for m_h=125 GeV. $\frac{v_C}{T_C} \gtrsim 1$ not satisfied

[Kajantie at al, PRL77,2887 ('96); Rummukainen et al, NPB532,283 ('98); Csikor et al, PRL82, 21 ('99); Aoki et al, PRD60,013001 ('99). Laine et al, NPB73,180('99)]

- MSSM EWBG was excluded.

∵ light stop scenario is inconsistent with LHC data $\frac{v_C}{T_C} \gtrsim 1$ not satisfied

[D. Curtin, P. Jaiswall, P. Meade., JHEP08(2012)005; T. Cohen, D. E. Morrissey, A. Pierce, PRD86, 013009 (2012); K. Krizka, A. Kumar, D. E. Morrissey, PRD87, 095016 (2013)]

Current status of EWBG

- SM EWBG was excluded.

$\because$ No 1st-order PT for m_h=125 GeV. $\quad \frac{v_C}{T_C} \gtrsim 1$ not satisfied

[Kajantie at al, PRL77,2887 ('96); Rummukainen et al, NPB532,283 ('98); Csikor et al, PRL82, 21 ('99); Aoki et al, PRD60,013001 ('99). Laine et al, NPB73,180('99)]

- MSSM EWBG was excluded.

$\because$ light stop scenario is inconsistent with LHC data $\quad \frac{v_C}{T_C} \gtrsim 1$ not satisfied

[D. Curtin, P. Jaiswall, P. Meade., JHEP08(2012)005; T. Cohen, D. E. Morrissey, A. Pierce, PRD86, 013009 (2012); K. Krizka, A. Kumar, D. E. Morrissey, PRD87, 095016 (2013)]

- Not enough data to exclude other models (2HDM, NMSSM etc).

Anyway, collider test of EWBG will be done based on the sphaleron decoupling condition,

$$\frac{v_C}{T_C} \gtrsim 1$$

What's next?

- No benchmark scenario.

- Colored particles (squarks) may not play a role in realizing strong 1^{st}-order PT. (due to severe LHC bounds)

- EWPT may be simply described by extended Higgs sector.

SM + SU(2) n-tuplet Higgs, n=1,2,3,...

[N.B.] CP violation comes from (chargino, neutralino)-sector which would not be relevant in studying EWPT. (bosons are more important than fermions)

We will consider a simple case, SM+SU(2) singlet Higgs.

Electroweak phase transition in the real singlet-extended SM (rSM)

in collaboration with Kaori Fuyuto (Nagoya U)

Ref. Phys.Rev.D90, 015015 (2014), [arXiv:1406.0433]

Toward Higgs precision (Higgcision)

- Higgs sector will be clarified with better accuracy at the coming LHC and ILC.

- Theoretical uncertainties in the EWBG calculation also have to be minimized.

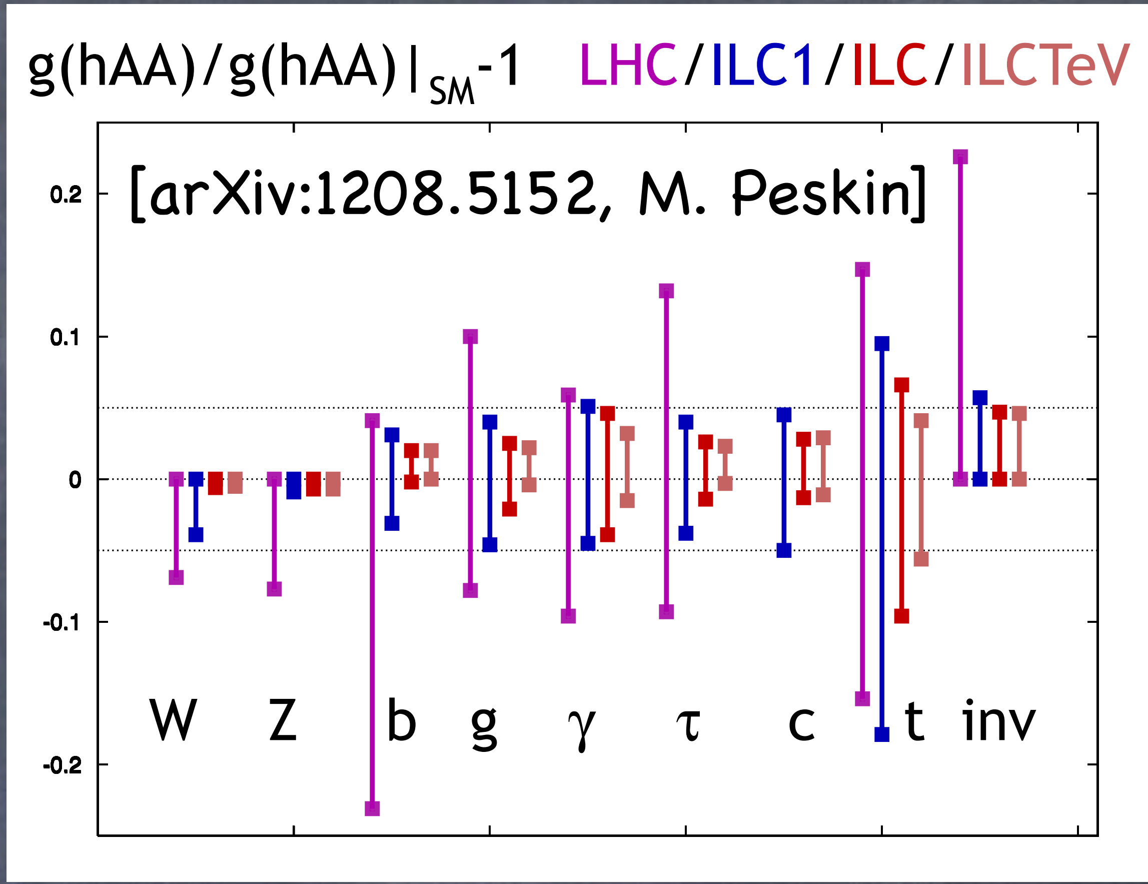

In the literature,

$$\boxed{\frac{v_C}{T_C} > 1}$$ is usually used.

But, r.h.s depends on Higgs mass

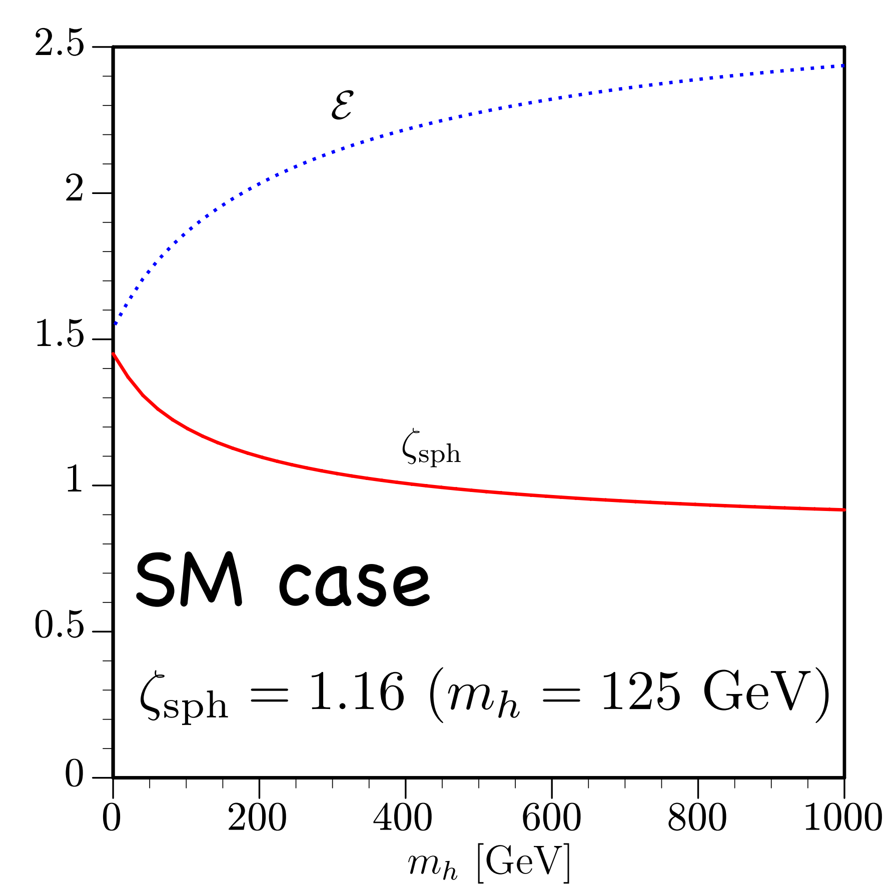

In this talk, we evaluate this condition more precisely, and study its impact on Higgs phenomenology.

Toward Higgs precision (Higgcision)

- Higgs sector will be clarified with better accuracy at the coming LHC and ILC.

- Theoretical uncertainties in the EWBG calculation also have to be minimized.

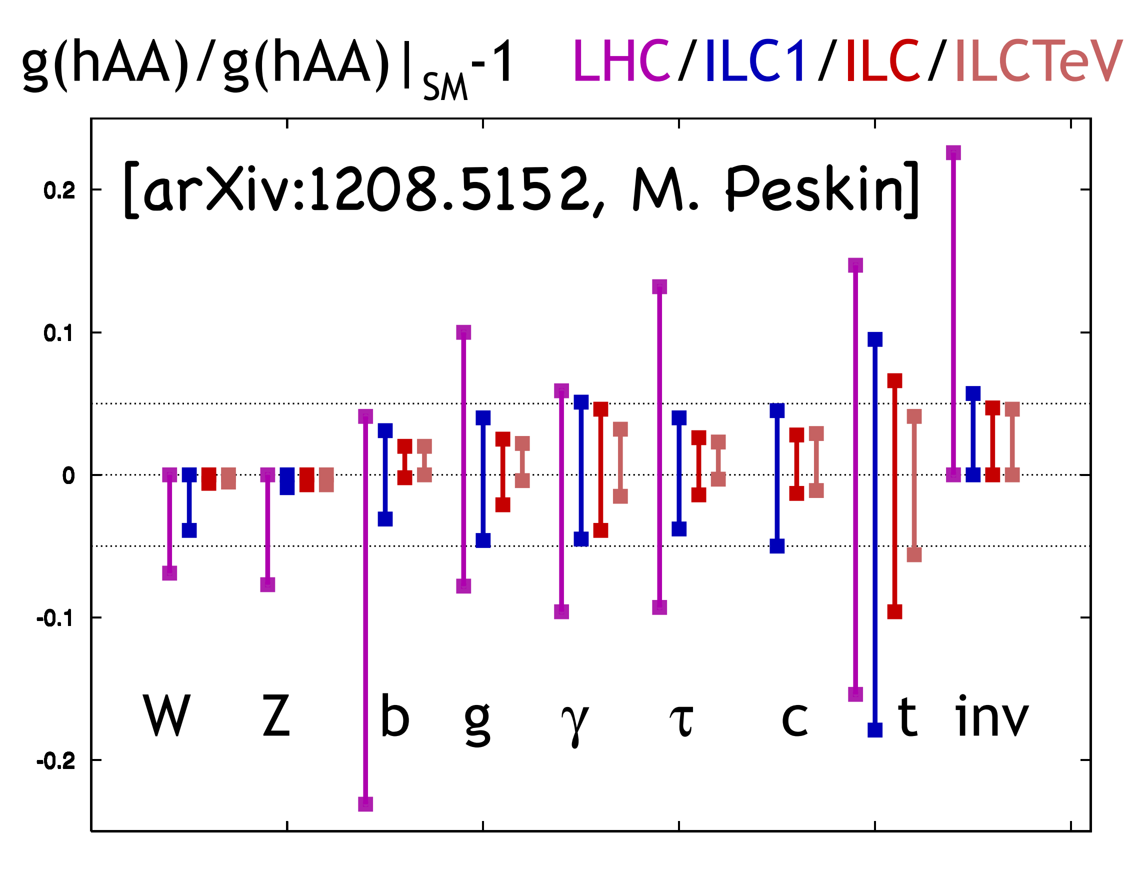

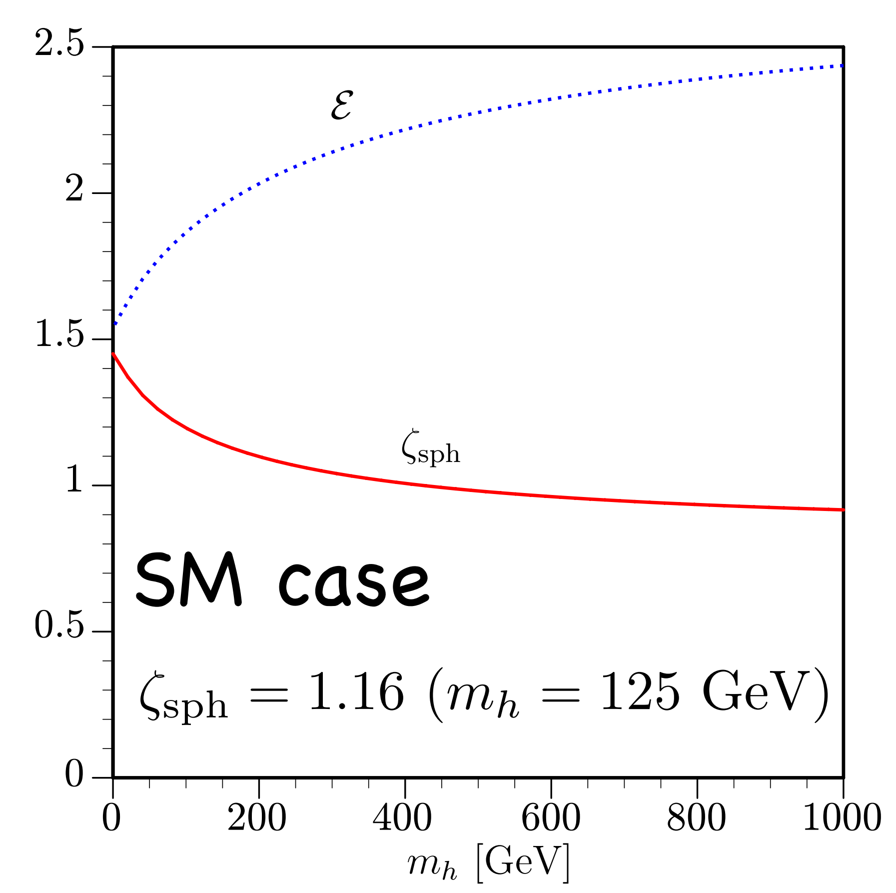

But, r.h.s depends on Higgs mass

In this talk, we evaluate this condition more precisely, and study its impact on Higgs phenomenology.

Toward Higgs precision (Higgcision)

- Higgs sector will be clarified with better accuracy at the coming LHC and ILC.

- Theoretical uncertainties in the EWBG calculation also have to be minimized.

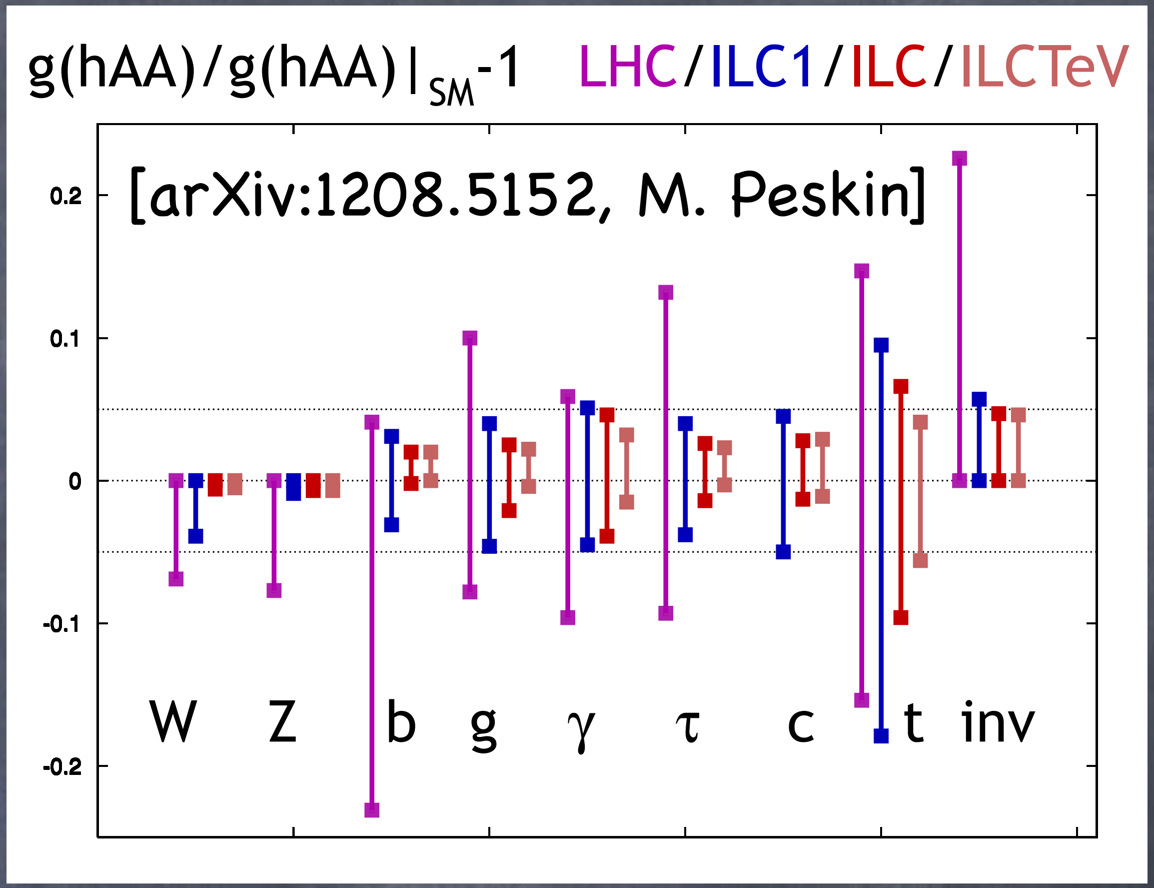

$$\boxed{\frac{v_C}{T_C} > \zeta_{\rm sph}}$$ must be used.

But, r.h.s depends on Higgs mass

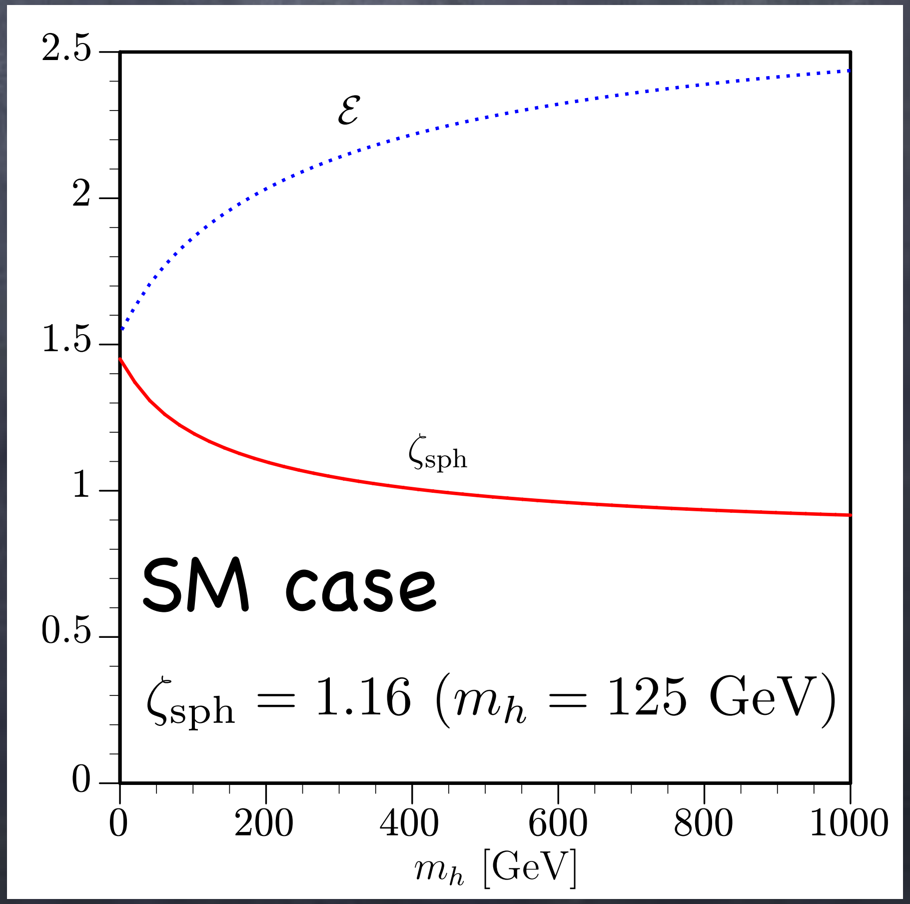

In this talk, we evaluate this condition more precisely, and study its impact on Higgs phenomenology.

Real singlet-extended SM (rSM)

Particle content: SM + S: (1,1,0)

- simple extension of the SM
- MSSM extended models have singlet Higgs (e.g., NMSSM)

Higgs potential:

$$
\boxed{
\begin{aligned}
V_0 = & -\mu_H^2 H^\dagger H + \lambda_H (H^\dagger H)^2 \\
& + \mu_{HS} H^\dagger H S + \frac{\lambda_{HS}}{2} H^\dagger H S^2 \\
& + \mu_S^3 S + \frac{m_S^2}{2} S^2 + \frac{\mu_S'}{3} S^3 + \frac{\lambda_S}{4} S^4,
\end{aligned}
}
$$

Scalar fields:

$$
H(x) = \begin{pmatrix} G^+(x) \\ \frac{1}{\sqrt{2}}\left(v + h(x) + iG^0(x)\right) \end{pmatrix}, \qquad S(x) = v_S + s(x).
$$

Real singlet-extended SM (rSM)

Particle content: SM + S: (1,1,0)

- simple extension of the SM
- MSSM extended models have singlet Higgs (e.g., NMSSM)

Higgs potential:

$$\boxed{\begin{aligned} V_0 = & -\mu_H^2 H^\dagger H + \lambda_H (H^\dagger H)^2 \\ & \boxed{+\mu_{HS} H^\dagger H S + \frac{\lambda_{HS}}{2} H^\dagger H S^2} \\ & + \mu_S^3 S + \frac{m_S^2}{2} S^2 + \frac{\mu'_S}{3} S^3 + \frac{\lambda_S}{4} S^4, \end{aligned}}$$

Scalar fields:

$$H(x) = \begin{pmatrix} G^+(x) \\ \frac{1}{\sqrt{2}}\left(v + h(x) + iG^0(x)\right) \end{pmatrix}, \qquad S(x) = v_S + s(x).$$

H-S mixings are important to have strong 1st-order PT.

Minimization (tadpole) conditions:

$$\left\langle \frac{\partial V}{\partial h} \right\rangle = v \left[-\mu_H^2 + \lambda_H v^2 + \mu_{HS} v_S + \frac{\lambda_{HS}}{2} v_S^2 \right] = 0,$$

$$\left\langle \frac{\partial V}{\partial s} \right\rangle = v_S \left[\frac{\mu_S^3}{v_S} + m_S^2 + \mu'_S v_S + \lambda_S v_S^2 + \frac{\mu_{HS}}{2} \frac{v^2}{v_S} + \frac{\lambda_{HS}}{2} v^2 \right] = 0,$$

Mass matrix: $$\frac{1}{2} \begin{pmatrix} h & s \end{pmatrix} \mathcal{M}_H^2 \begin{pmatrix} h \\ s \end{pmatrix}$$

$$\mathcal{M}_H^2 = \begin{pmatrix} 2\lambda_H v^2 & \mu_{HS} v + \lambda_{HS} v v_S \\ \mu_{HS} v + \lambda_{HS} v v_S & -\frac{\mu_S^3}{v_S} + \mu'_S v_S + 2\lambda_S v_S^2 - \frac{\mu_{HS}}{2} \frac{v^2}{v_S} \end{pmatrix},$$

which can be diagonalized by

$$\begin{pmatrix} h \\ s \end{pmatrix} = \begin{pmatrix} \cos\alpha & -\sin\alpha \\ \sin\alpha & \cos\alpha \end{pmatrix} \begin{pmatrix} H_1 \\ H_2 \end{pmatrix} \qquad \alpha \in [-\pi/4, \pi/4]$$

Minimization (tadpole) conditions:

$$\left\langle \frac{\partial V}{\partial h} \right\rangle = v\left[-\mu_H^2 + \lambda_H v^2 + \mu_{HS} v_S + \frac{\lambda_{HS}}{2} v_S^2\right] = 0,$$

$$\left\langle \frac{\partial V}{\partial s} \right\rangle = v_S\left[\frac{\mu_S^3}{v_S} + m_S^2 + \mu_S' v_S + \lambda_S v_S^2 + \frac{\mu_{HS}}{2}\frac{v^2}{v_S} + \frac{\lambda_{HS}}{2} v^2\right] = 0,$$

Mass matrix: $$\frac{1}{2}\begin{pmatrix} h & s \end{pmatrix} \mathcal{M}_H^2 \begin{pmatrix} h \\ s \end{pmatrix}$$

$$\mathcal{M}_H^2 = \begin{pmatrix} 2\lambda_H v^2 & \mu_{HS} v + \lambda_{HS} v v_S \\ \mu_{HS} v + \lambda_{HS} v v_S & -\frac{\mu_S^3}{v_S} + \mu_S' v_S + 2\lambda_S v_S^2 - \frac{\mu_{HS}}{2}\frac{v^2}{v_S} \end{pmatrix},$$

which can be diagonalized by

125 GeV Higgs

$$\begin{pmatrix} h \\ s \end{pmatrix} = \begin{pmatrix} \cos\alpha & -\sin\alpha \\ \sin\alpha & \cos\alpha \end{pmatrix} \begin{pmatrix} H_1 \\ H_2 \end{pmatrix} \qquad \alpha \in [-\pi/4, \pi/4]$$

Vacuum structure

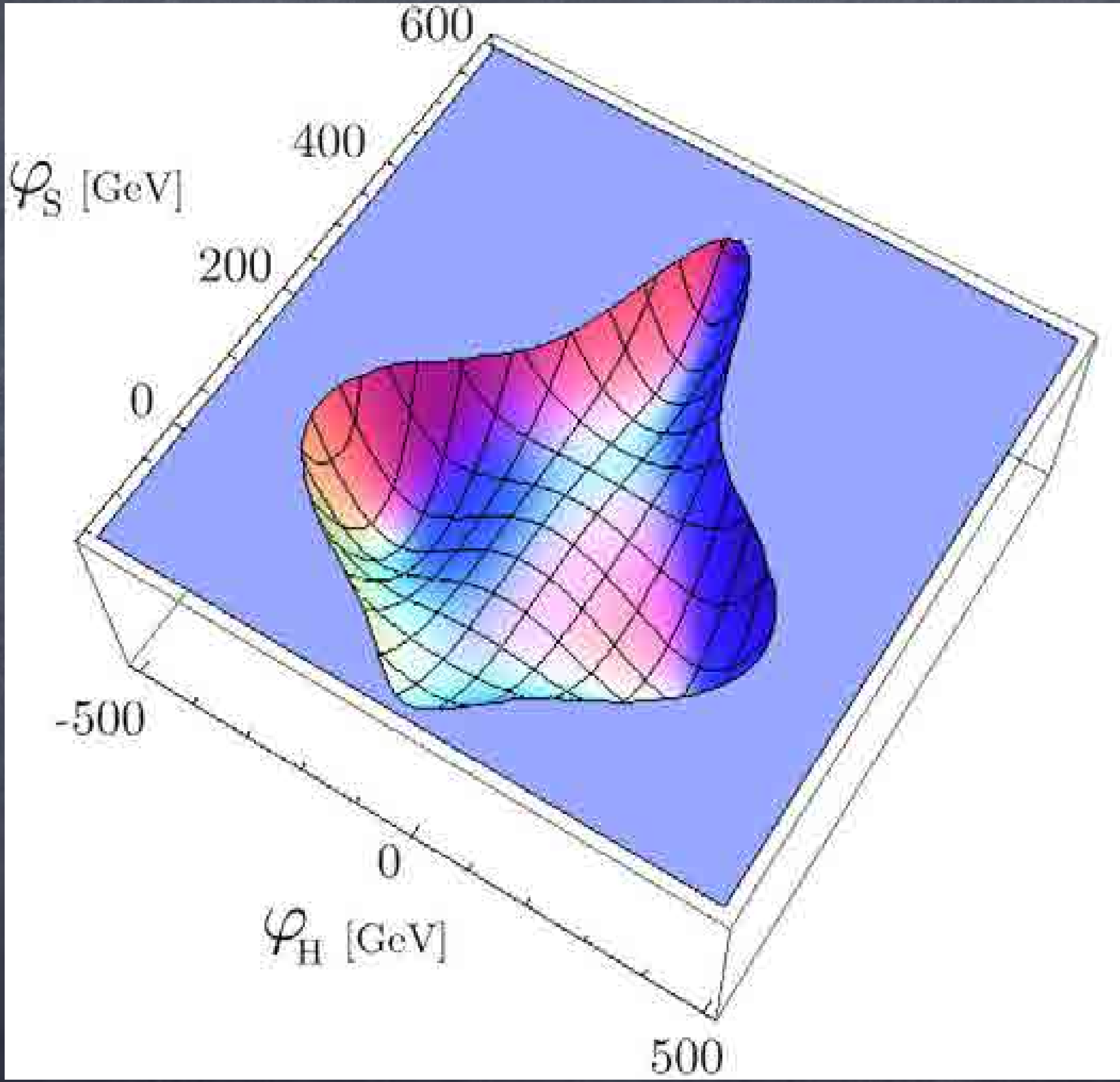

- Shape of the T=0 Higgs potential in an example.
- Vacuum structure is complex. EW vac. is not always global.

Vacuum structure

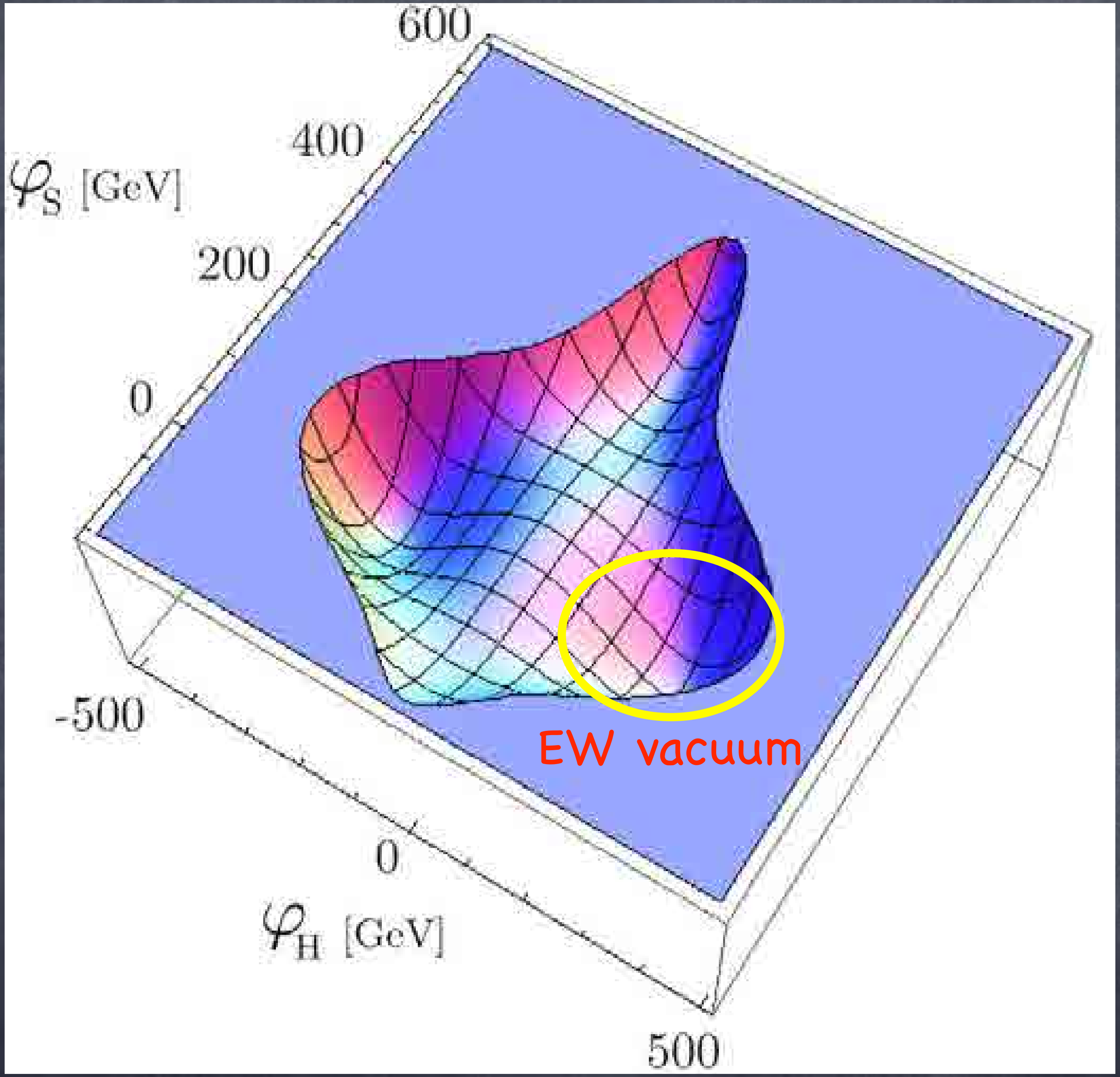

- Shape of the T=0 Higgs potential in an example.
- Vacuum structure is complex. EW vac. is not always global.

Vacuum structure

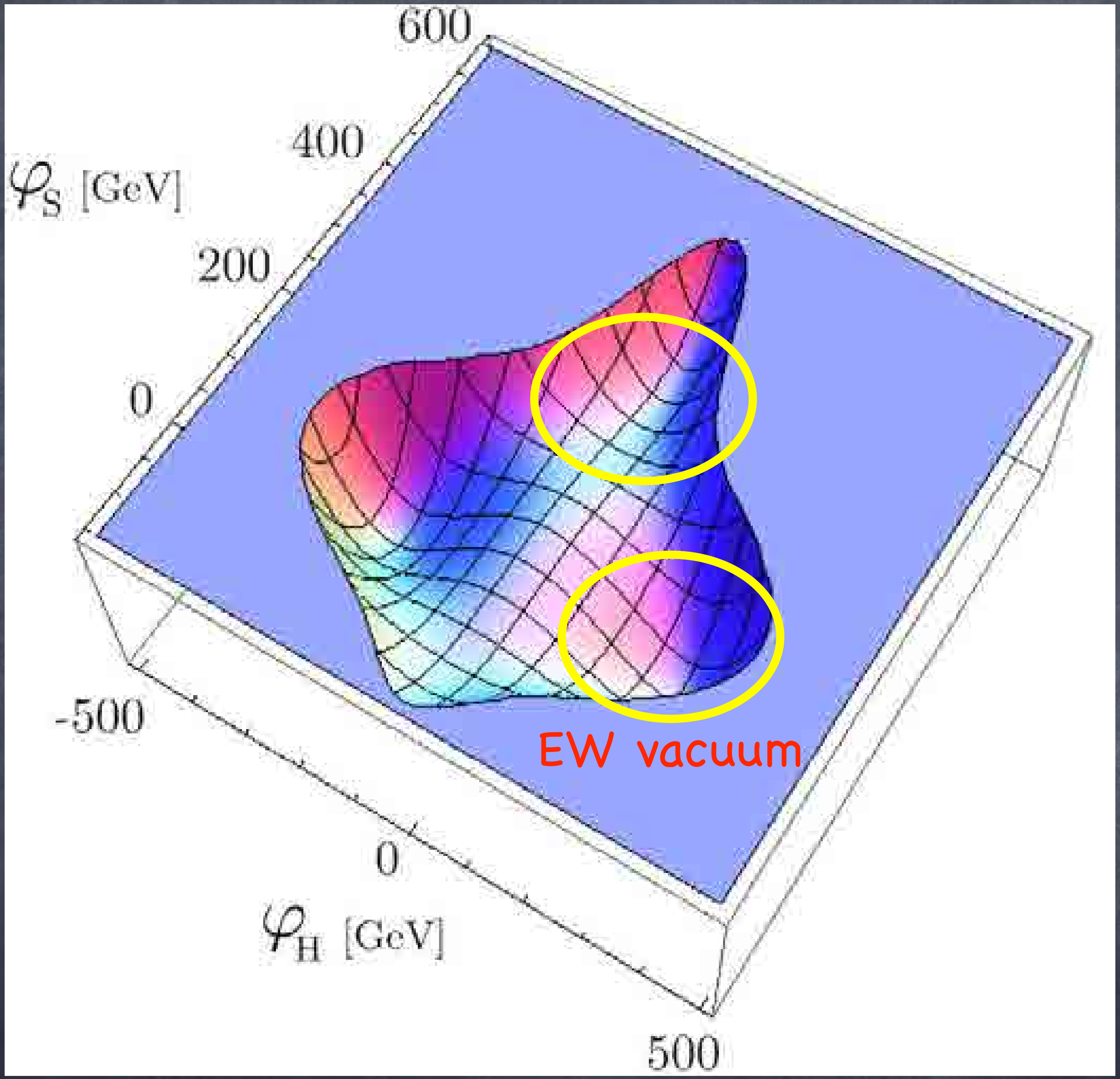

- Shape of the T=0 Higgs potential in an example.
- Vacuum structure is complex. EW vac. is not always global.

Vacuum structure

various vacua:

[Funakubo, Tao, Toyoda, PTP114, ('05) 369]

$$\mathrm{EW}: v \neq 0,\ v_S \neq 0,$$
$$\mathrm{I}: v = 0,\ v_S \neq 0,$$
$$\mathrm{II}: v \neq 0,\ v_S = 0,$$
$$\mathrm{SYM}: v = v_S = 0$$

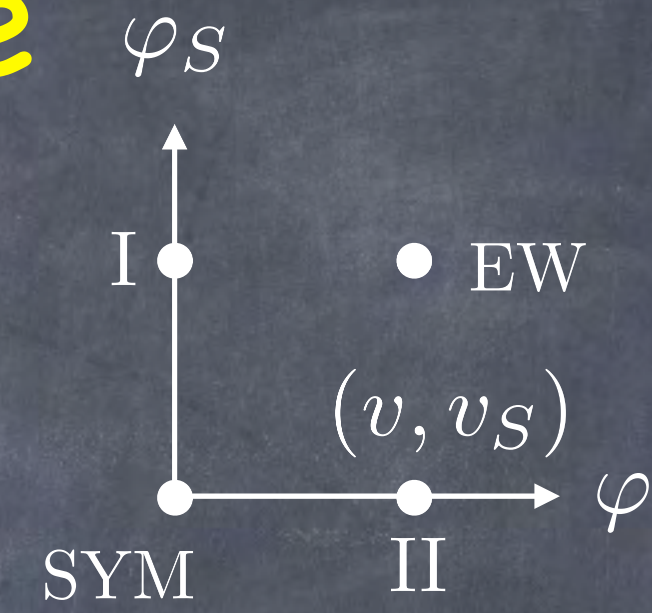

Global min. condition: $V^{(\mathrm{EW})}(v, v_S) < V(\varphi, \varphi_S)$

For example,

$$\Delta V_0 = V_0^{(\mathrm{I})}(0, \bar{v}_S) - V_0^{(\mathrm{EW})}(v, v_S)$$
$$= \frac{\lambda_H}{4} v^4 + \frac{\mu_{HS}}{4} v^2 v_S + \frac{\lambda_{HS}}{4} v^2 v_S^2 + \frac{\mu_S^3}{2}(\bar{v}_S - v_S) - \frac{\mu'_S}{6}(\bar{v}_S^3 - v_S^3) - \frac{\lambda_S}{4}(\bar{v}_S^4 - v_S^4).$$

ΔV_0 has to be positive.

$$\bar{v}_S = \frac{1}{2\lambda_S}\left[-\mu'_S \pm \sqrt{\mu'^2_S - 4\lambda_S m_S^2}\right]$$

However, $\Delta V_0 < 0$ would occur if $\bar{v}_S$ gets large. (small λ_S)

[NOTE]: Relatively large $\bar{v}_S$ is needed for "type-B EWPT" (see later)

Higgs couplings

Higgs-gauge bosons

$$\mathcal{L}_{\mathrm{HVV}} = \frac{1}{v}\left(\cos\alpha\ H_1 - \sin\alpha\ H_2\right)\left(2m_W^2 W_\mu^+ W^{-\mu} + m_Z^2 Z_\mu Z^\mu\right),$$

Higgs-fermions

$$\mathcal{L}_{\mathrm{Yukawa}} = -\sum_f \frac{m_f}{v}\left(\cos\alpha\ H_1 - \sin\alpha\ H_2\right)\bar{f}f.$$

Normalized couplings:

$$\boxed{\kappa_V = \frac{g_{H_1VV}}{g_{hVV}^{\mathrm{SM}}} = \cos\alpha, \qquad \kappa_F = \frac{g_{H_1ff}}{g_{hff}^{\mathrm{SM}}} = \cos\alpha.}$$

We collectively denote $\kappa \equiv \kappa_V = \kappa_F$

Higgs couplings

Higgs-gauge bosons

$$\mathcal{L}_{\rm HVV} = \frac{1}{v}\left(\boxed{\cos\alpha}\, H_1 - \sin\alpha\ H_2\right)\left(2m_W^2 W_\mu^+ W^{-\mu} + m_Z^2 Z_\mu Z^\mu\right),$$

Higgs-fermions

$$\mathcal{L}_{\rm Yukawa} = -\sum_f \frac{m_f}{v}\left(\boxed{\cos\alpha}\, H_1 - \sin\alpha\ H_2\right)\bar{f} f.$$

Normalized couplings:

$$\boxed{\kappa_V = \frac{g_{H_1VV}}{g_{hVV}^{\rm SM}} = \cos\alpha, \qquad \kappa_F = \frac{g_{H_1ff}}{g_{hff}^{\rm SM}} = \cos\alpha.}$$

We collectively denote $\kappa \equiv \kappa_V = \kappa_F$

Higgs couplings

Higgs-gauge bosons

$$\mathcal{L}_{\mathrm{HVV}} = \frac{1}{v}\left(\boxed{\cos\alpha}\, H_1 - \boxed{\sin\alpha}\, H_2\right)\left(2m_W^2 W_\mu^+ W^{-\mu} + m_Z^2 Z_\mu Z^\mu\right),$$

Higgs-fermions

$$\mathcal{L}_{\mathrm{Yukawa}} = -\sum_f \frac{m_f}{v}\left(\boxed{\cos\alpha}\, H_1 - \boxed{\sin\alpha}\, H_2\right)\bar{f} f.$$

Normalized couplings:

$$\boxed{\kappa_V = \frac{g_{H_1VV}}{g_{hVV}^{\mathrm{SM}}} = \cos\alpha, \qquad \kappa_F = \frac{g_{H_1ff}}{g_{hff}^{\mathrm{SM}}} = \cos\alpha.}$$

We collectively denote $\kappa \equiv \kappa_V = \kappa_F$

LHC constraints

Constraints from 125 GeV Higgs

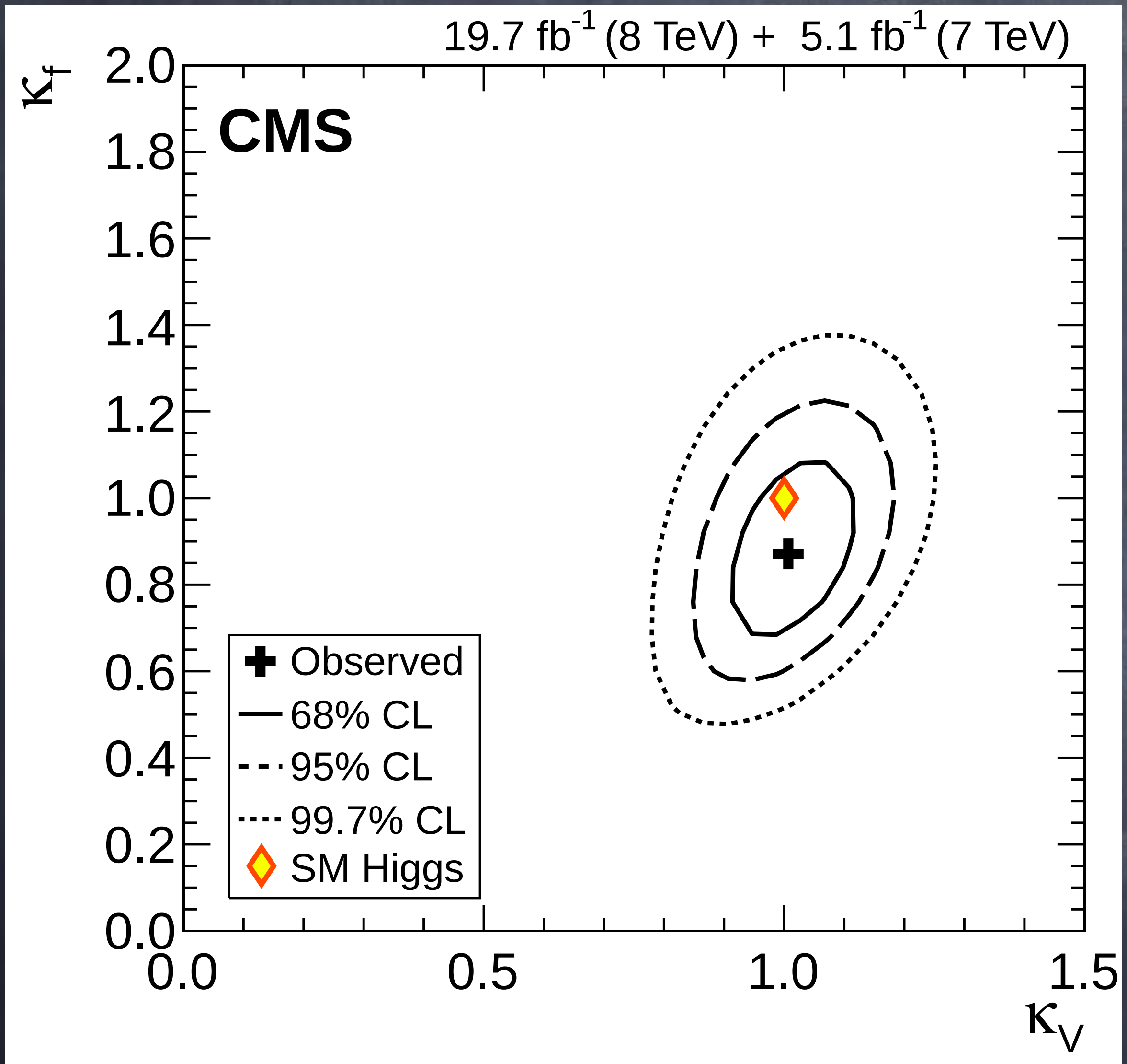

Direct search of 2nd Higgs

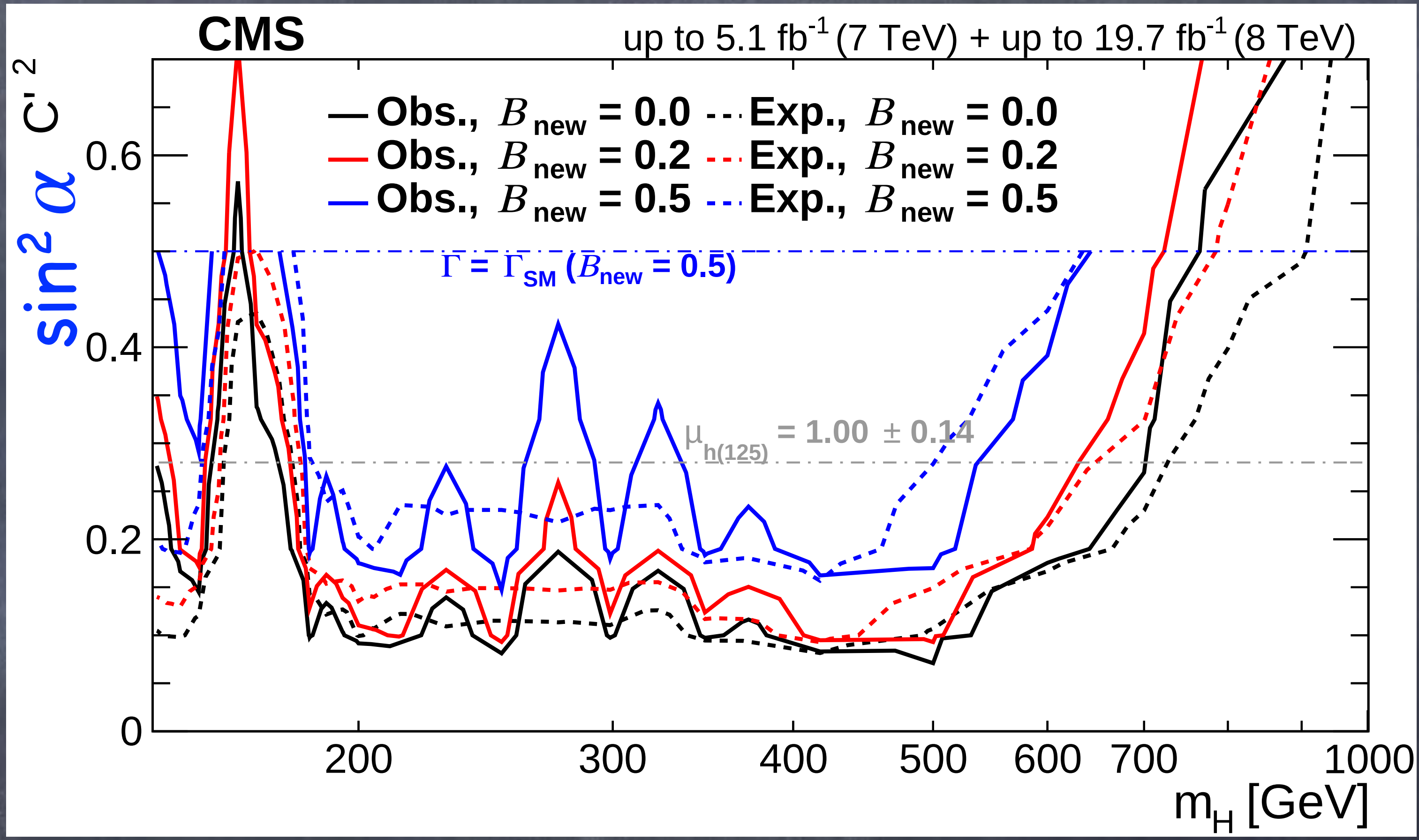

Signal strength of the 2nd Higgs

$$\mu' = C'^2(1 - \mathcal{B}_{\rm new})$$

- Direct/Indirect searches put some constraints on the 2nd Higgs mass and coupling.

LHC constraints

Constraints from 125 GeV Higgs

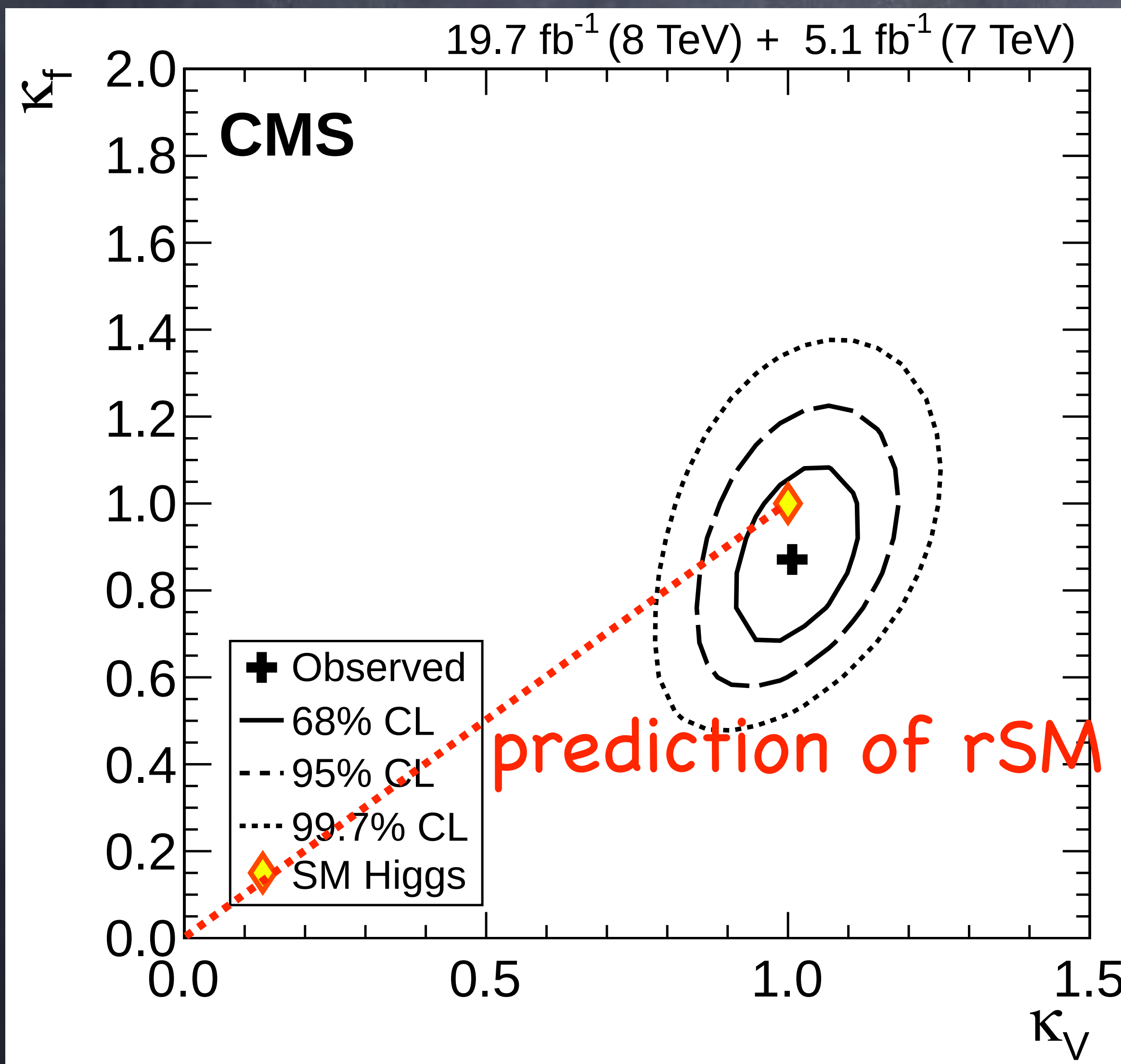

Direct search of 2nd Higgs

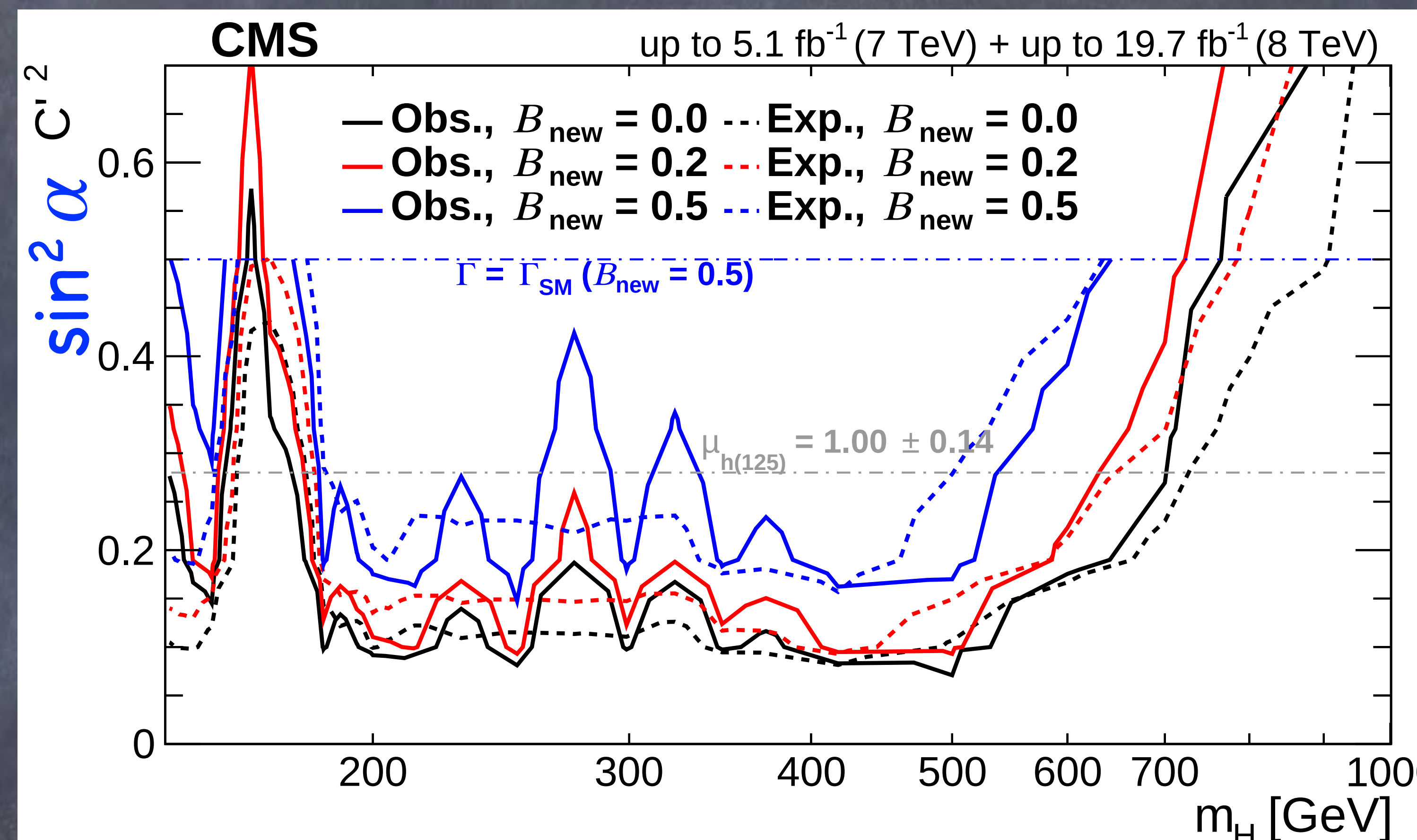

Signal strength of the 2nd Higgs

$$\mu' = C'^2(1 - \mathcal{B}_{\mathrm{new}})$$

- Direct/Indirect searches put some constraints on the 2nd Higgs mass and coupling.

Effective potential

To discuss EWPT, we use the effective potential.

$$V_{\rm eff}(\varphi_H,\varphi_S,T) = V_0(\varphi_H,\varphi_S) + V_1(\varphi_H,\varphi_S) + V_1(\varphi_H,\varphi_S,T) + V_{\rm daisy}(\varphi_H,\varphi_S,T).$$

where

$$V_1(\varphi_H,\varphi_S) = \sum_i n_i \frac{\bar{m}_i^4(\varphi_H,\varphi_S)}{64\pi^2}\left(\ln\frac{\bar{m}_i^2(\varphi_H,\varphi_S)}{\mu^2} - c_i\right),$$

$$V_1(\varphi_H,\varphi_S,T) = \sum_i n_i \frac{T^4}{2\pi^2} I_{B,F}\left(\frac{\bar{m}_i^2(\varphi_H,\varphi_S)}{T^2}\right),$$

with $I_{B,F}(a^2) = \int_0^\infty dx\, x^2 \ln\left(1 \mp e^{-\sqrt{x^2+a^2}}\right),$

$$V_{\rm daisy}(\varphi_H,\varphi_S,T) = -\sum_j n_j \frac{T}{12\pi}\left[\left\{\bar{M}_j^2(\varphi_H,\varphi_S,T)\right\}^{3/2} - \left\{\bar{m}_j^2(\varphi_H,\varphi_S)\right\}^{3/2}\right],$$

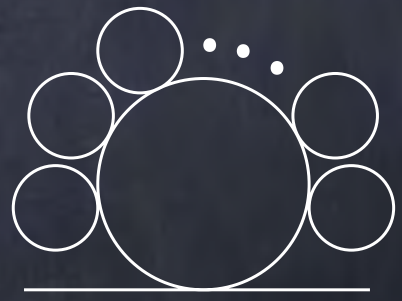

$$n_{H_1} = n_{H_2} = n_{G^0} = 1, \quad n_{G^\pm} = 2, \quad n_W = 2\cdot 3, \quad n_Z = 3, \quad n_t = n_b = -4N_c,$$

Patterns of EWPT

❒ Diverse patterns of the phase transitions.

[K.Funakubo, S. Tao, F. Toyoda., PTP114,369 (2005)]

A: SYM $\rightarrow$ I $\Rightarrow$ EW   B: SYM $\rightarrow$ I$'$ $\Rightarrow$ EW

C: SYM $\Rightarrow$ II $\rightarrow$ EW   D: SYM $\Rightarrow$ EW

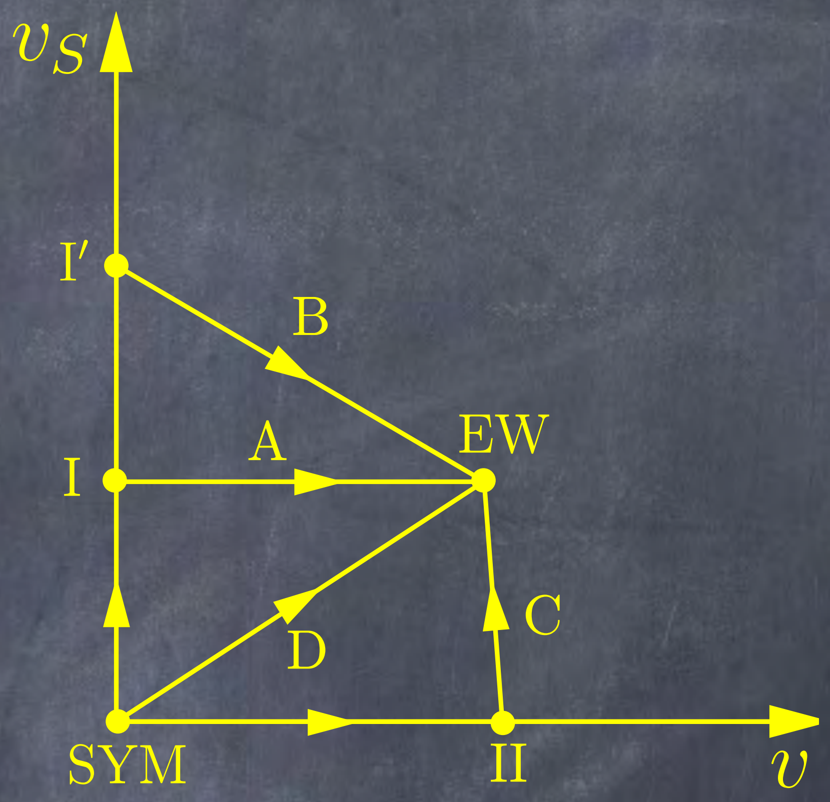

Type B

❒ Before EW symmetry breaking, singlet develops a VEV.

❒ Difference between type A and type B:

barrier exists in type B,   no barrier in type A

Type-B PT

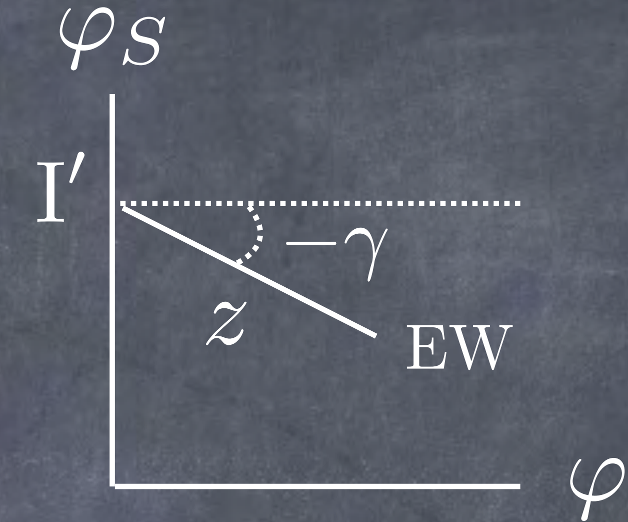

$$\varphi = z\cos\gamma, \quad \varphi_S = z\sin\gamma + \bar{v}_S$$

$$\mathrm{EW}:(v, v_S) \qquad \mathrm{I}':(0, \bar{v}_S)$$

$$\boxed{V(z,\gamma;T) = c_0 + c_1 z + c_2 z^2 - c_3 z^3 + c_4 z^4 \underset{T=T_C}{\longrightarrow} c_4 z^2 (z - z_C)^2.}$$

$$\frac{v_C}{T_C} = \frac{z_C}{T_C} c_\gamma = \frac{Ec_\gamma^4 - s_\gamma c_\gamma \left[(\mu_{HS} + \lambda_{HS}\bar{v}_S)c_\gamma^2/2 + (\mu_S'/3 + \lambda_S \bar{v}_S)s_\gamma^2\right]/T_C}{(\lambda_H c_\gamma^4 + \lambda_{HS} s_\gamma^2 c_\gamma^2 + \lambda_S s_\gamma^4)/2}$$

To get the strong 1st-order PT,

numerator ↗ and/or denominator ↘

- Size of $\bar{v}_S$ is constrained by the vacuum stability
- EWPT is reduced to the SM-like as $\gamma \to 0$ ($\bar{v}_S \to v_S$).

type B —> type A

Type-B PT

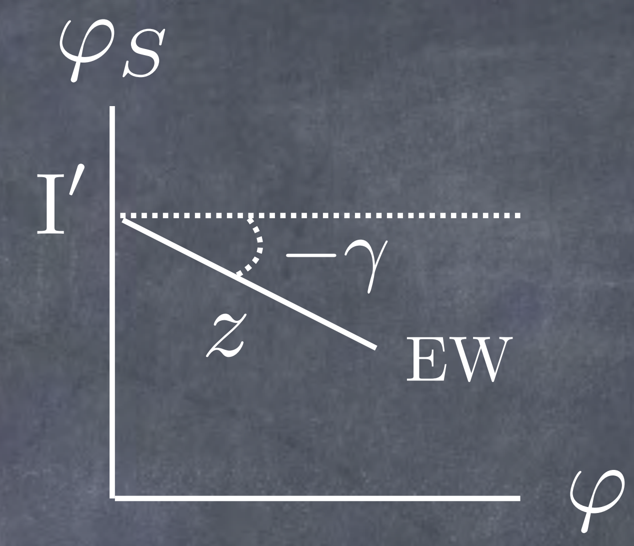

$$\varphi = z\cos\gamma, \quad \varphi_S = z\sin\gamma + \bar{v}_S$$

$$\mathrm{EW}: (v, v_S) \qquad \mathrm{I}': (0, \bar{v}_S)$$

$$\boxed{V(z,\gamma;T) = \cancel{c_0} + c_1 z + c_2 z^2 - c_3 z^3 + c_4 z^4 \underset{T=T_C}{\longrightarrow} c_4 z^2 (z - z_C)^2.}$$

$$\frac{v_C}{T_C} = \frac{z_C}{T_C}c_\gamma = \frac{Ec_\gamma^4 - s_\gamma c_\gamma \left[(\mu_{HS} + \lambda_{HS}\bar{v}_S)c_\gamma^2/2 + (\mu_S'/3 + \lambda_S \bar{v}_S)s_\gamma^2\right]/T_C}{(\lambda_H c_\gamma^4 + \lambda_{HS}s_\gamma^2 c_\gamma^2 + \lambda_S s_\gamma^4)/2}$$

To get the strong 1st-order PT,

numerator ↗ and/or denominator ↘

- Size of $\bar{v}_S$ is constrained by the vacuum stability
- EWPT is reduced to the SM-like as $\gamma \to 0$ $(\bar{v}_S \to v_S)$.

type B —> type A

Type-B PT

$$\varphi = z\cos\gamma, \quad \varphi_S = z\sin\gamma + \bar{v}_S$$

$$\mathrm{EW}: (v, v_S) \qquad \mathrm{I}': (0, \bar{v}_S)$$

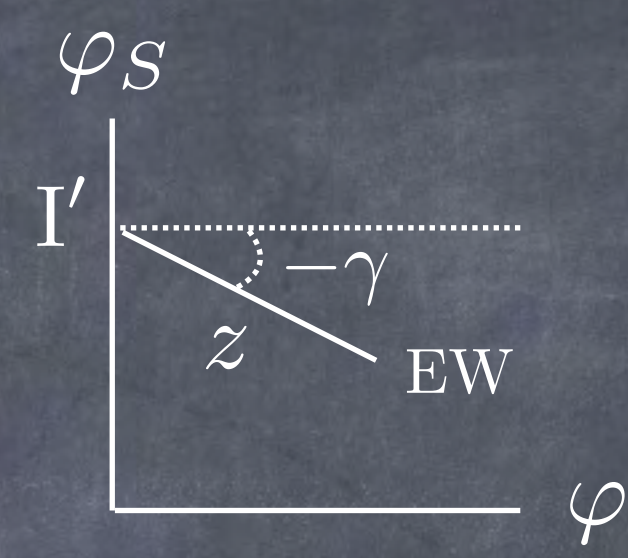

$$\boxed{V(z,\gamma;T) = \cancel{c_0} + \cancel{c_1} z + c_2 z^2 - c_3 z^3 + c_4 z^4 \underset{T=T_C}{\longrightarrow} c_4 z^2 (z - z_C)^2.}$$

$$\frac{v_C}{T_C} = \frac{z_C}{T_C} c_\gamma = \frac{E c_\gamma^4 - s_\gamma c_\gamma \Big[(\mu_{HS} + \lambda_{HS}\bar{v}_S) c_\gamma^2/2 + (\mu_S'/3 + \lambda_S \bar{v}_S) s_\gamma^2\Big]/T_C}{(\lambda_H c_\gamma^4 + \lambda_{HS} s_\gamma^2 c_\gamma^2 + \lambda_S s_\gamma^4)/2}$$

To get the strong 1st-order PT,

numerator $\nearrow$ and/or denominator $\searrow$

- Size of $\bar{v}_S$ is constrained by the vacuum stability
- EWPT is reduced to the SM-like as $\gamma \to 0$ $(\bar{v}_S \to v_S)$.

type B —> type A

Type-B PT

$$\varphi = z\cos\gamma, \quad \varphi_S = z\sin\gamma + \bar{v}_S$$

$$\mathrm{EW}: (v, v_S) \qquad \mathrm{I}': (0, \bar{v}_S)$$

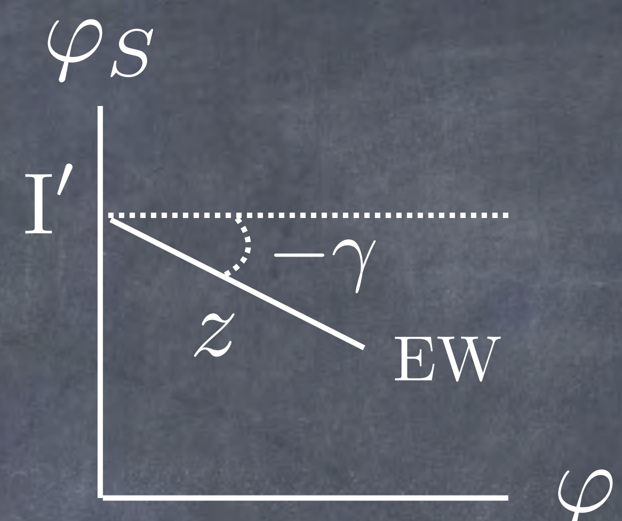

$$\boxed{V(z,\gamma;T) = \cancel{c_0} + \cancel{c_1} z + c_2 z^2 - c_3 z^3 + c_4 z^4 \underset{T=T_C}{\longrightarrow} c_4 z^2 (z - z_C)^2.}$$

thermal loop origin

$$\frac{v_C}{T_C} = \frac{z_C}{T_C} c_\gamma = \frac{\boxed{Ec_\gamma^4} - s_\gamma c_\gamma \left[(\mu_{HS} + \lambda_{HS}\bar{v}_S)c_\gamma^2/2 + (\mu_S'/3 + \lambda_S \bar{v}_S)s_\gamma^2\right]/T_C}{(\lambda_H c_\gamma^4 + \lambda_{HS} s_\gamma^2 c_\gamma^2 + \lambda_S s_\gamma^4)/2}$$

To get the strong 1st-order PT,

numerator ↗ and/or denominator ↘

- ❐ Size of $\bar{v}_S$ is constrained by the vacuum stability
- ❐ EWPT is reduced to the SM-like as $\gamma \to 0$ $(\bar{v}_S \to v_S)$.

type B —> type A

Type-B PT

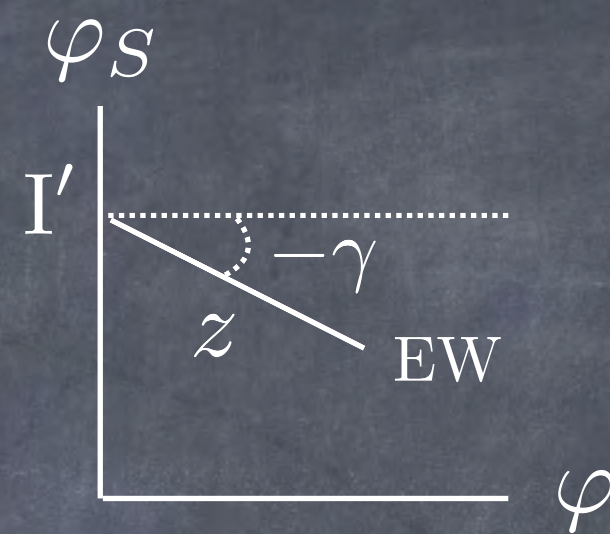

$$\varphi = z\cos\gamma, \quad \varphi_S = z\sin\gamma + \bar{v}_S$$

$$\mathrm{EW}: (v, v_S) \qquad \mathrm{I}': (0, \bar{v}_S)$$

$$\boxed{V(z,\gamma;T) = \cancel{c_0} + \cancel{c_1}z + c_2 z^2 - c_3 z^3 + c_4 z^4 \underset{T=T_C}{\longrightarrow} c_4 z^2 (z - z_C)^2.}$$

thermal loop origin tree origin

$$\frac{v_C}{T_C} = \frac{z_C}{T_C}c_\gamma = \frac{\boxed{Ec_\gamma^4}\boxed{-s_\gamma c_\gamma\left[(\mu_{HS} + \lambda_{HS}\bar{v}_S)c_\gamma^2/2 + (\mu_S'/3 + \lambda_S\bar{v}_S)s_\gamma^2\right]/T_C}}{(\lambda_H c_\gamma^4 + \lambda_{HS}s_\gamma^2 c_\gamma^2 + \lambda_S s_\gamma^4)/2}$$

To get the strong 1st-order PT,

numerator ↗ and/or denominator ↘

- ❒ Size of $\bar{v}_S$ is constrained by the vacuum stability
- ❒ EWPT is reduced to the SM-like as $\gamma \to 0$ $(\bar{v}_S \to v_S)$.

type B —> type A

Strong 1st order PT

$$m_{H_2} = 170 \text{ GeV}, \; v_S = 90 \text{ GeV}, \; \mu'_S = -30 \text{ GeV}, \; \mu_{HS} = -80 \text{ GeV}.$$

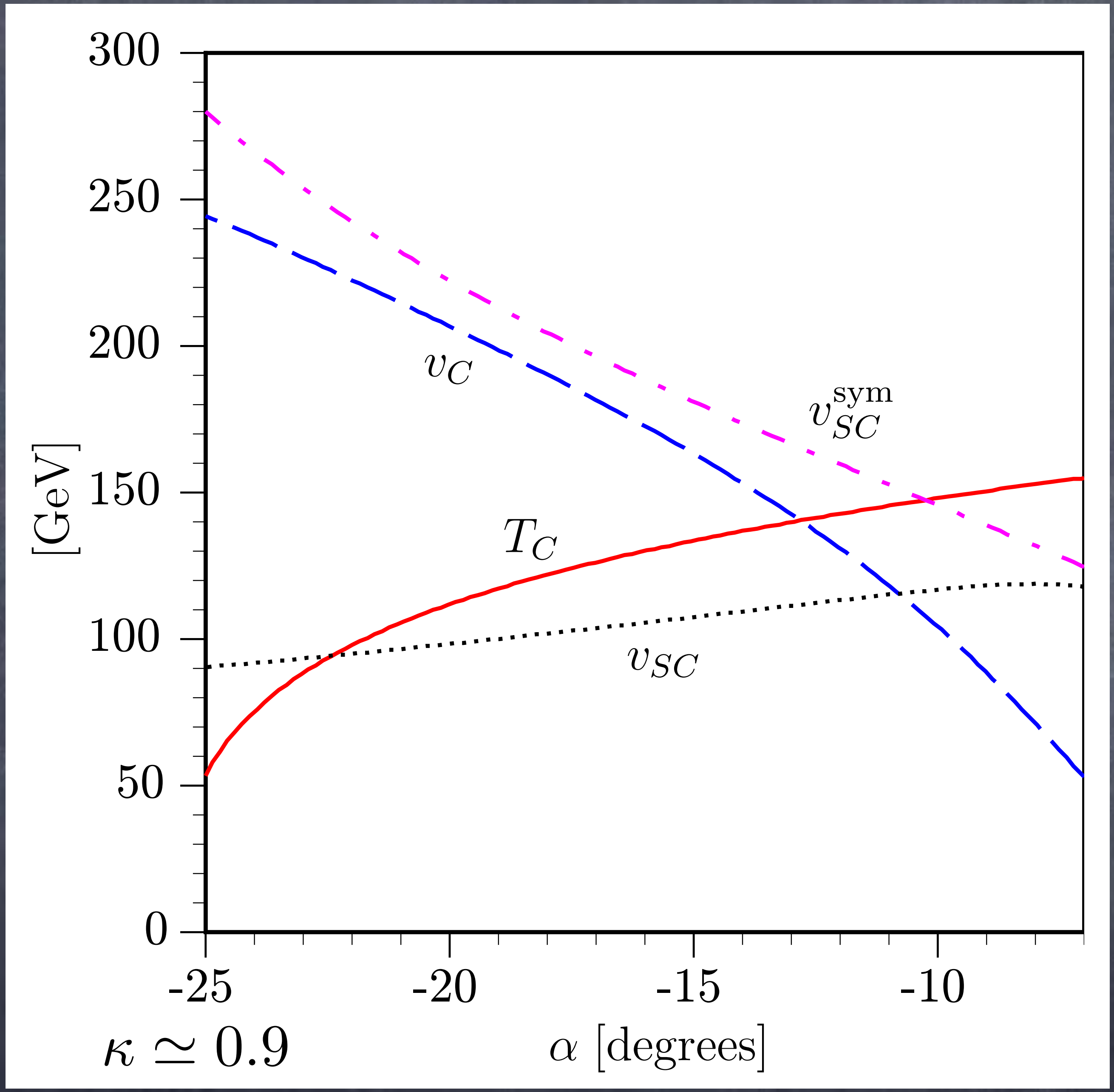

- ❒ α is mixing angle between H and S.
- ❒ larger α gives strong 1st-order PT. ($v_C/T_C > 1$ for $|\alpha| > 13$ deg.)

Strong 1st order PT

$$m_{H_2} = 170 \text{ GeV},\ v_S = 90 \text{ GeV},\ \mu'_S = -30 \text{ GeV},\ \mu_{HS} = -80 \text{ GeV}.$$

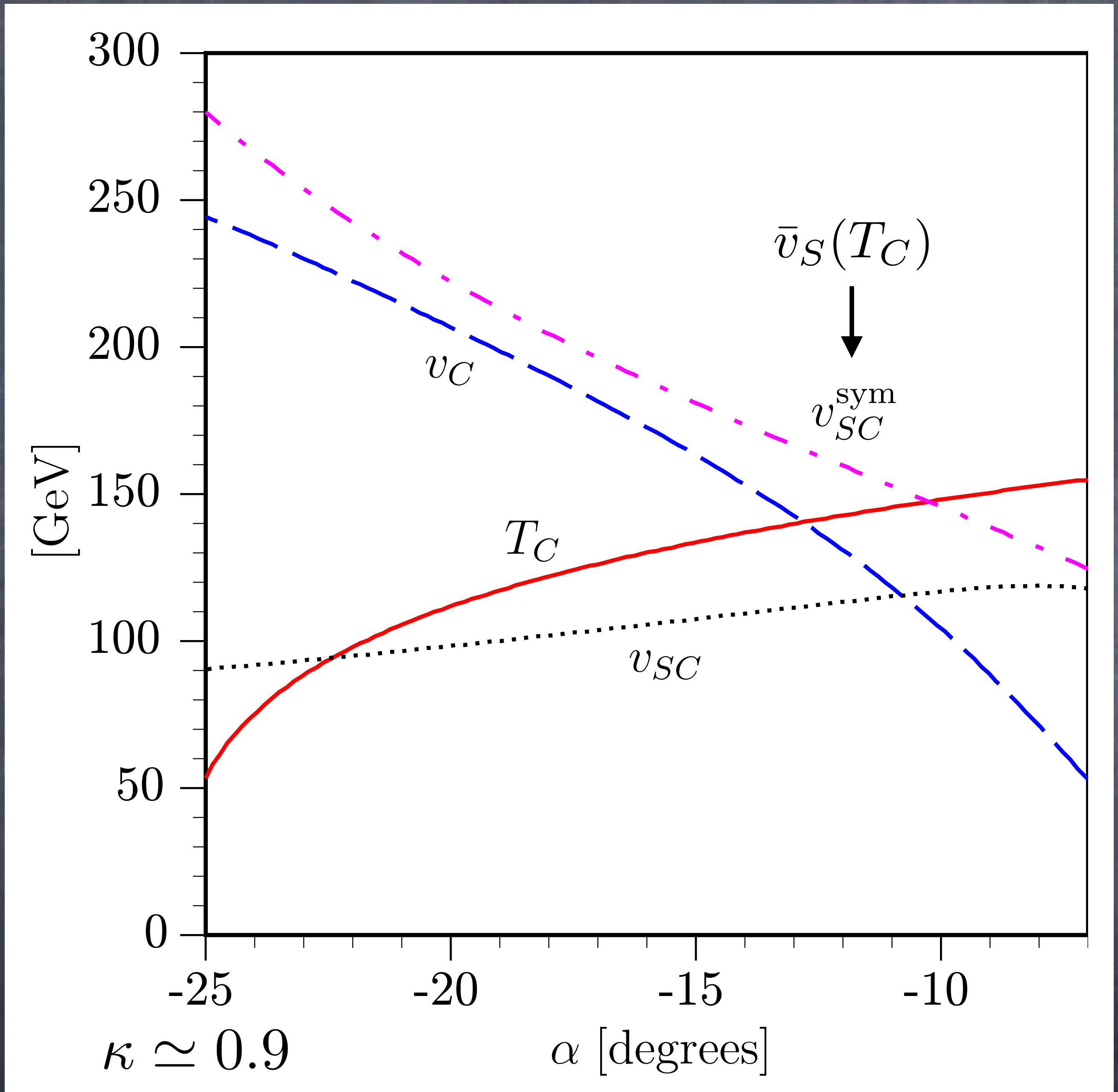

- α is mixing angle between H and S.
- larger α gives strong 1st-order PT. ($v_C/T_C > 1$ for $|\alpha| > 13$ deg.)

Strong 1st order PT

$m_{H_2} = 170$ GeV, $v_S = 90$ GeV, $\mu'_S = -30$ GeV, $\mu_{HS} = -80$ GeV.

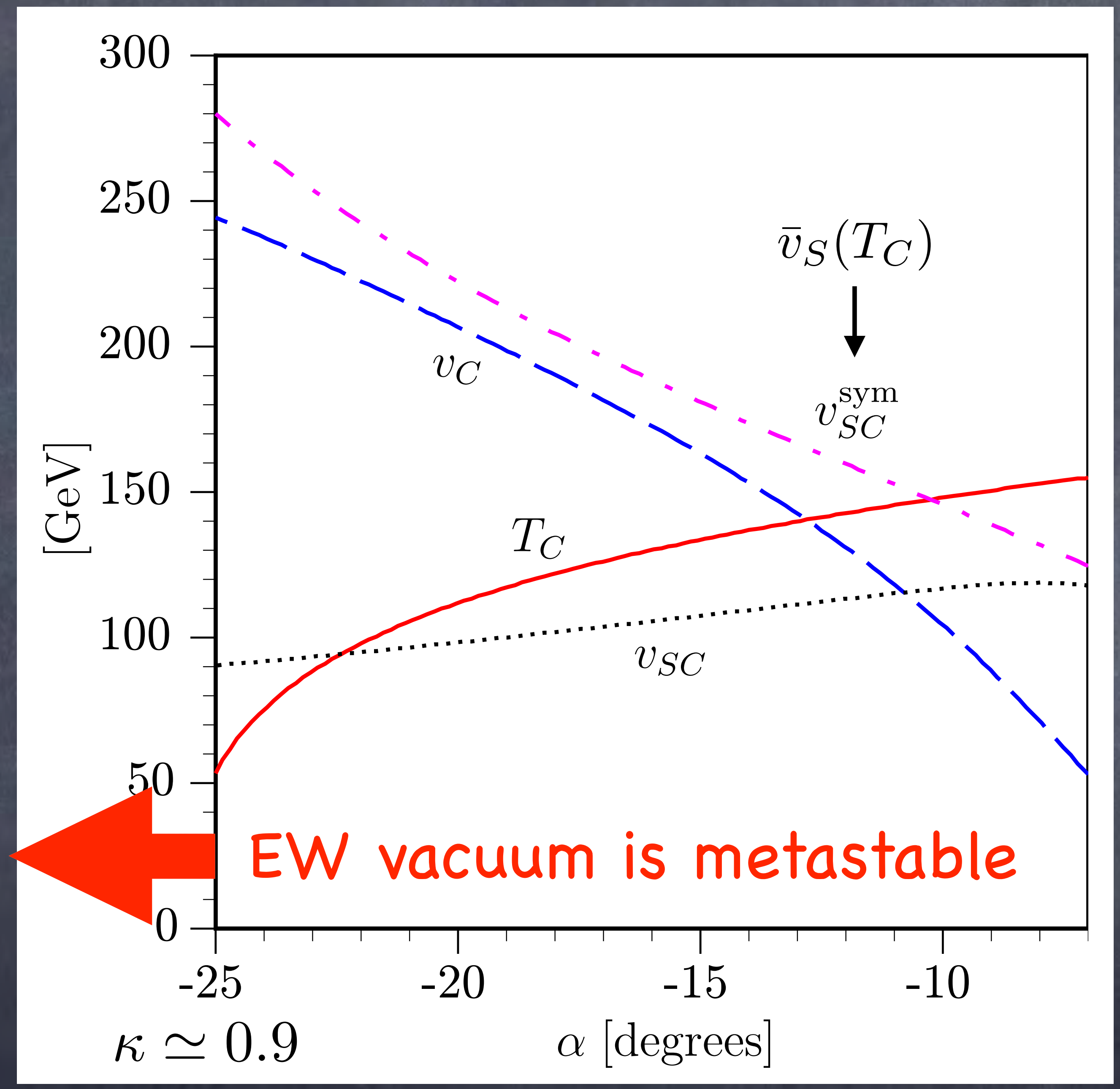

- ❒ α is mixing angle between H and S.
- ❒ larger α gives strong 1st-order PT. ($v_C/T_C > 1$ for $|\alpha| > 13$ deg.)

Sphaleron decoupling condition

After the EWPT, the sphaleron process has to be decoupled.

$$\boxed{\Gamma_B^{(b)}(T) \simeq (\text{prefactor})e^{-E_{\text{sph}}/T} < H(T) \simeq 1.66\sqrt{g_*}T^2/m_{\text{P}}}$$

g_* massless dof, 106.75 (SM) m_{P} Planck mass ≃ 1.22x10[19] GeV

$E_{\text{sph}} = 4\pi v\mathcal{E}/g_2$ (g_2: SU(2) gauge coupling),

$$\boxed{\frac{v(T)}{T} > \frac{g_2}{4\pi\mathcal{E}(T)}\left[42.97 + \ln\mathcal{N} - 2\ln\left(\frac{T}{100\ \text{GeV}}\right) + \cdots\right] \equiv \zeta_{\text{sph}}(T),}$$

- Sphaleron energy gives the dominant effect.

- We evaluate E(Tc), ζ(Tc).

Sphaleron decoupling condition

After the EWPT, the sphaleron process has to be decoupled.

$$\boxed{\Gamma_B^{(b)}(T) \simeq (\text{prefactor})e^{-E_{\rm sph}/T} < H(T) \simeq 1.66\sqrt{g_*}T^2/m_{\rm P}}$$

g_* massless dof, 106.75 (SM) $m_{\rm P}$ Planck mass ≃ 1.22x10[19] GeV

$E_{\rm sph} = 4\pi v\mathcal{E}/g_2$ (g_2: SU(2) gauge coupling),

$$\boxed{\frac{v(T)}{T} > \frac{g_2}{4\pi\mathcal{E}(T)}\left[42.97 + \ln\cancel{\mathcal{N}} - 2\ln\left(\frac{T}{100\ \text{GeV}}\right) + \cdots\right] \equiv \zeta_{\rm sph}(T),}$$

- Sphaleron energy gives the dominant effect.
- We evaluate E(Tc), ζ (Tc).

Sphaleron decoupling condition

$$m_{H_2} = 170 \text{ GeV},\ v_S = 90 \text{ GeV},\ \mu'_S = -30 \text{ GeV},\ \mu_{HS} = -80 \text{ GeV}.$$

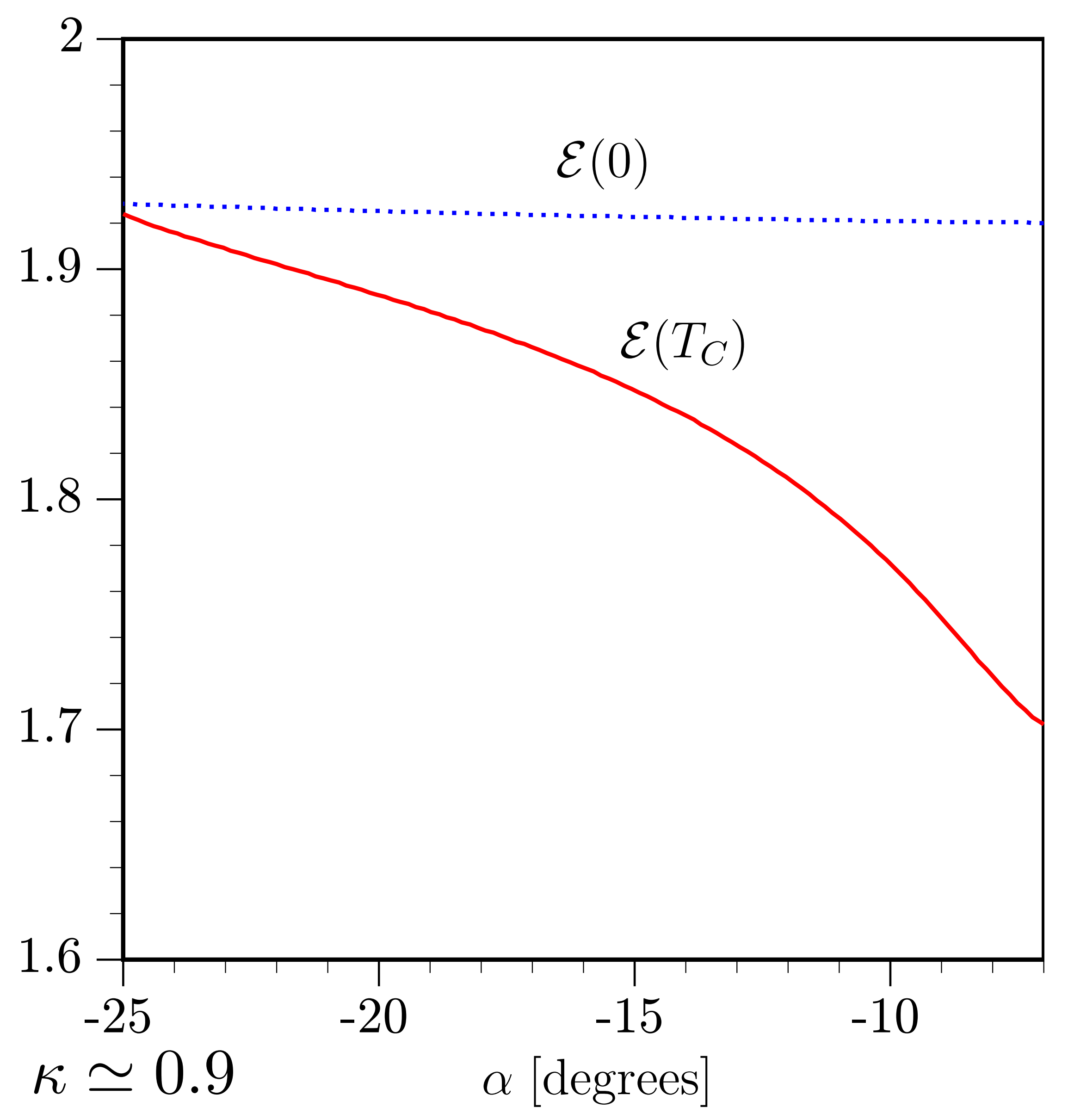

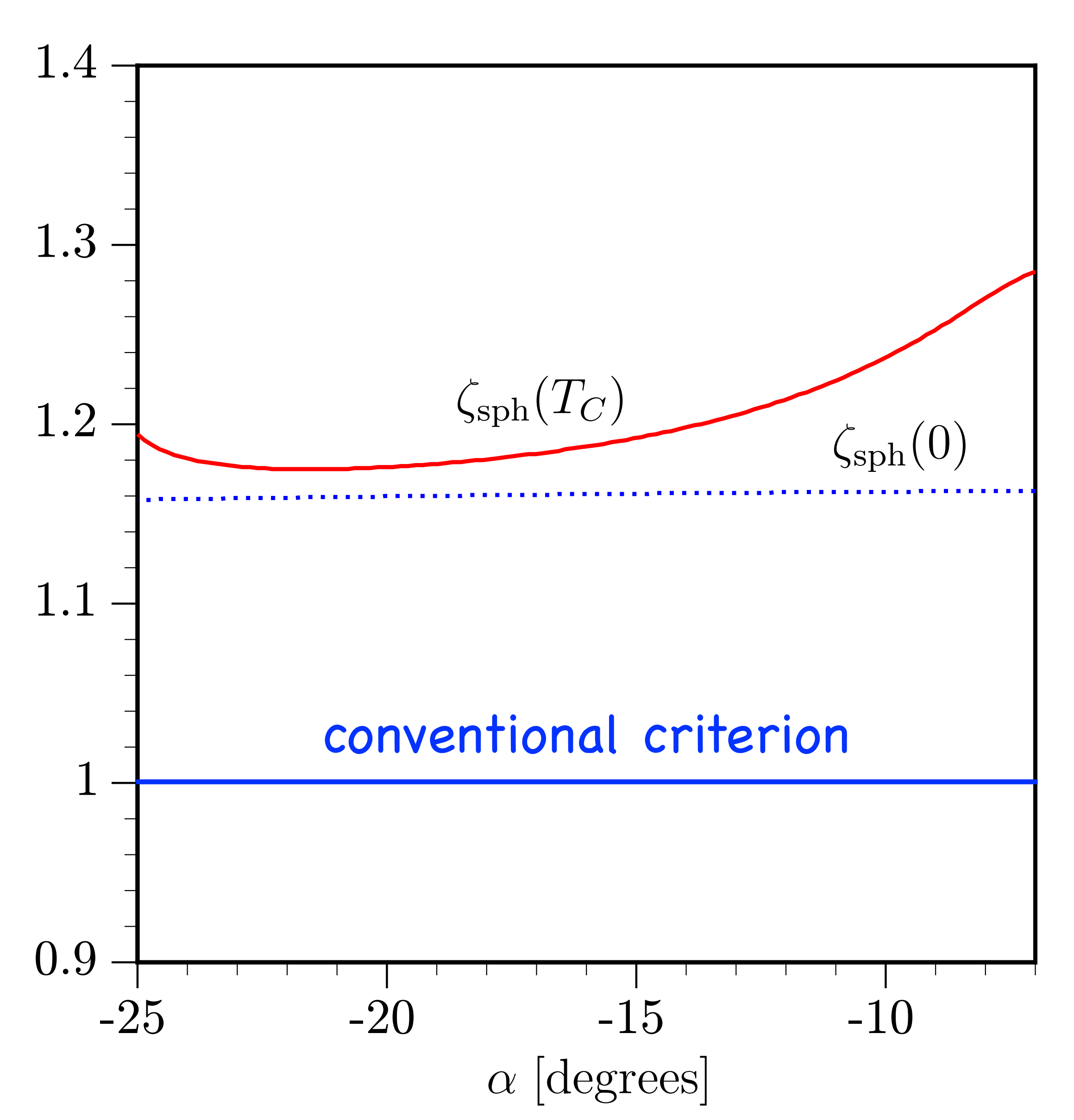

Sphaleron decoupling condition

$$m_{H_2} = 170 \text{ GeV}, \; v_S = 90 \text{ GeV}, \; \mu'_S = -30 \text{ GeV}, \; \mu_{HS} = -80 \text{ GeV}.$$

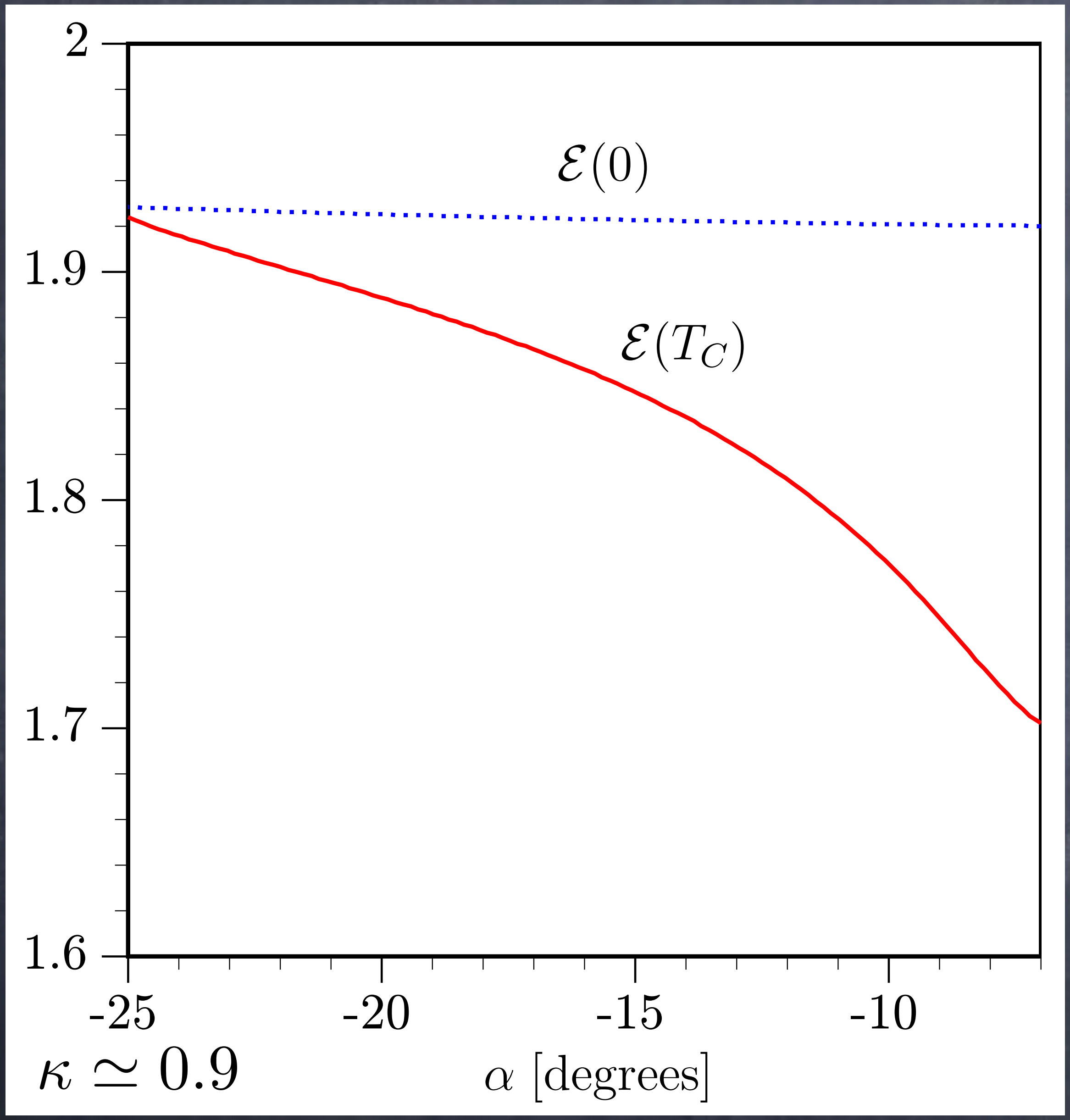

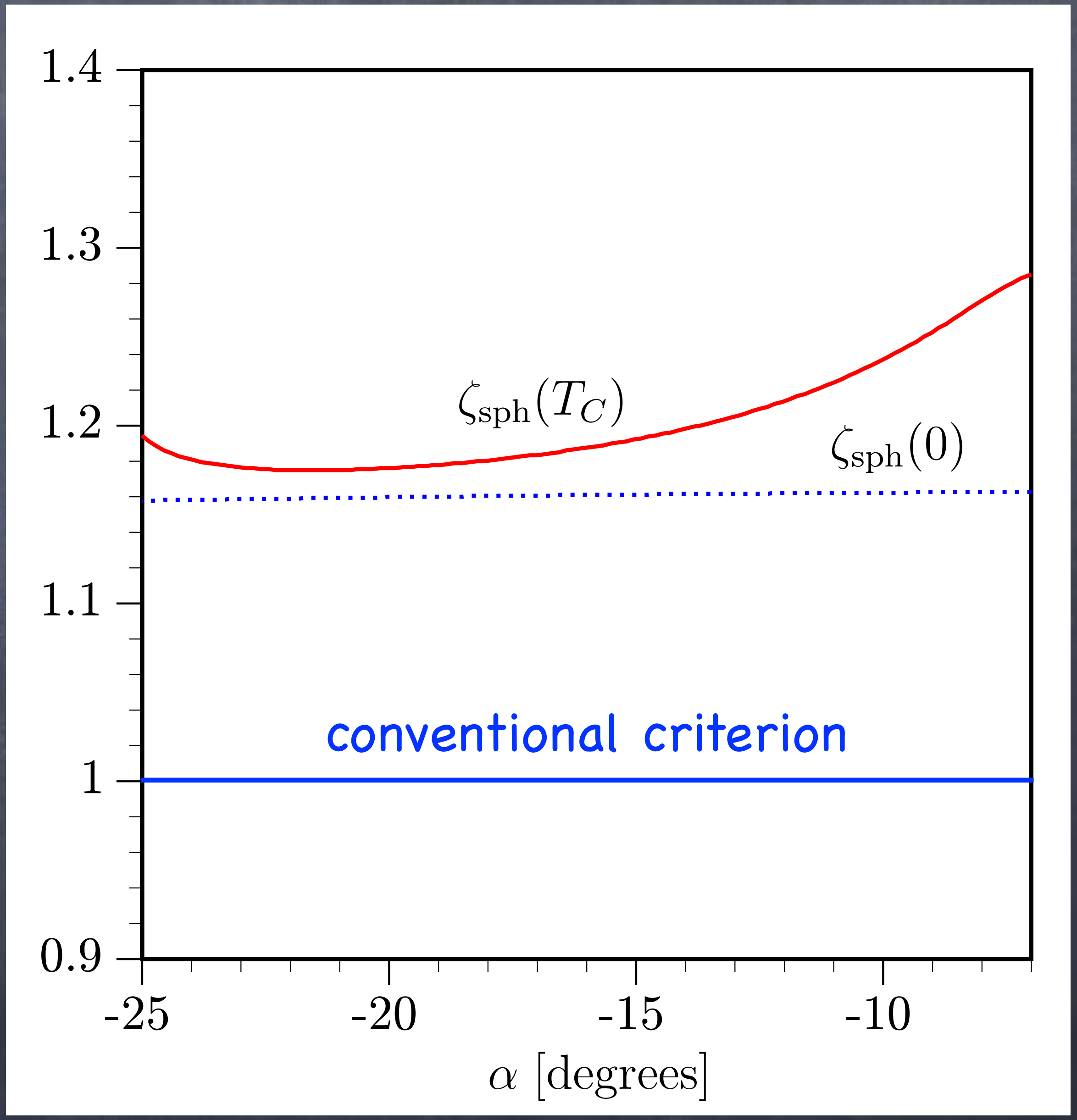

- ζ (T_C)= (1.2–1.3)

Sphaleron decoupling condition

$$m_{H_2} = 170 \text{ GeV}, \; v_S = 90 \text{ GeV}, \; \mu'_S = -30 \text{ GeV}, \; \mu_{HS} = -80 \text{ GeV}.$$

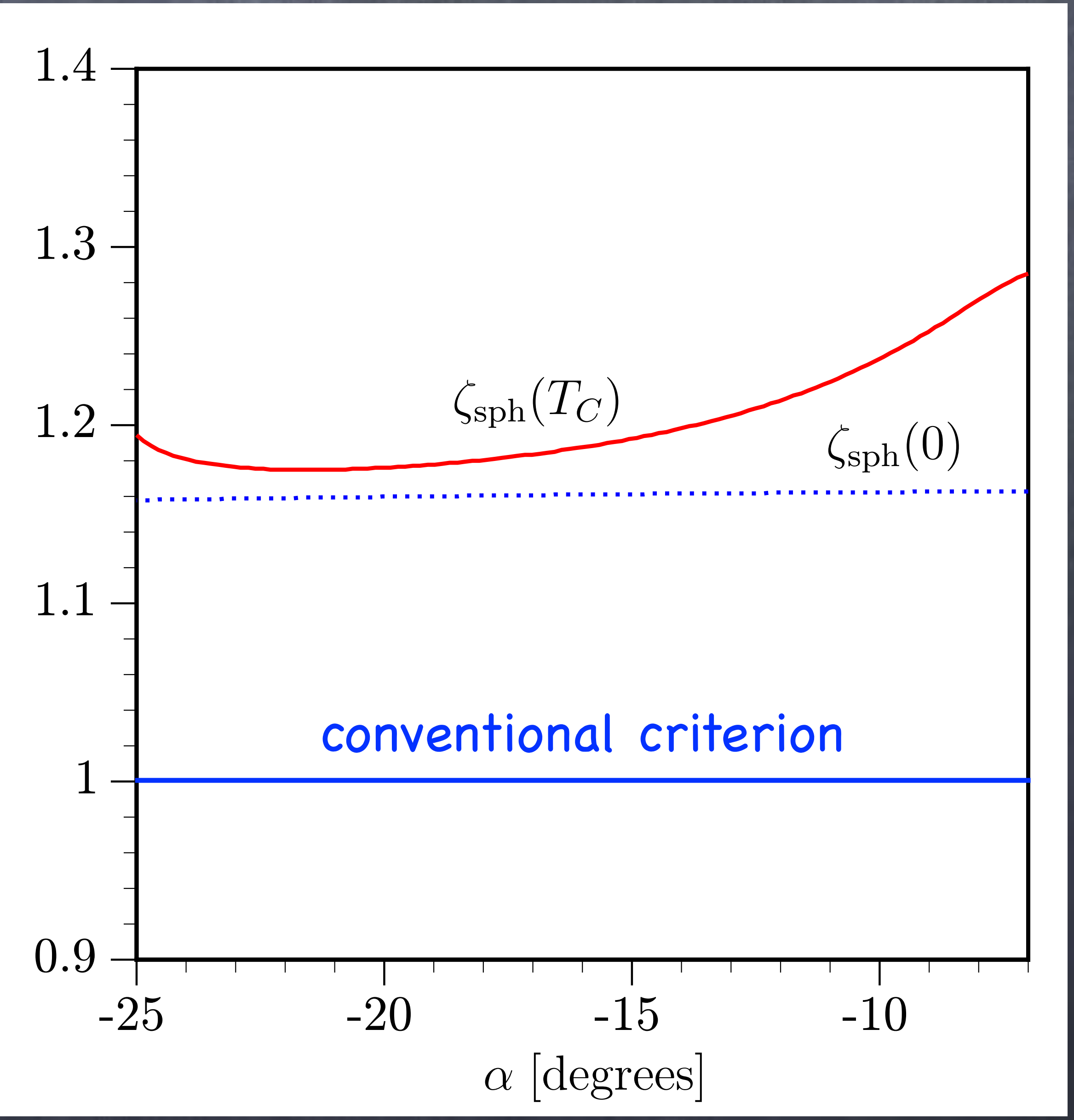

- $\zeta\,(T_C)$= (1.2–1.3)

Sphaleron decoupling condition

$$m_{H_2} = 170 \text{ GeV},\ v_S = 90 \text{ GeV},\ \mu'_S = -30 \text{ GeV},\ \mu_{HS} = -80 \text{ GeV}.$$

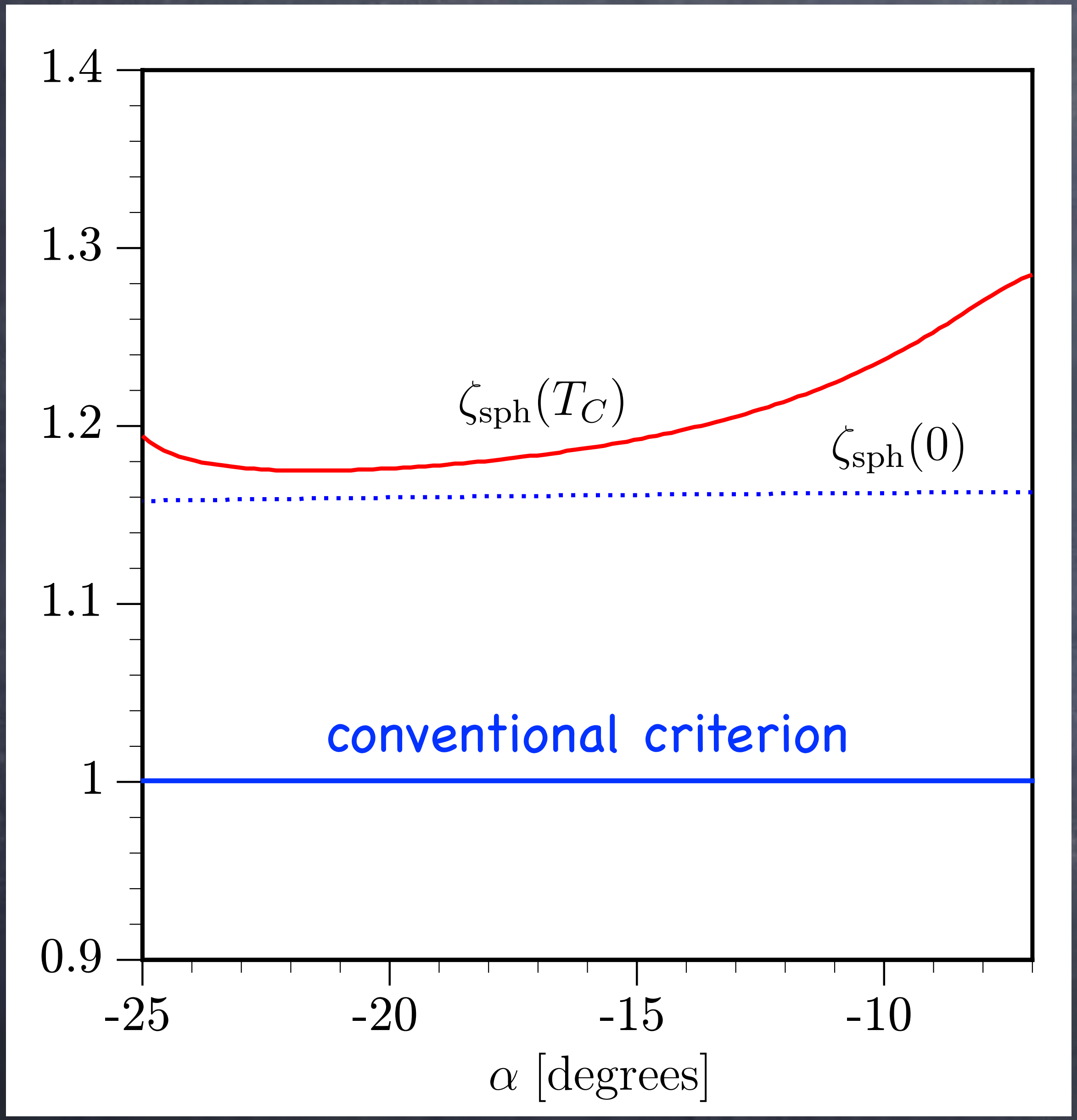

- ζ (T_C)= (1.2–1.3)

Sphaleron decoupling condition

$$m_{H_2} = 170 \text{ GeV},\ v_S = 90 \text{ GeV},\ \mu'_S = -30 \text{ GeV},\ \mu_{HS} = -80 \text{ GeV}.$$

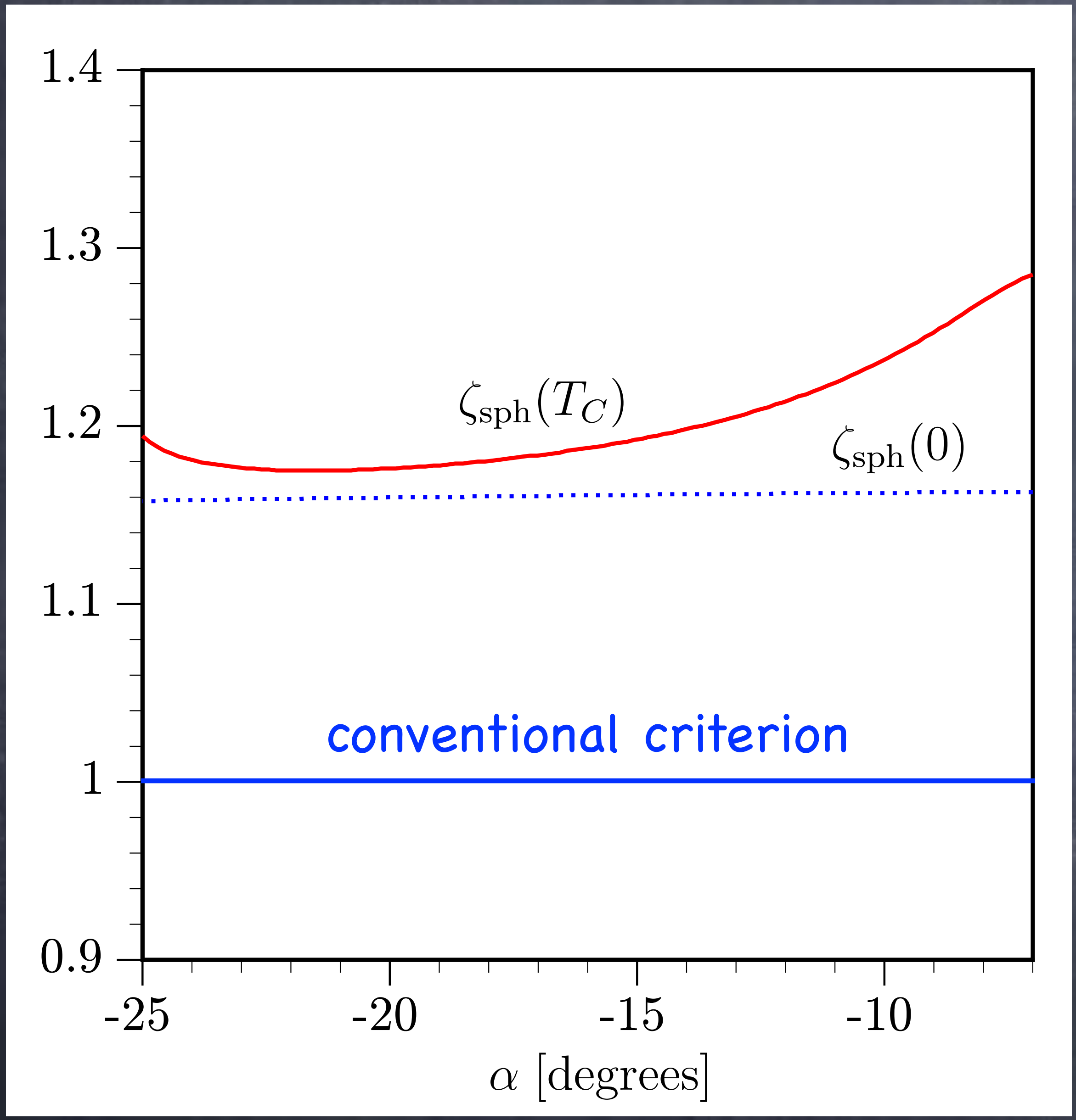

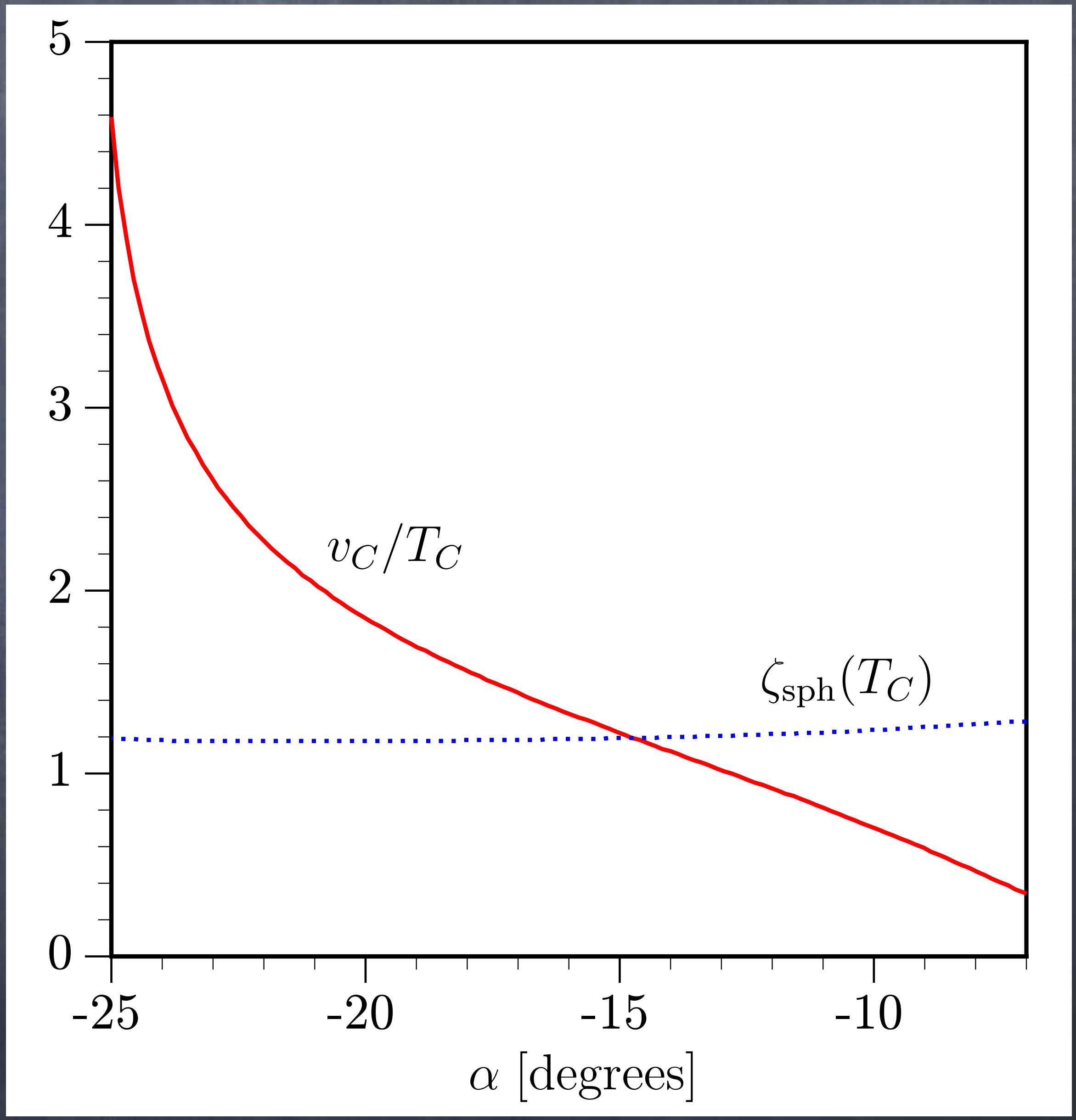

- $\zeta\,(T_C)$= (1.2–1.3)

Sphaleron decoupling condition

$$m_{H_2} = 170 \text{ GeV}, \; v_S = 90 \text{ GeV}, \; \mu'_S = -30 \text{ GeV}, \; \mu_{HS} = -80 \text{ GeV}.$$

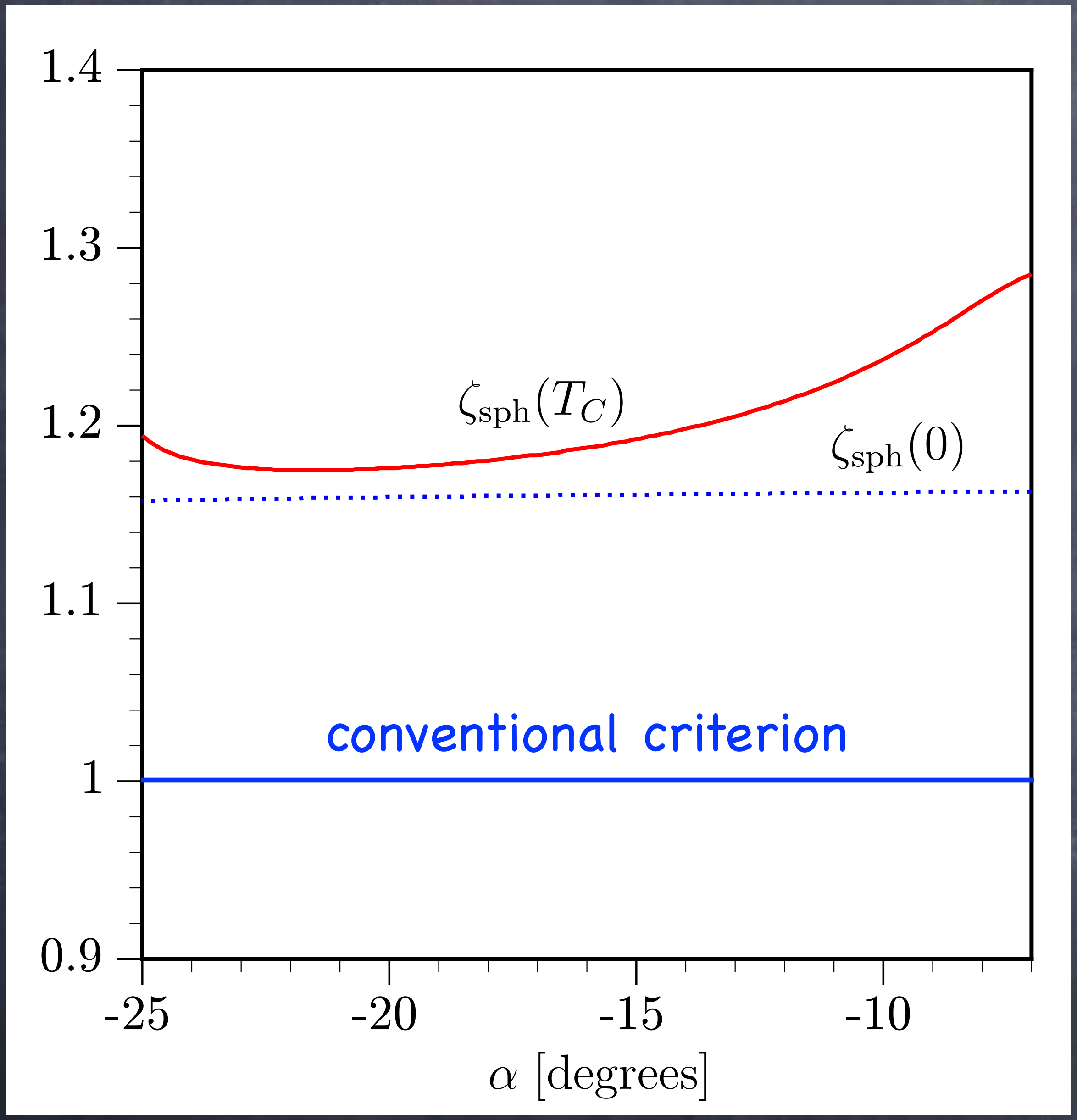

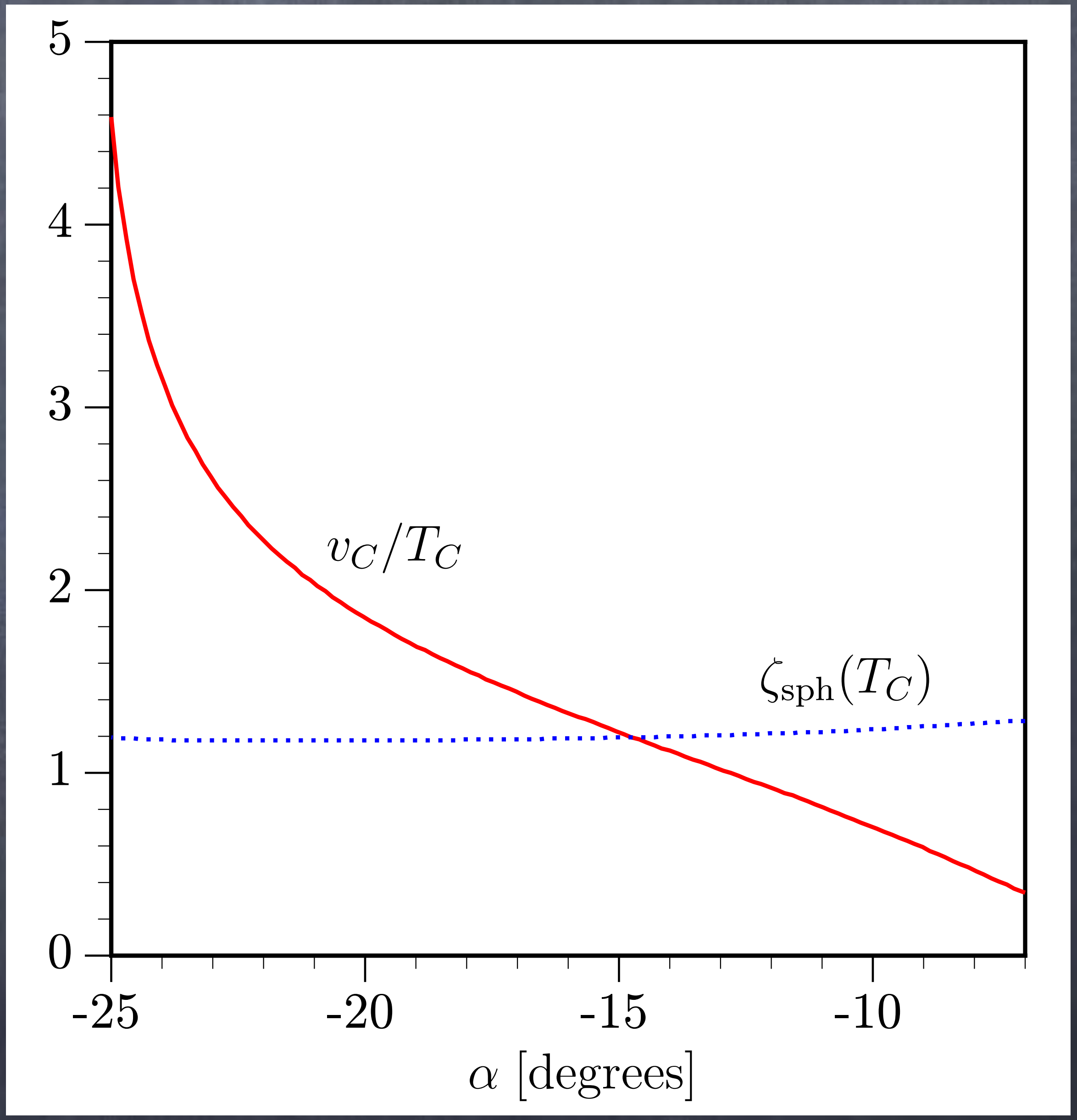

- $\zeta(T_C)$= (1.2-1.3)
- $v_C/T_C > \zeta(T_C)$ is satisfied for $|\alpha| > 15$ deg.

hhh coupling

- We may see a remnant of 1st-order EWPT by measuring Higgs self-coupling.

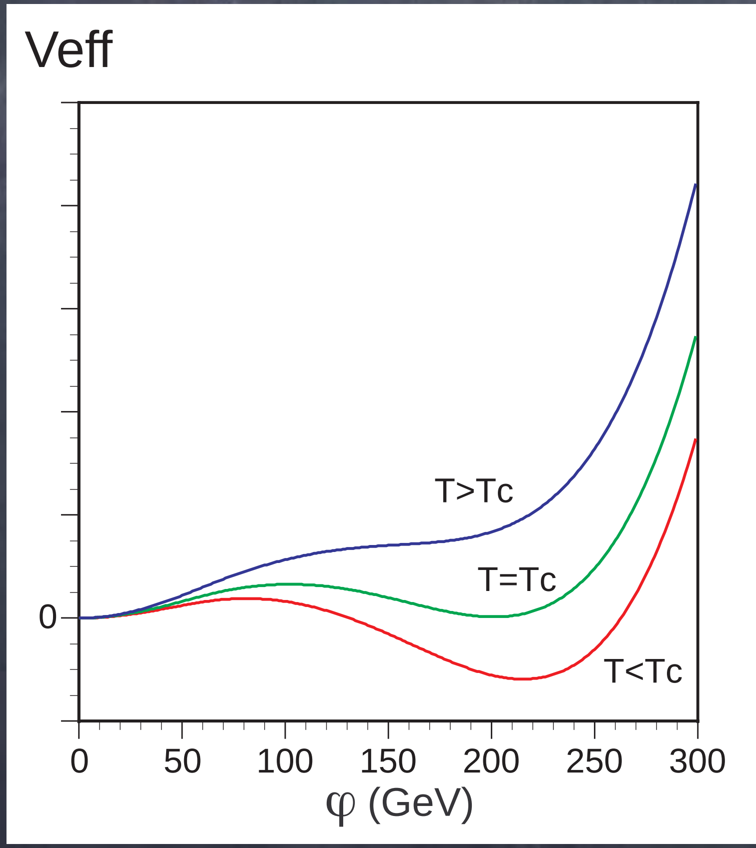

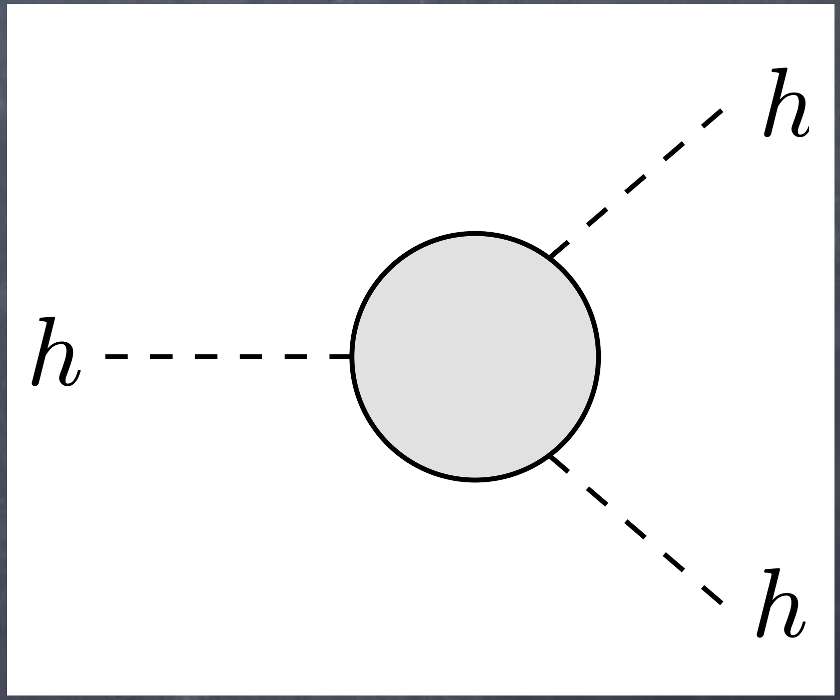

$v_c/T_c \nearrow$ -> Δhhh $\nearrow$

e.g., 2HDM [Kanemura, Okada, E.S., PLB606,(2005)361]

$\zeta(T_c)$ determines the minimum deviation of Δhhh.

hhh coupling

❒ hhh coupling in the SM.

$$\lambda^{\rm SM}_{H_1H_1H_1} = \frac{3m^2_{H_1}}{v}\left[1+\frac{9m^2_{H_1}}{32\pi^2 v^2}+\sum_{i=W,Z,t,b} n_i \frac{m_i^4}{12\pi^2 m^2_{H_1} v^2}\right]$$

The dominant one-loop correction comes from top loop

❒ hhh coupling in the rSM.

$$\lambda^{\rm rSM}_{H_1H_1H_1} = \lambda^{\rm rSM,tree}_{H_1H_1H_1} + \lambda^{\rm rSM,loop}_{H_1H_1H_1},$$

$$\lambda^{\rm rSM,tree}_{H_1H_1H_1} = 6\left[\lambda_H v c_\alpha^3 + \frac{\mu_{HS}}{2} s_\alpha c_\alpha^2 + \frac{\lambda_{HS}}{2} s_\alpha c_\alpha (v s_\alpha + v_S c_\alpha) + \left(\frac{\mu'_S}{3} + \lambda_S v_S\right) s_\alpha^3\right],$$

$$\lambda^{\rm rSM,loop}_{H_1H_1H_1} = c_\alpha^3 \left\langle \frac{\partial^3 V_1}{\partial \varphi_H^3}\right\rangle + c_\alpha^2 s_\alpha \left\langle \frac{\partial^3 V_1}{\partial \varphi_H^2 \partial \varphi_S}\right\rangle + c_\alpha s_\alpha^2 \left\langle \frac{\partial^3 V_1}{\partial \varphi_H \partial \varphi_S^2}\right\rangle + s_\alpha^3 \left\langle \frac{\partial^3 V_1}{\partial \varphi_S^3}\right\rangle,$$

Larger α gives the larger deviation from the SM value.

(To have strong 1st order PT, (λ_{HS}, μ_{HS}) have to be large.)

$\Delta\lambda_{H_1H_1H_1}$ contours in (m_{H_2}, κ) plane

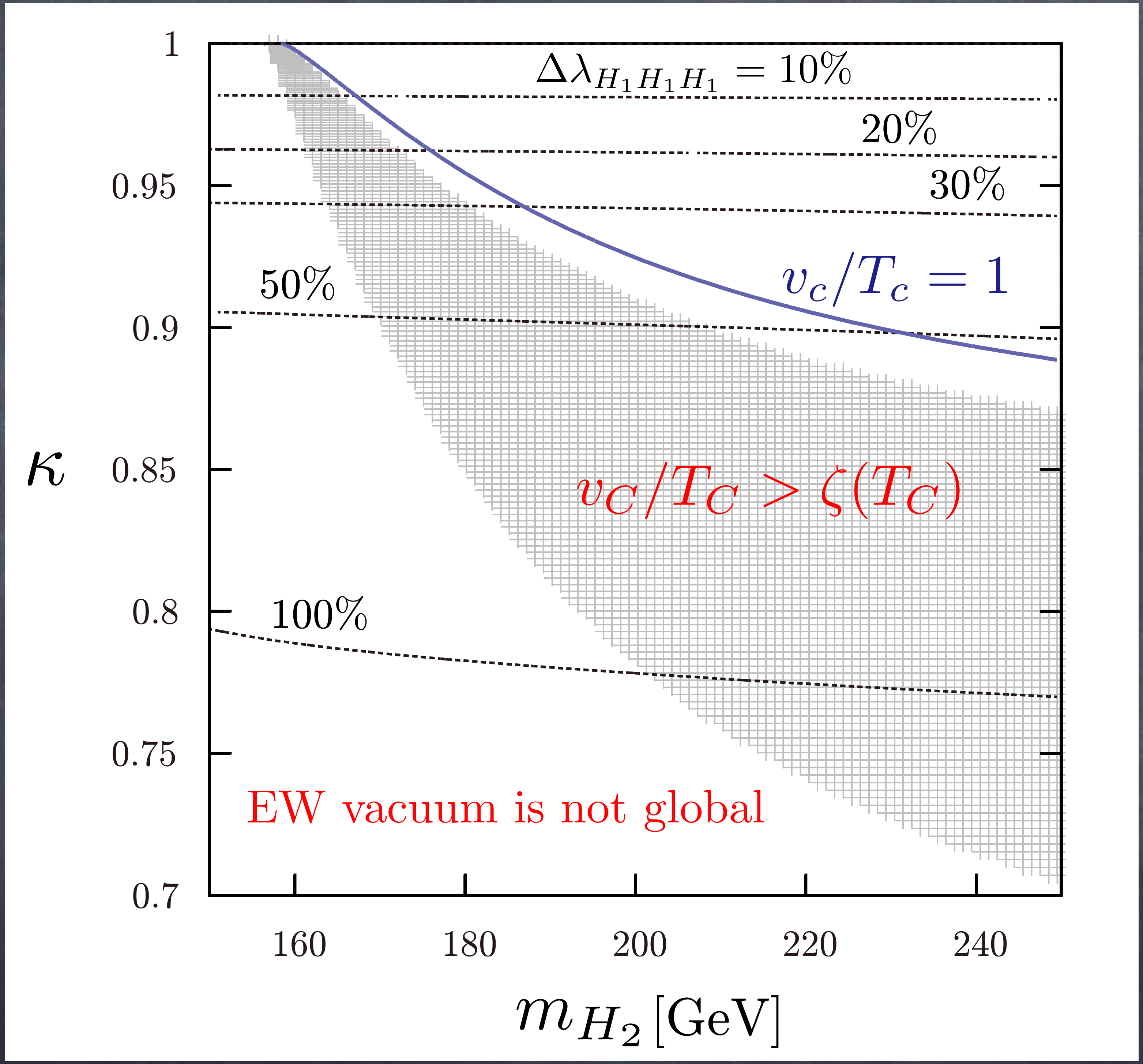

- $\Delta\lambda_{H_1H_1H_1} \simeq 16\%$ for $\kappa \simeq 0.97$ and 160 GeV $\lesssim m_{H_2} \lesssim$ 169 GeV,
- $\Delta\lambda_{H_1H_1H_1} \simeq 27\%$ for $\kappa \simeq 0.95$, and 163 GeV $\lesssim m_{H_2} \lesssim$ 176 GeV.

$\Delta\lambda_{H_1H_1H_1}$ contours in (m_{H_2}, κ) plane

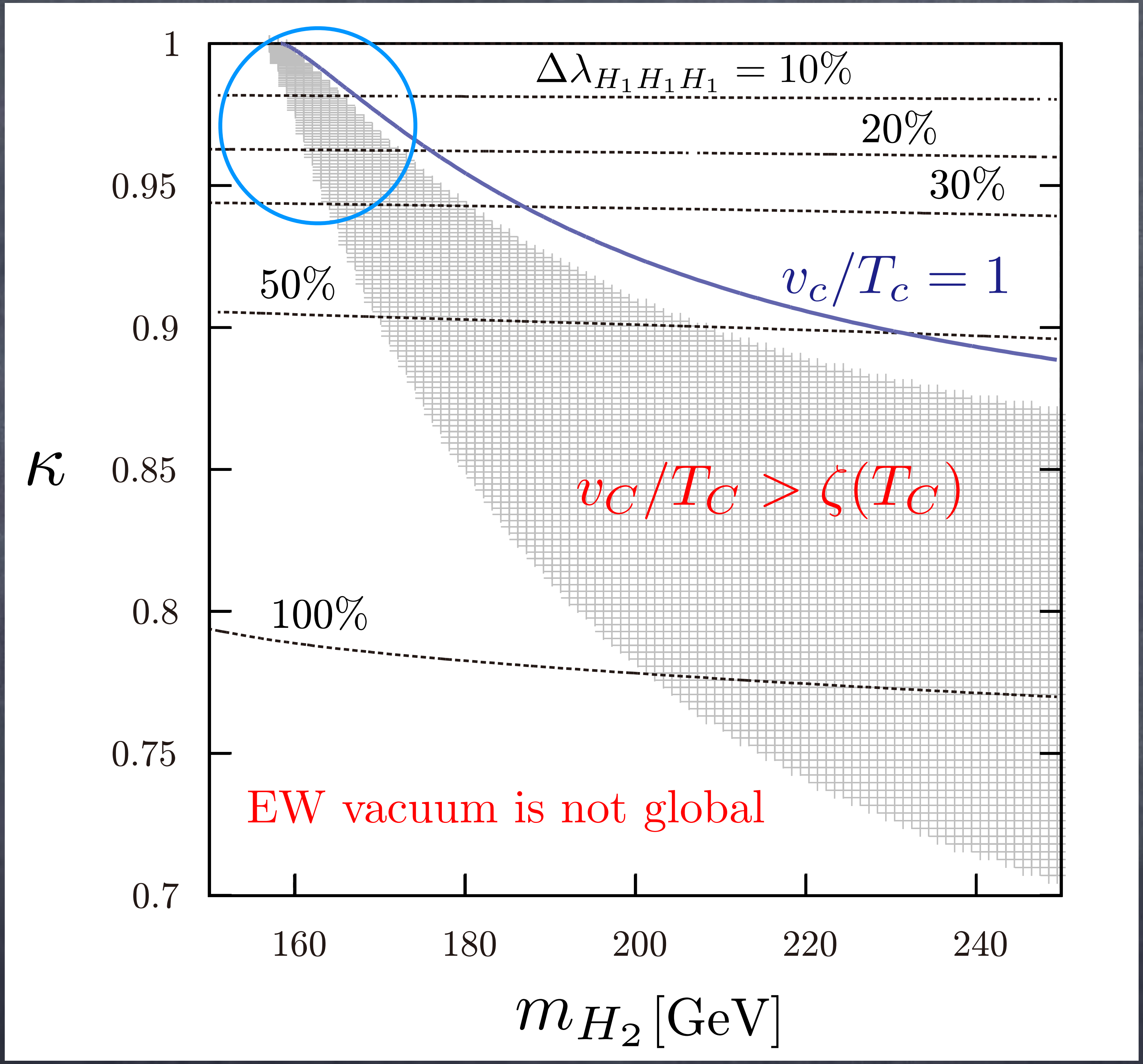

- $\Delta\lambda_{H_1H_1H_1} \simeq 16\%$ for $\kappa \simeq 0.97$ and 160 GeV $\lesssim m_{H_2} \lesssim$ 169 GeV,
- $\Delta\lambda_{H_1H_1H_1} \simeq 27\%$ for $\kappa \simeq 0.95$, and 163 GeV $\lesssim m_{H_2} \lesssim$ 176 GeV.

$\Delta\lambda_{H_1H_1H_1}$ contours in (m_{H_2}, κ) plane

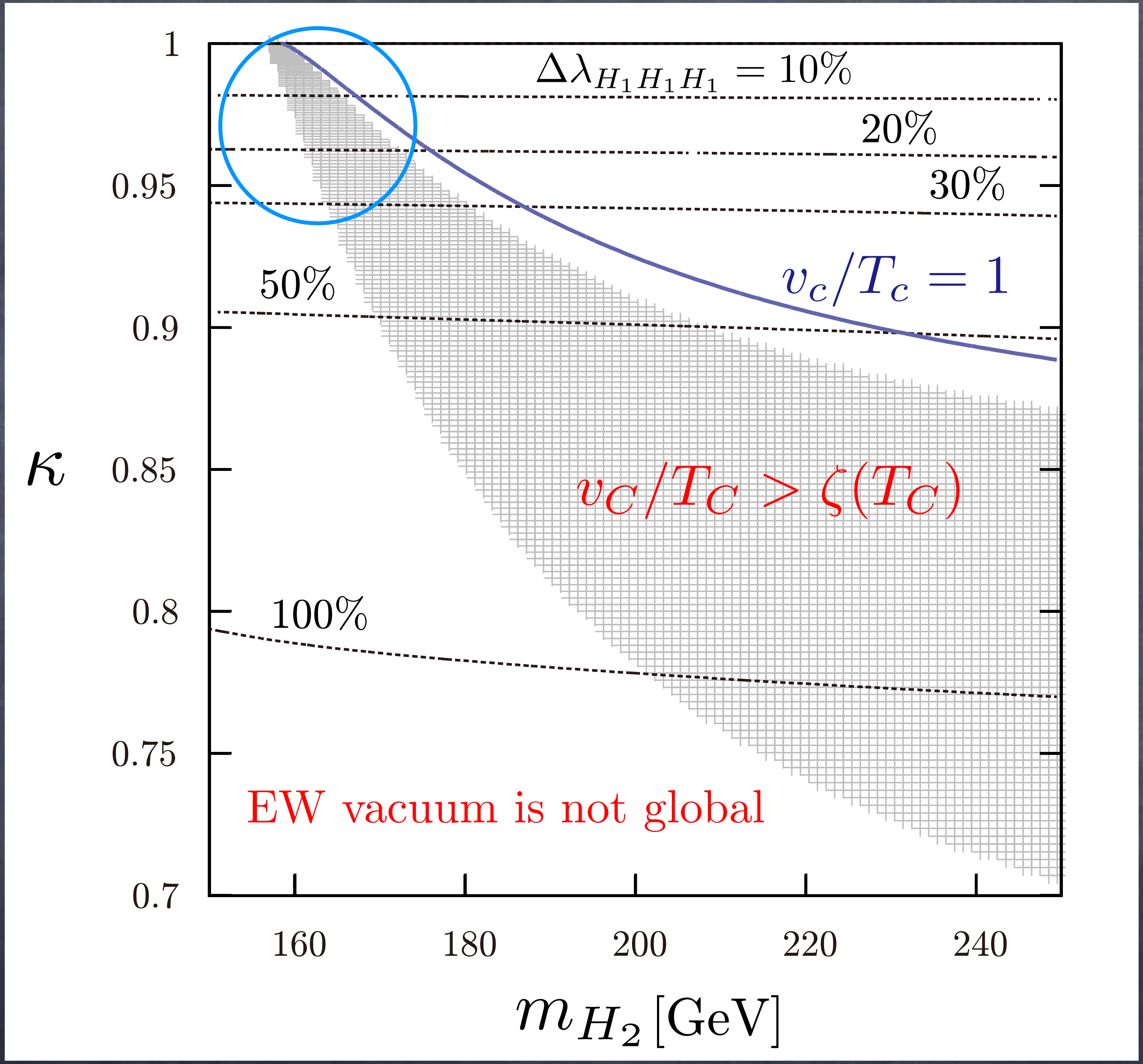

If $\dfrac{v_C}{T_C} > 1$

- $\Delta\lambda_{H_1H_1H_1} \simeq 16\%$ for $\kappa \simeq 0.97$ and $160\ \mathrm{GeV} \lesssim m_{H_2} \lesssim 169\ \mathrm{GeV}$,
- $\Delta\lambda_{H_1H_1H_1} \simeq 27\%$ for $\kappa \simeq 0.95$, and $163\ \mathrm{GeV} \lesssim m_{H_2} \lesssim 176\ \mathrm{GeV}$.

$\Delta\lambda_{H_1 H_1 H_1}$ contours in (m_{H_2}, κ) plane

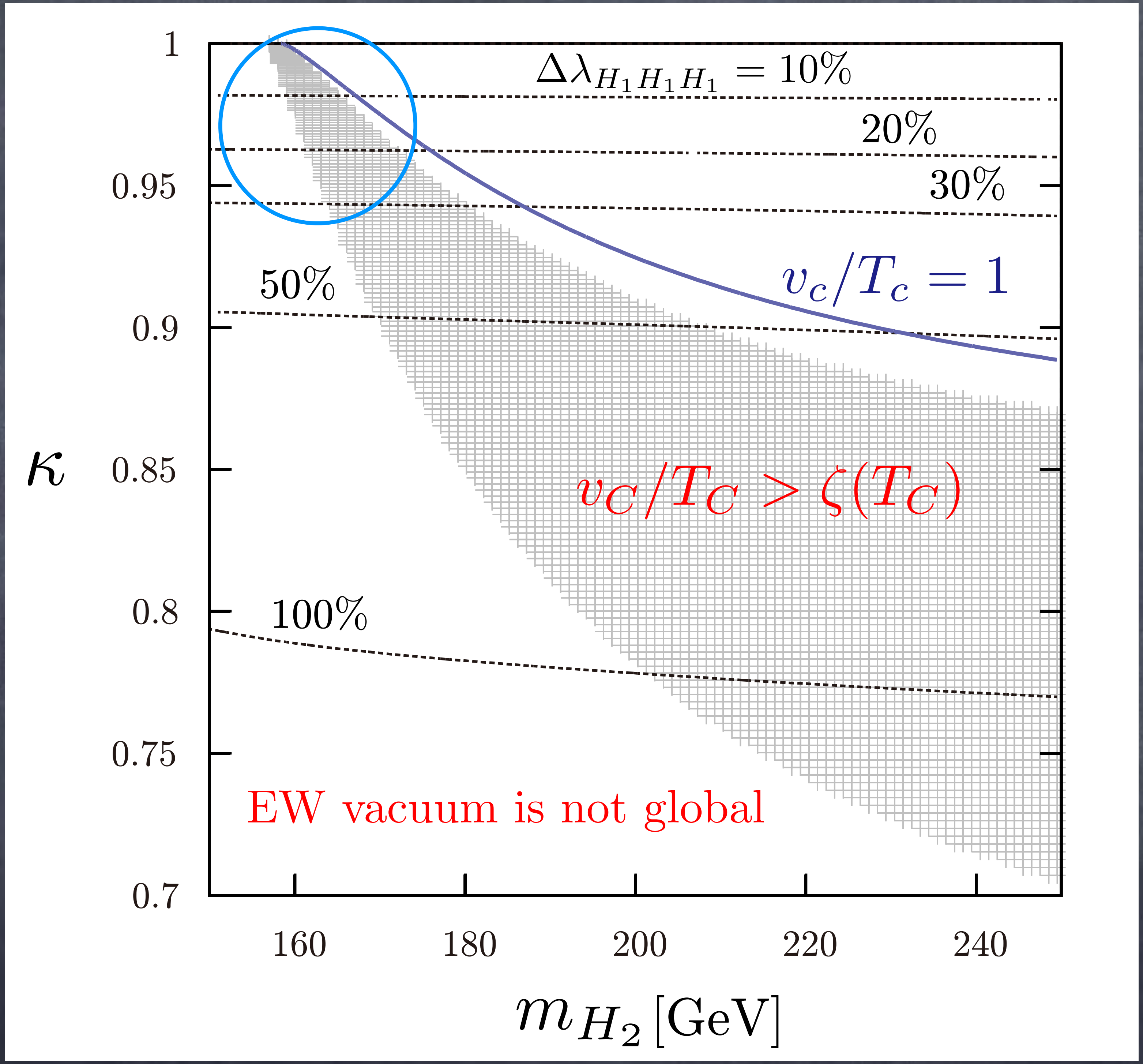

If $\dfrac{v_C}{T_C} > 1$

172

- $\Delta\lambda_{H_1 H_1 H_1} \simeq 16\%$ for $\kappa \simeq 0.97$ and 160 GeV $\lesssim m_{H_2} \lesssim 169$ GeV,
- $\Delta\lambda_{H_1 H_1 H_1} \simeq 27\%$ for $\kappa \simeq 0.95$, and 163 GeV $\lesssim m_{H_2} \lesssim 176$ GeV.

$\Delta\lambda_{H_1H_1H_1}$ contours in (m_{H_2}, κ) plane

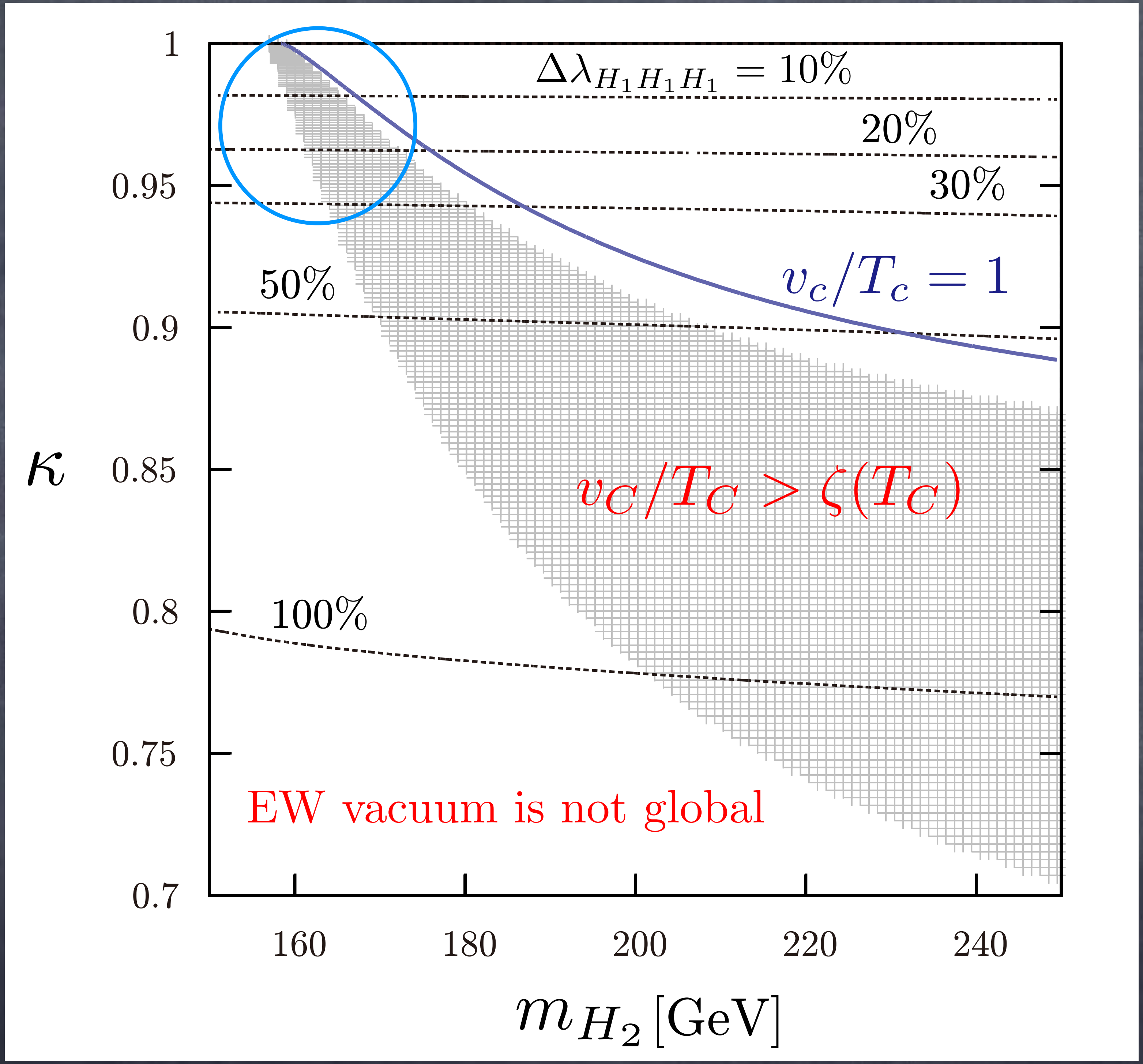

If $\dfrac{v_C}{T_C} > 1$

172

182

- $\Delta\lambda_{H_1H_1H_1} \simeq 16\%$ for $\kappa \simeq 0.97$ and 160 GeV $\lesssim m_{H_2} \lesssim$ 169 GeV,
- $\Delta\lambda_{H_1H_1H_1} \simeq 27\%$ for $\kappa \simeq 0.95$, and 163 GeV $\lesssim m_{H_2} \lesssim$ 176 GeV.

Higgs coupling measurements@LHC/ILC

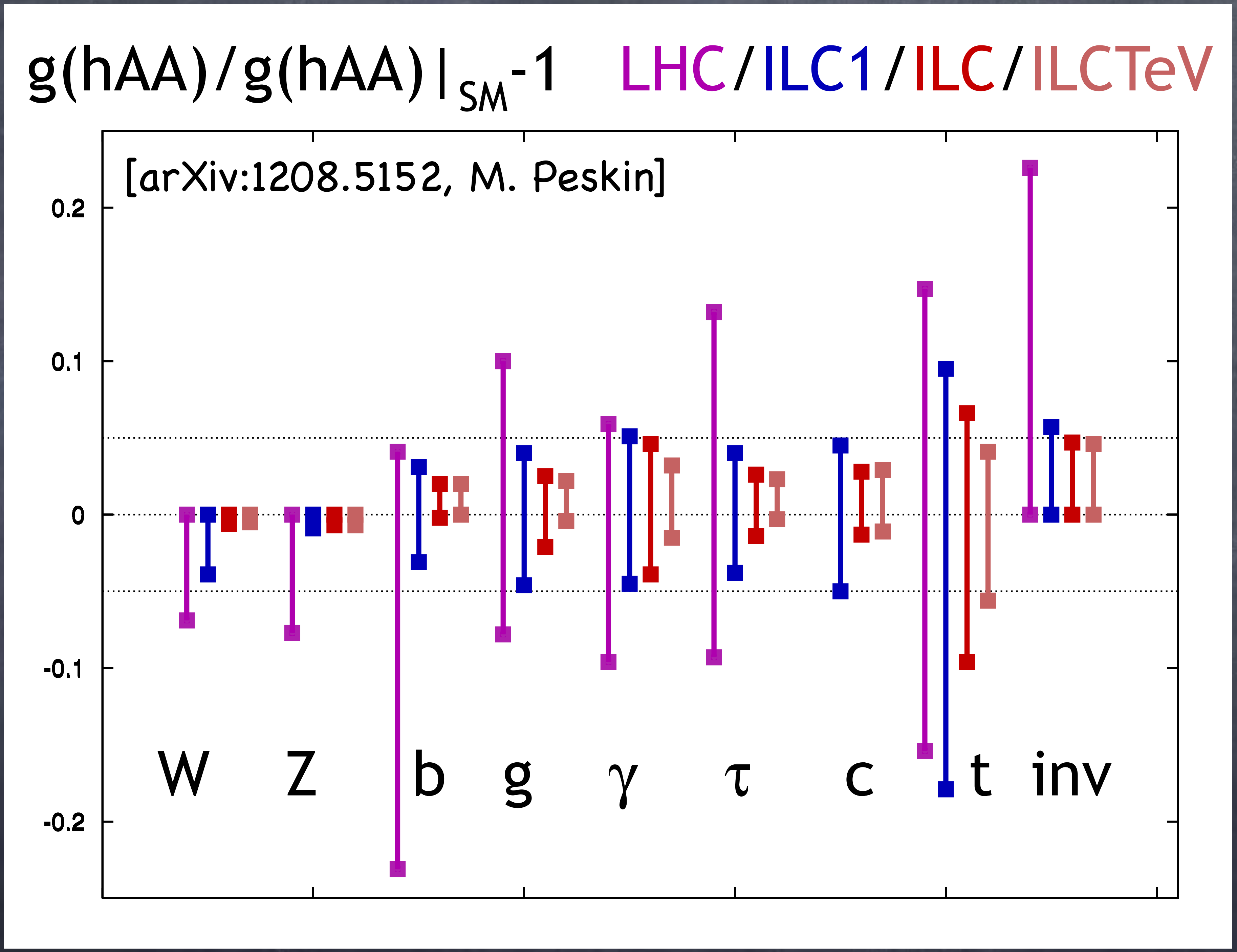

LHC/ILC can probe EWBG-favored region.

hhh coupling at LHC

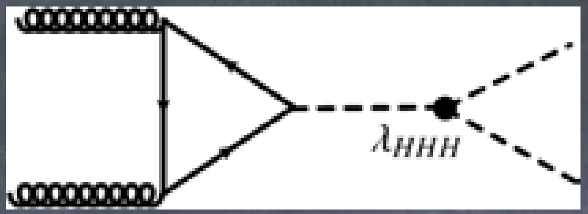

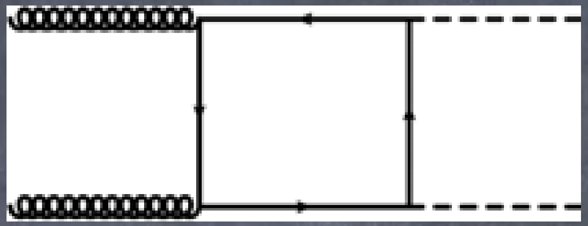

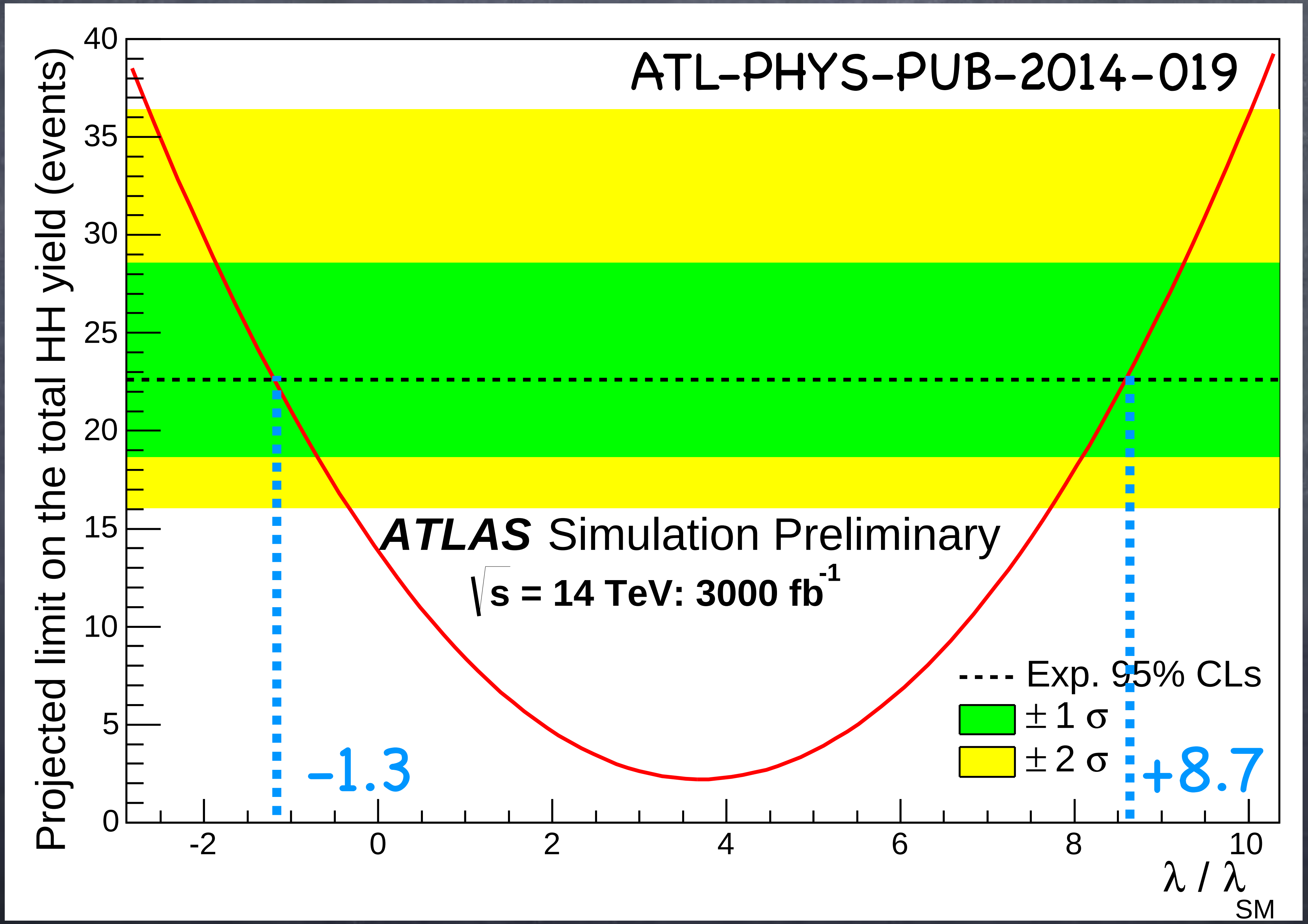

c.f. @ILC $\Delta\lambda_{hhh}/\lambda_{hhh} = 13\%$ [ILC white paper, 1310.0763]

Summary

❒ In the light of LHC data, MSSM EWBG was excluded. Other models are still viable.

❒ As a simple example, we have discussed the EW phase transition and sphaleron decoupling condition in SM+S.

❒ v_C/T_C > (1.1-1.2) in the typical cases.

❒ We also studied the deviation of the hhh coupling from the SM value based on the improved sphaleron decoupling condition.

❒ The deviation is greater than that based on the conventional criterion $v_C/T_C>1$. -> Δhhh ⤴

Backup

κ vs. $\Delta\lambda_{H_1 H_1 H_1}$

$$\Delta\lambda_{H_1H_1H_1} = \frac{\lambda^{\rm rSM}_{H_1H_1H_1} - \lambda^{\rm SM}_{H_1H_1H_1}}{\lambda^{\rm SM}_{H_1H_1H_1}}$$

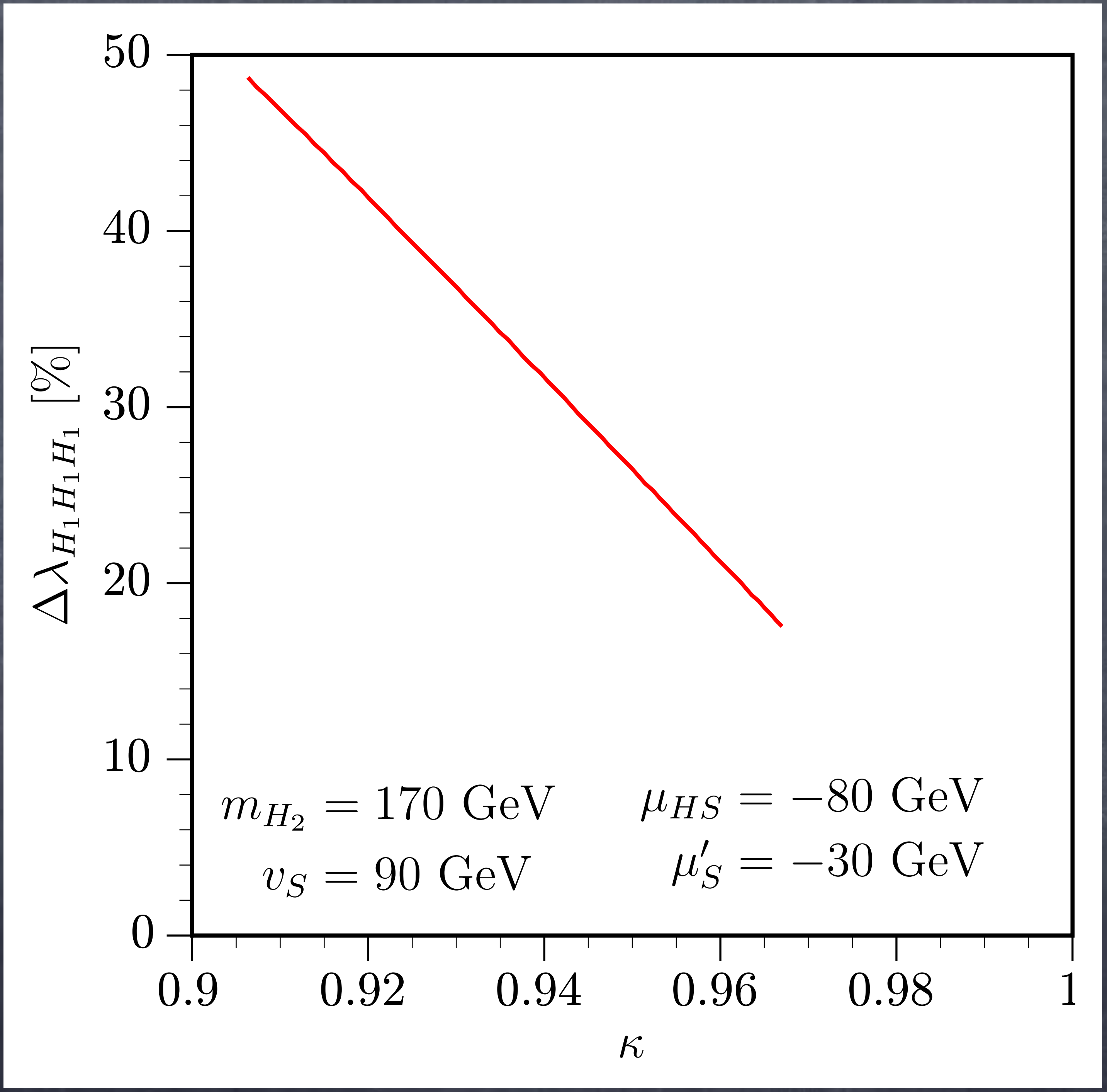

- Smaller κ gives larger $\Delta\lambda_{H1H1H1}$.

κ vs. $\Delta\lambda_{H_1H_1H_1}$

$$\Delta\lambda_{H_1H_1H_1} = \frac{\lambda^{\rm rSM}_{H_1H_1H_1} - \lambda^{\rm SM}_{H_1H_1H_1}}{\lambda^{\rm SM}_{H_1H_1H_1}}$$

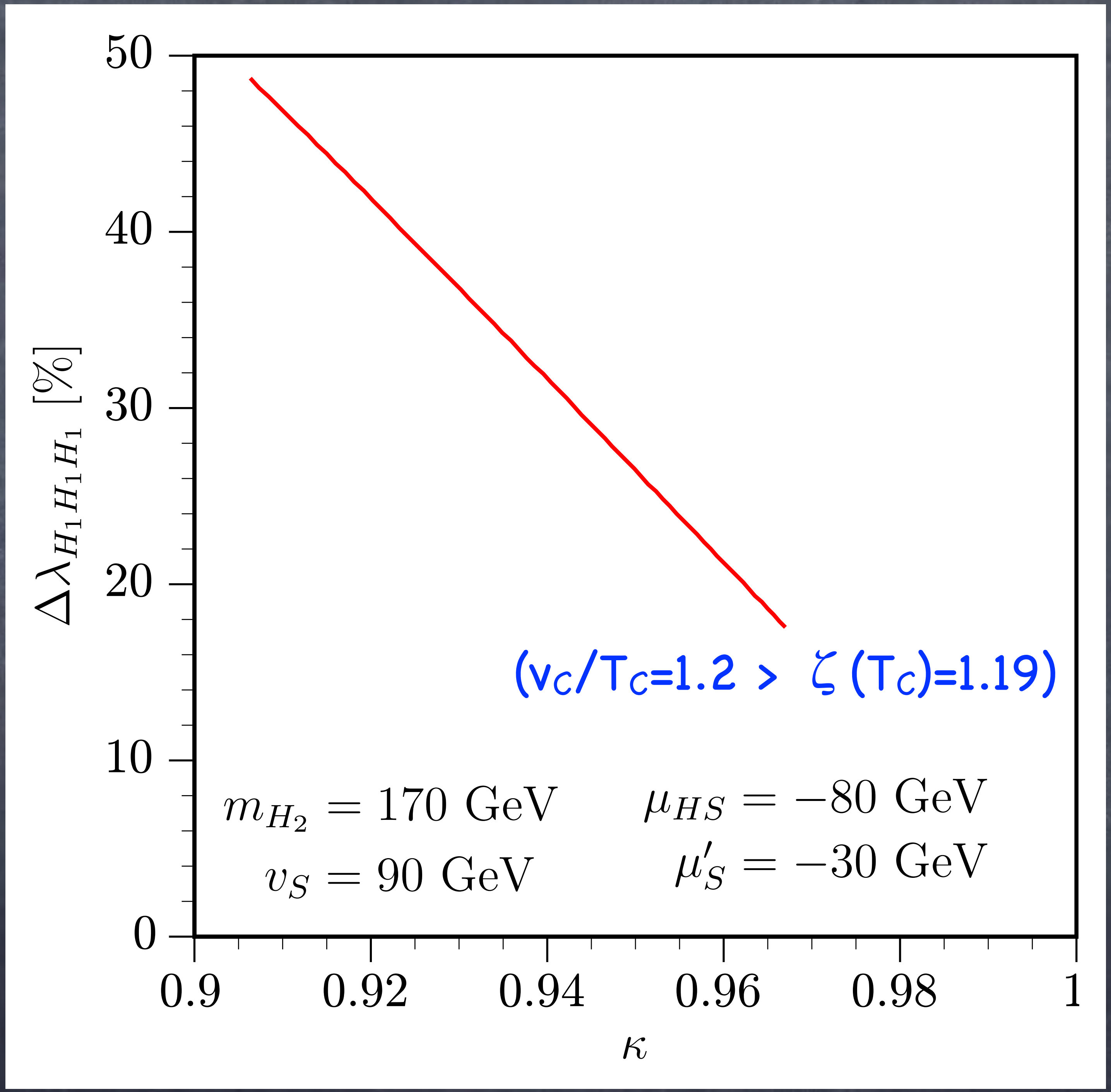

- Smaller κ gives larger $\Delta\lambda_{H1H1H1}$.

κ vs. $\Delta\lambda_{H_1H_1H_1}$

$$\Delta\lambda_{H_1H_1H_1} = \frac{\lambda^{\rm rSM}_{H_1H_1H_1} - \lambda^{\rm SM}_{H_1H_1H_1}}{\lambda^{\rm SM}_{H_1H_1H_1}}$$

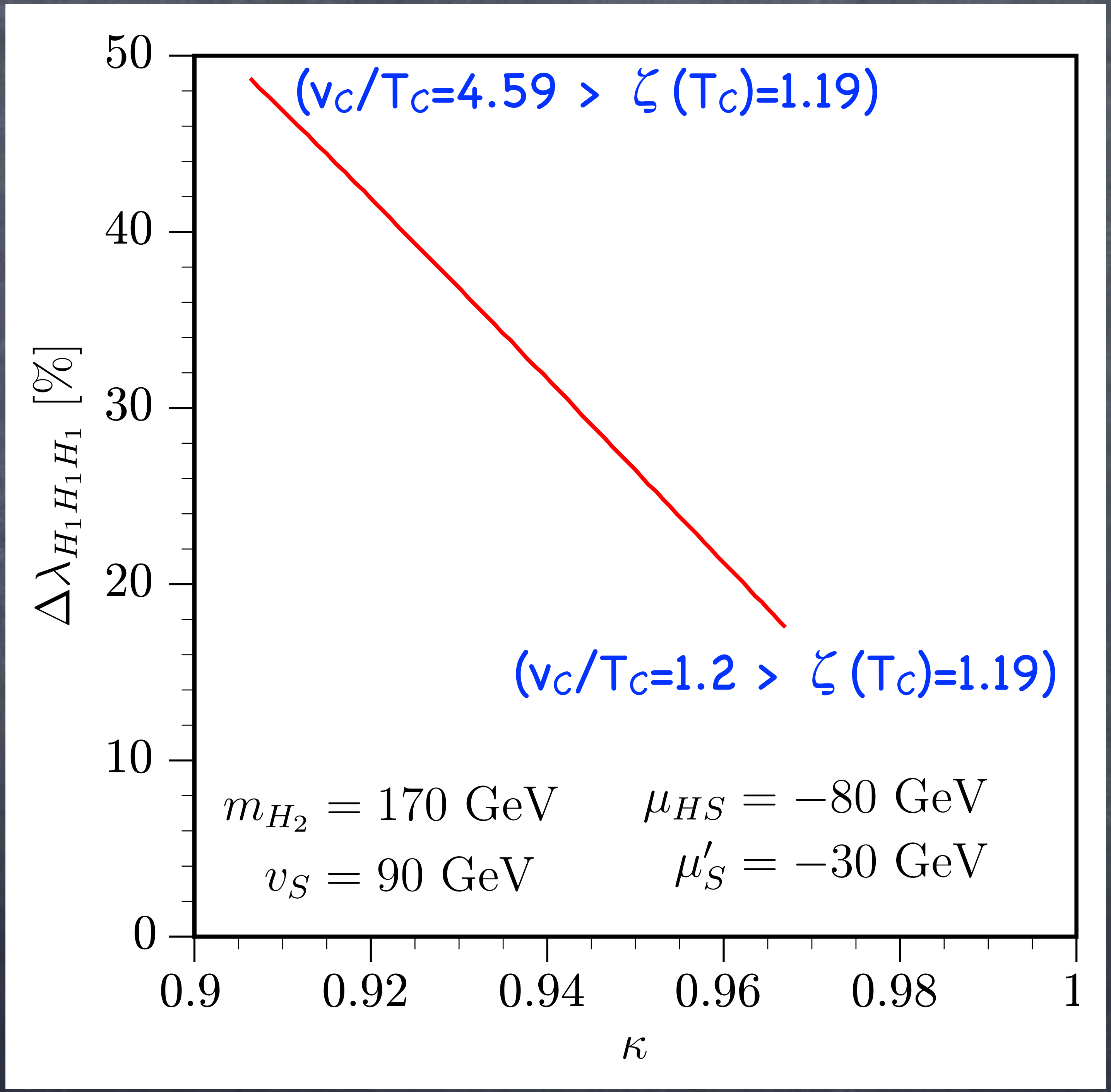

- Smaller κ gives larger $\Delta\lambda_{H1H1H1}$.

Benchmark points

	Z2-symmetric S1	S2	S3	S4
H-S mixing parameters	λ_{HS}	λ_{HS}, μ_{HS}	λ_{HS}, μ_{HS}	μ_{HS}
PT type	D	B	B	B
m_{H_2} [GeV]	500	170	148	500
α [degrees]	38	-20	0	20
v_S [GeV]	200	90	100	200
μ_{HS} [GeV]	0.00	-80.00	-80.00	-310.72
μ'_S [GeV]	0	-30	-30	0

κ	0.79	0.94	1.0	0.94
$\Delta\lambda_{H_1H_1H_1}$ [%]	-23.7	31.8	0.58	41.1
$\log_{10}(\Lambda/\mathrm{GeV})$	3.90	9.68	13.78	3.90

Benchmark points

Z2-symmetric

	S1	S2	S3	S4
H-S mixing parameters	λ_{HS}	λ_{HS}, μ_{HS}	λ_{HS}, μ_{HS}	μ_{HS}
PT type	D	B	B	B
m_{H_2} [GeV]	500	170	148	500
α [degrees]	38	-20	0	20
v_S [GeV]	200	90	100	200
μ_{HS} [GeV]	0.00	-80.00	-80.00	-310.72
μ'_S [GeV]	0	-30	-30	0

κ	0.79	0.94	1.0	0.94
$\Delta\lambda_{H_1H_1H_1}$ [%]	-23.7	31.8	0.58	41.1
$\log_{10}(\Lambda/\mathrm{GeV})$	3.90	9.68	13.78	3.90

Benchmark points

Z2-symmetric

	S1	S2	S3	S4
H-S mixing parameters	λ_{HS}	λ_{HS}, μ_{HS}	λ_{HS}, μ_{HS}	μ_{HS}
PT type	D	B	B	B
m_{H_2} [GeV]	500	170	148	500
α [degrees]	38	-20	0	20
v_S [GeV]	200	90	100	200
μ_{HS} [GeV]	0.00	-80.00	-80.00	-310.72
μ'_S [GeV]	0	-30	-30	0
κ	0.79	0.94	1.0	0.94
$\Delta\lambda_{H_1H_1H_1}$ [%]	-23.7	31.8	0.58	41.1
$\log_{10}(\Lambda/\mathrm{GeV})$	3.90	9.68	13.78	3.90

excluded

Benchmark points

Z2-symmetric

	S1	S2	S3	S4
H-S mixing parameters	λ_{HS}	λ_{HS}, μ_{HS}	λ_{HS}, μ_{HS}	μ_{HS}
PT type	D	B	B	B
m_{H_2} [GeV]	500	170	148	500
α [degrees]	38	-20	0	20
v_S [GeV]	200	90	100	200
μ_{HS} [GeV]	0.00	-80.00	-80.00	-310.72
μ'_S [GeV]	0	-30	-30	0
κ	0.79	0.94	1.0	0.94
$\Delta\lambda_{H_1H_1H_1}$ [%]	-23.7	31.8	0.58	41.1
$\log_{10}(\Lambda/\mathrm{GeV})$	3.90	9.68	13.78	3.90

excluded

Benchmark points

	Z2-symmetric S1	S2	S3	S4
H-S mixing parameters	λ_{HS}	λ_{HS}, μ_{HS}	λ_{HS}, μ_{HS}	μ_{HS}
PT type	D	B	B	B
m_{H_2} [GeV]	500	170	148	500
α [degrees]	38	-20	0	20
v_S [GeV]	200	90	100	200
μ_{HS} [GeV]	0.00	-80.00	-80.00	-310.72
μ'_S [GeV]	0	-30	-30	0
κ	0.79	0.94	1.0	0.94
$\Delta\lambda_{H_1H_1H_1}$ [%]	-23.7	31.8	0.58	41.1
$\log_{10}(\Lambda/\mathrm{GeV})$	3.90	9.68	13.78	3.90

excluded

no significant deviation

Benchmark points

Z2-symmetric

	S1	S2	S3	S4
H-S mixing parameters	λ_{HS}	λ_{HS}, μ_{HS}	λ_{HS}, μ_{HS}	μ_{HS}
PT type	D	B	B	B
m_{H_2} [GeV]	500	170	148	500
α [degrees]	38	-20	0	20
v_S [GeV]	200	90	100	200
μ_{HS} [GeV]	0.00	-80.00	-80.00	-310.72
μ'_S [GeV]	0	-30	-30	0
κ	0.79	0.94	1.0	0.94
$\Delta\lambda_{H_1H_1H_1}$ [%]	-23.7	31.8	0.58	41.1
$\log_{10}(\Lambda/\mathrm{GeV})$	3.90	9.68	13.78	3.90

excluded

no significant deviation

Benchmark points

Z2-symmetric

	S1	S2	S3	S4
H-S mixing parameters	λ_{HS}	λ_{HS}, μ_{HS}	λ_{HS}, μ_{HS}	μ_{HS}
PT type	D	B	B	B
m_{H_2} [GeV]	500	170	148	500
α [degrees]	38	-20	0	20
v_S [GeV]	200	90	100	200
μ_{HS} [GeV]	0.00	-80.00	-80.00	-310.72
μ'_S [GeV]	0	-30	-30	0
κ	0.79	0.94	1.0	0.94
$\Delta\lambda_{H_1H_1H_1}$ [%]	-23.7	31.8	0.58	41.1
$\log_{10}(\Lambda/\mathrm{GeV})$	3.90	9.68	13.78	3.90

below GUT scale

excluded

no significant deviation

MSSM EWBG

light stop scenario

$$m^2_{\tilde{t}_1}(\varphi) \simeq \frac{y_t^2 \sin^2\beta}{2}\varphi^2 \quad (m^2_{\tilde{q}_L} \gg m^2_{\tilde{t}_R}, |A_t - \mu/\tan\beta|^2 \simeq 0)$$

Strong 1^{st}-order EWPT is driven by the light stop with a mass below 120 GeV. [M. Carena et al, NPB812, (2009) 243].

Prediction: σ(gg -> H -> VV)/ σ(gg -> H -> VV)$_{SM}$ ≃ (2-3)

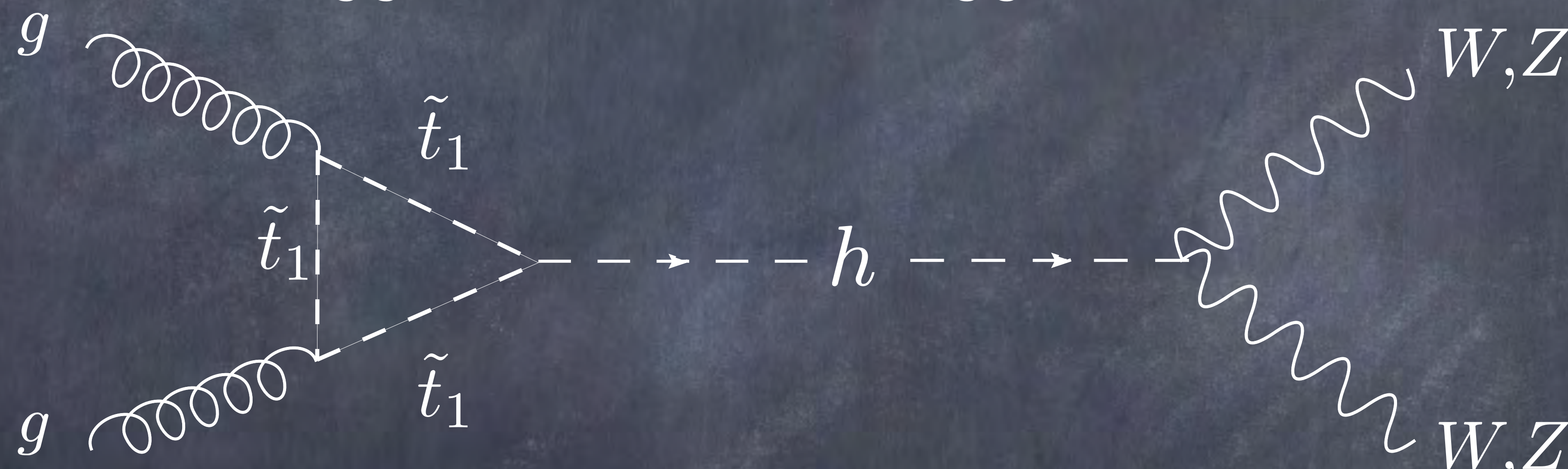

MSSM EWBG

light stop scenario

$$m_{\tilde{t}_1}^2(\varphi) \simeq \frac{y_t^2 \sin^2\beta}{2}\varphi^2 \quad (m_{\tilde{q}_L}^2 \gg m_{\tilde{t}_R}^2, |A_t - \mu/\tan\beta|^2 \simeq 0)$$

Strong 1^{st}-order EWPT is driven by the light stop with a mass below 120 GeV. [M. Carena et al, NPB812, (2009) 243].

Prediction: σ(gg -> H -> VV)/ σ(gg -> H -> VV)$_{SM}$ ≃ (2-3)

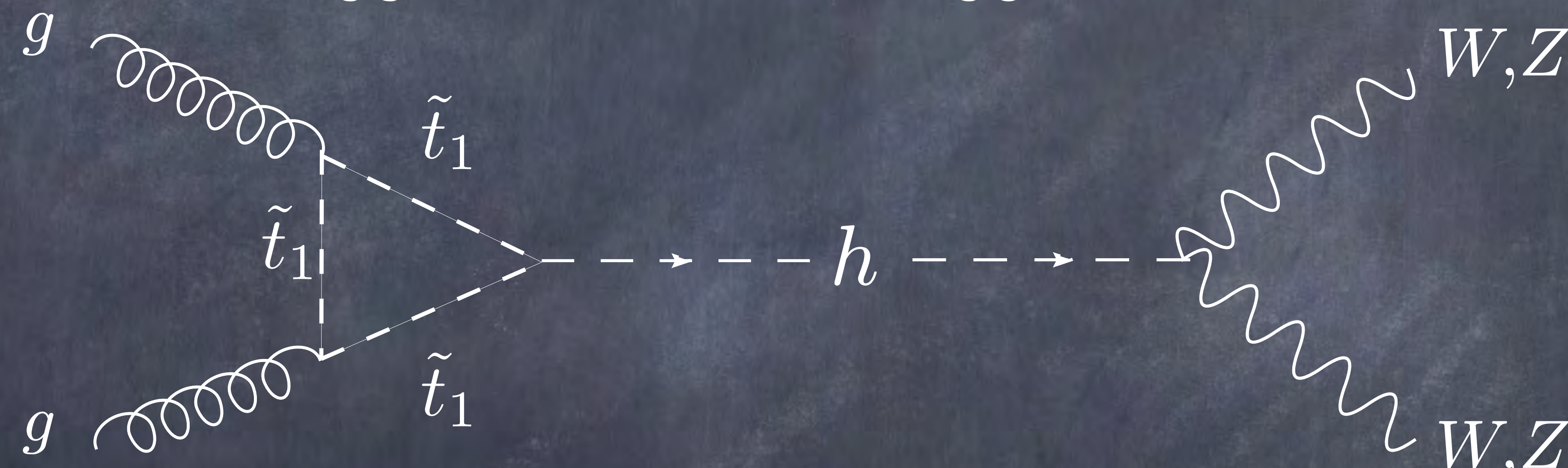

Confronting this scenario with LHC data,

MSSM EWBG is ruled out
at greater than 98% CL (m_A>1 TeV),
at least 90% CL for light value of m_A (~300 GeV)

∵ σ(gg -> H -> VV) is inconsistent.

[D. Curtin, P. Jaiswall, P. Meade., JHEP08(2012)005]

MSSM EWBG

light stop scenario

$$m_{\tilde{t}_1}^2(\varphi) \simeq \frac{y_t^2 \sin^2\beta}{2}\varphi^2 \quad (m_{\tilde{q}_L}^2 \gg m_{\tilde{t}_R}^2, |A_t - \mu/\tan\beta|^2 \simeq 0)$$

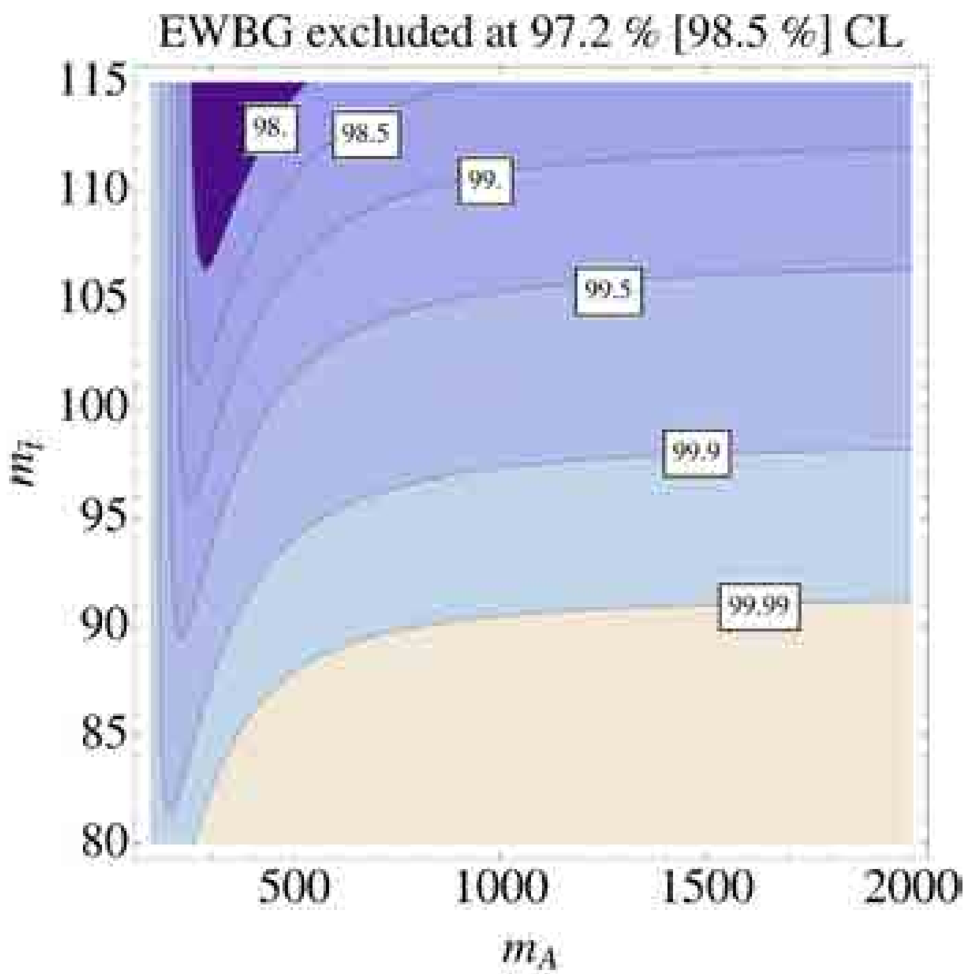

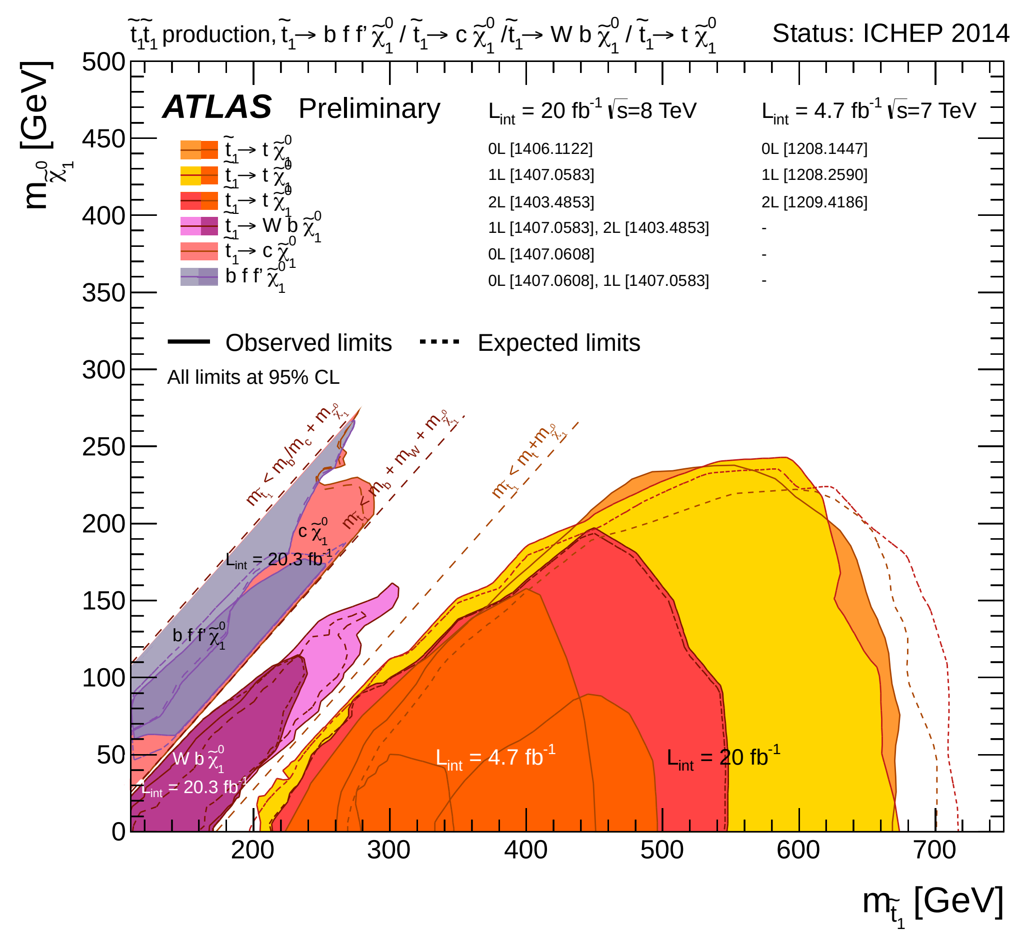

Confronting this scenario with LHC data,

MSSM EWBG is ruled out
at greater than 98% CL (m_A>1 TeV),
at least 90% CL for light value of m_A (~300 GeV)

$\because \sigma$(gg -> H -> VV) is inconsistent.

[D. Curtin, P. Jaiswall, P. Meade., JHEP08(2012)005]

MSSM EWBG

light stop scenario

$$m_{\tilde{t}_1}^2(\varphi) \simeq \frac{y_t^2 \sin^2\beta}{2}\varphi^2 \quad (m_{\tilde{q}_L}^2 \gg m_{\tilde{t}_R}^2, |A_t - \mu/\tan\beta|^2 \simeq 0)$$

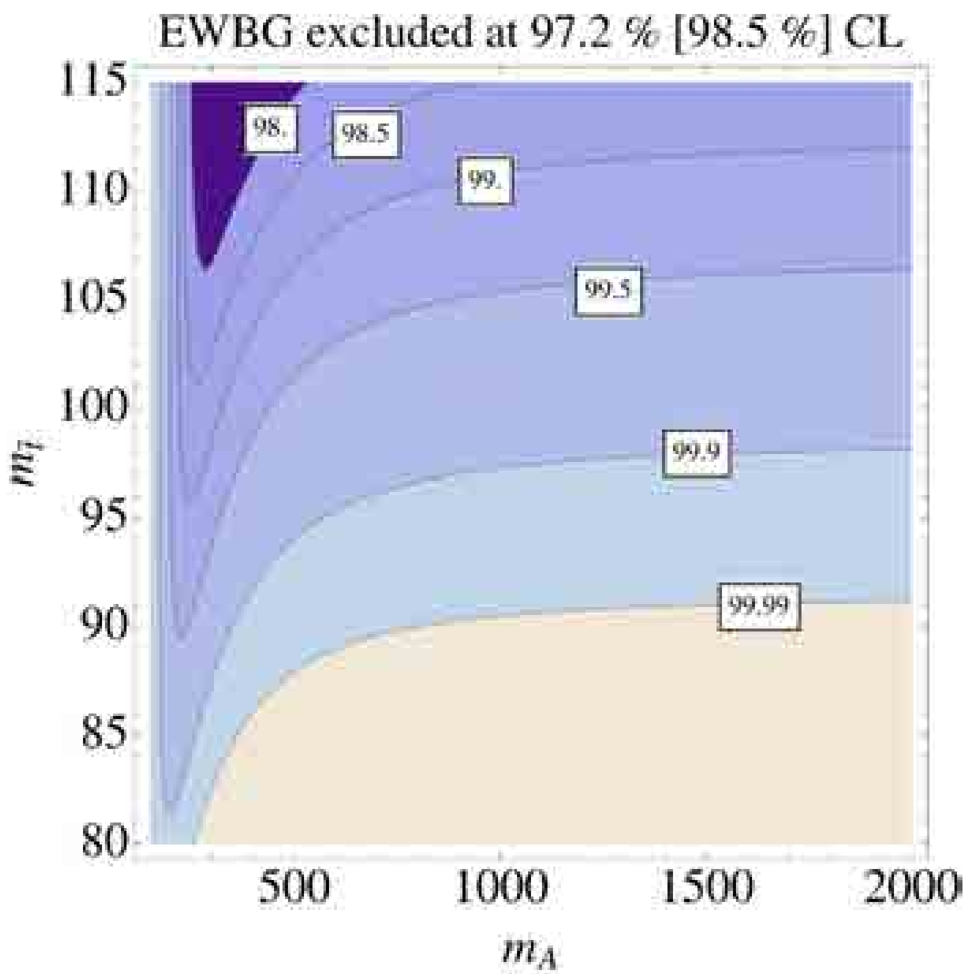

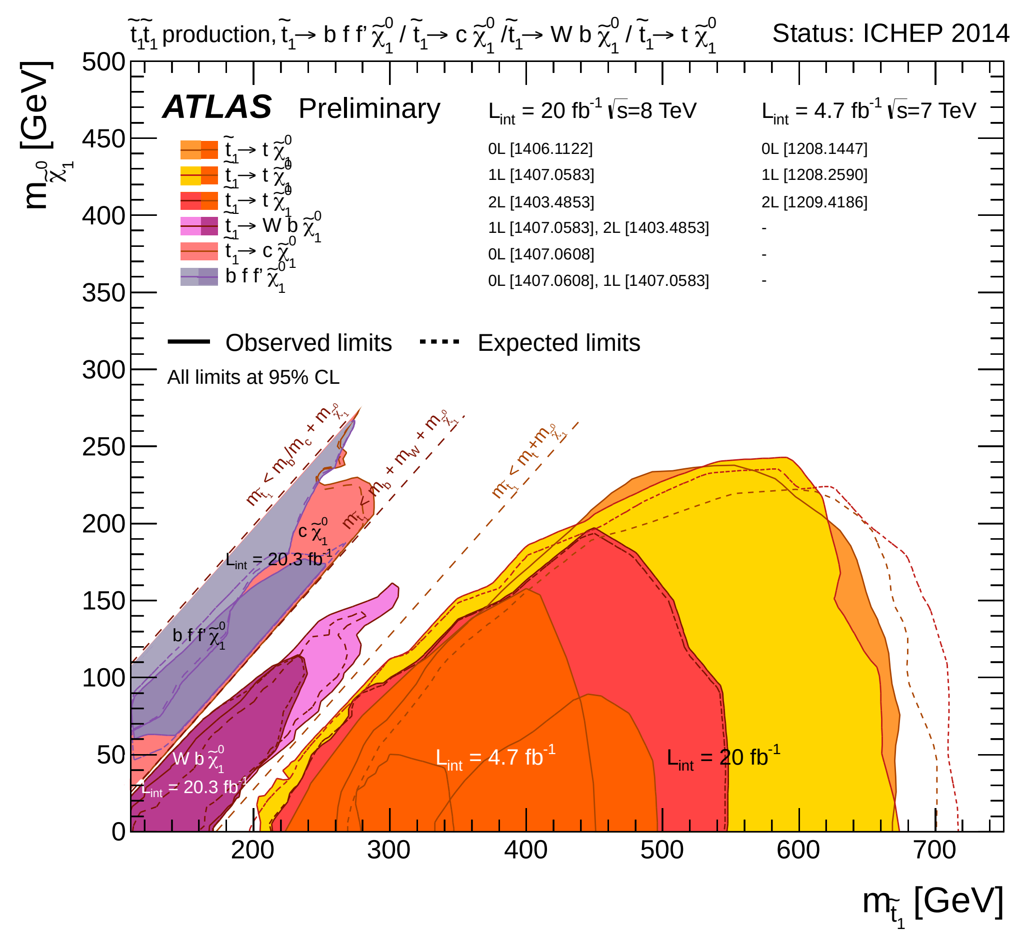

Confronting this scenario with LHC data,

MSSM EWBG is ruled out
at greater than 98% CL (m_A>1 TeV),
at least 90% CL for light value of m_A (~300 GeV)

[D. Curtin, P. Jaiswall, P. Meade., JHEP08(2012)005]

$\because \sigma$(gg -> H -> VV)

is inconsistent.

$\dfrac{v_C}{T_C} \gtrsim 1$ not satisfied

4 Higgs doublets+singlets-extended MSSM

- Strong 1st-order EWPT is driven by the charged Higgs bosons.

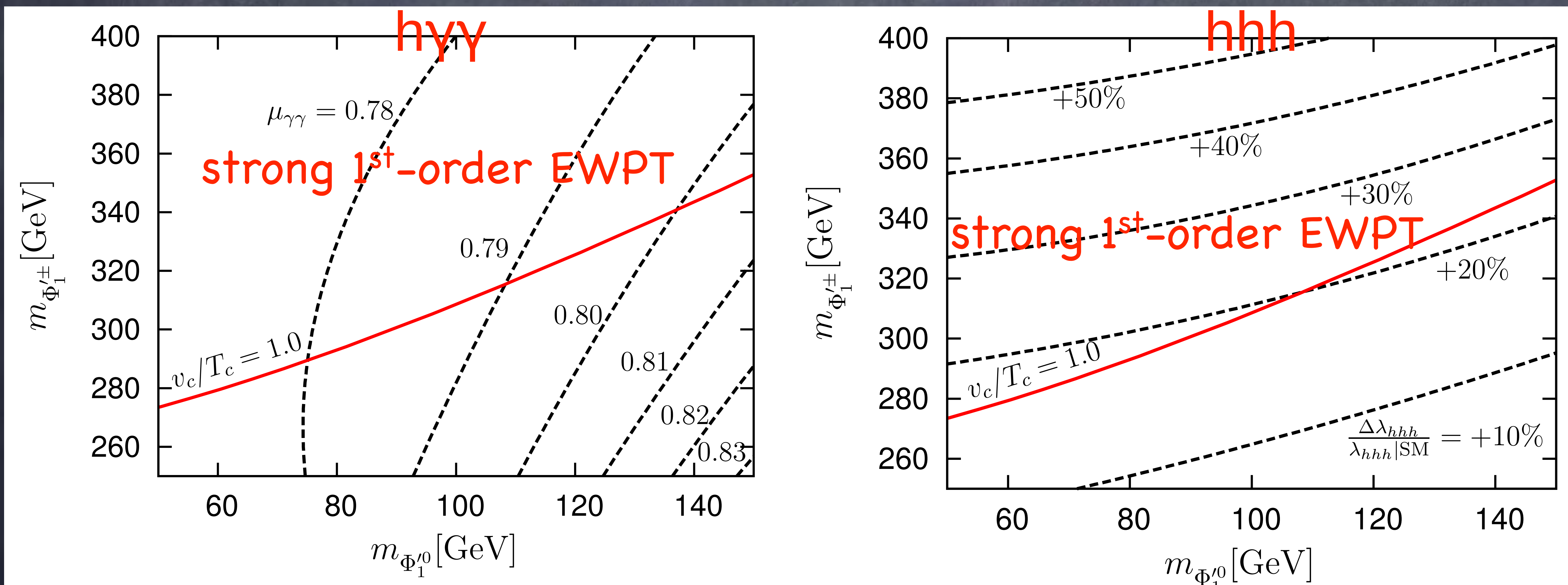

[S. Kanemura, E.S., T. Shindou, T. Yamada, JHEP05 (2013) 066]

If the EWPT is strong 1st order,

- $\mu_{\gamma\gamma}$ is reduced by more than 20%,
- hhh coupling is enhanced by more than 20%.

4 Higgs doublets+singlets-extended MSSM

❒ Strong 1st-order EWPT is driven by the charged Higgs bosons.

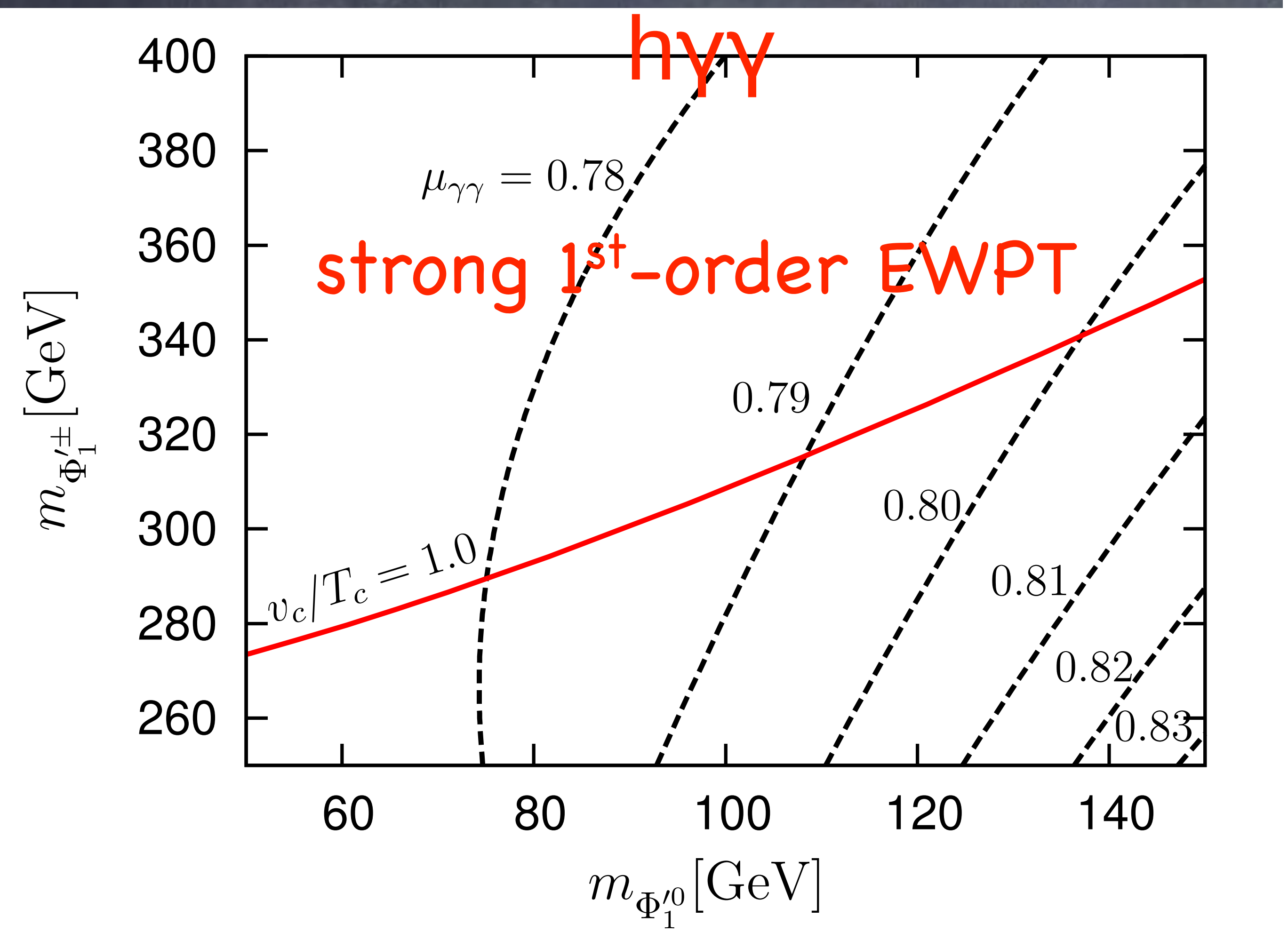

$$\mu_{\gamma\gamma} = 1.17 \pm 0.27 \text{ (ATLAS)}$$

$$\mu_{\gamma\gamma} = 1.14^{+0.26}_{-0.23} \text{ (CMS)}$$

[S. Kanemura, E.S., T. Shindou, T. Yamada, JHEP05 (2013) 066]

If the EWPT is strong 1st order,

- $\mu_{\gamma\gamma}$ is reduced by more than 20%,
- hhh coupling is enhanced by more than 20%.

Singlino-driven EWBG in the NMSSM

[K. Cheung, TJ. Hou, JS. Lee, E.S., PLB710 (2012) 188]

- Strong 1st-order EWPT is driven by the doublet-singlet mixing effects.
- CP-violation relevant to the BAU comes from Higgsino-singlino int.

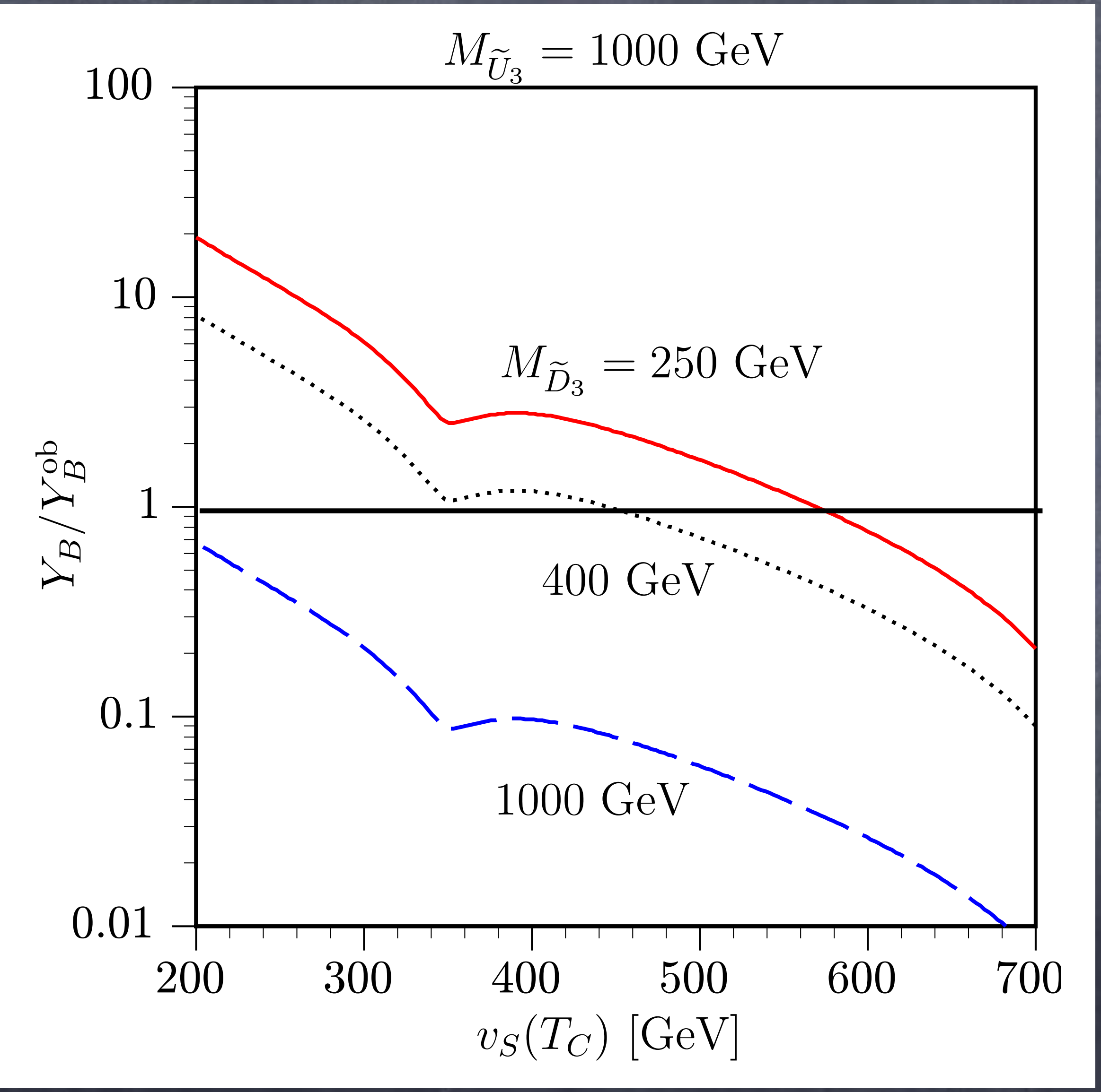

Singlino-driven EWBG in the NMSSM

[K. Cheung, TJ. Hou, JS. Lee, E.S., PLB710 (2012) 188]

- Strong 1st-order EWPT is driven by the doublet-singlet mixing effects.
- CP-violation relevant to the BAU comes from Higgsino-singlino int.

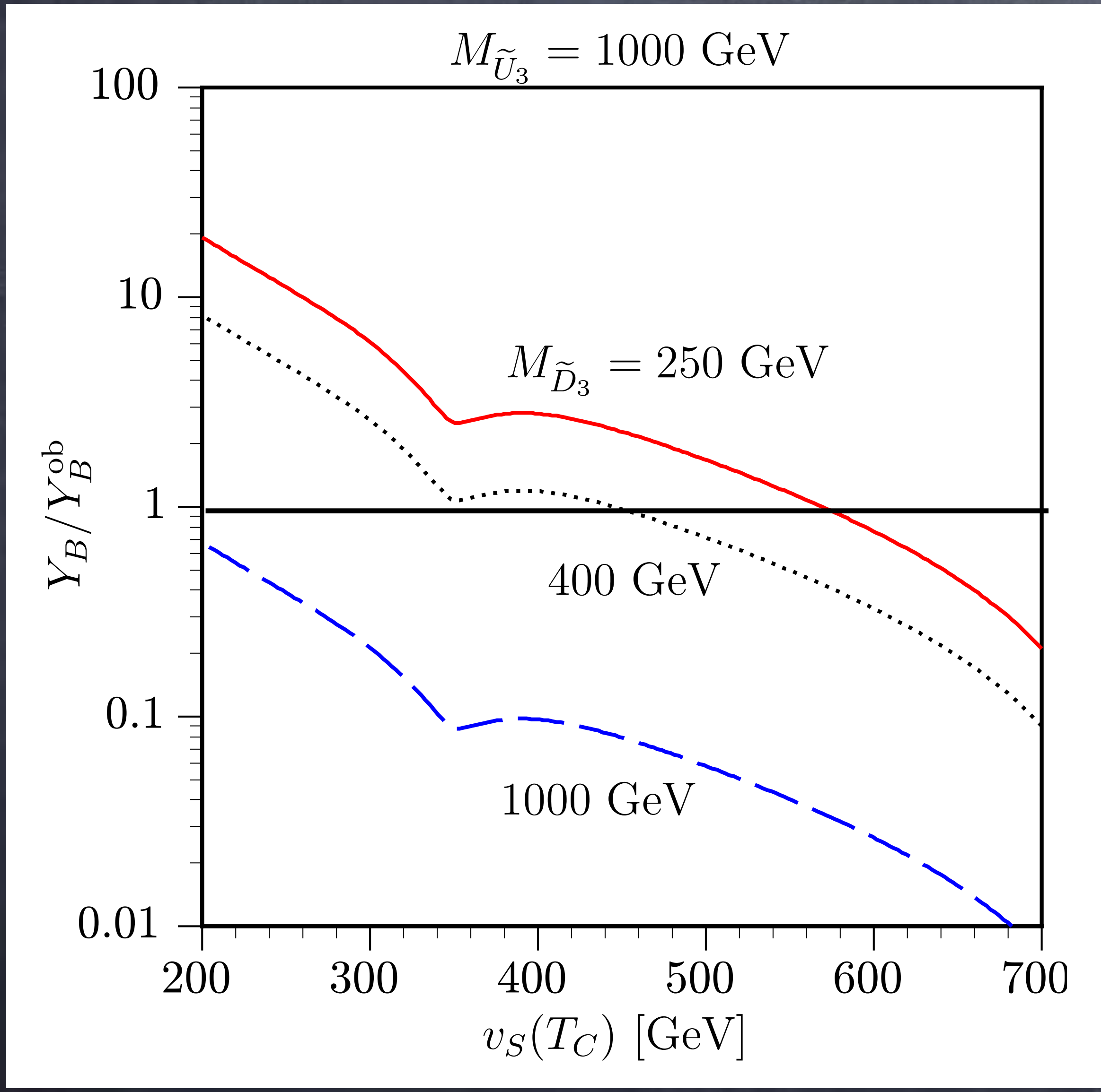

Singlino-driven EWBG in the NMSSM

[K. Cheung, TJ. Hou, JS. Lee, E.S., PLB710 (2012) 188]

- Strong 1st-order EWPT is driven by the doublet-singlet mixing effects.
- CP-violation relevant to the BAU comes from Higgsino-singlino int.

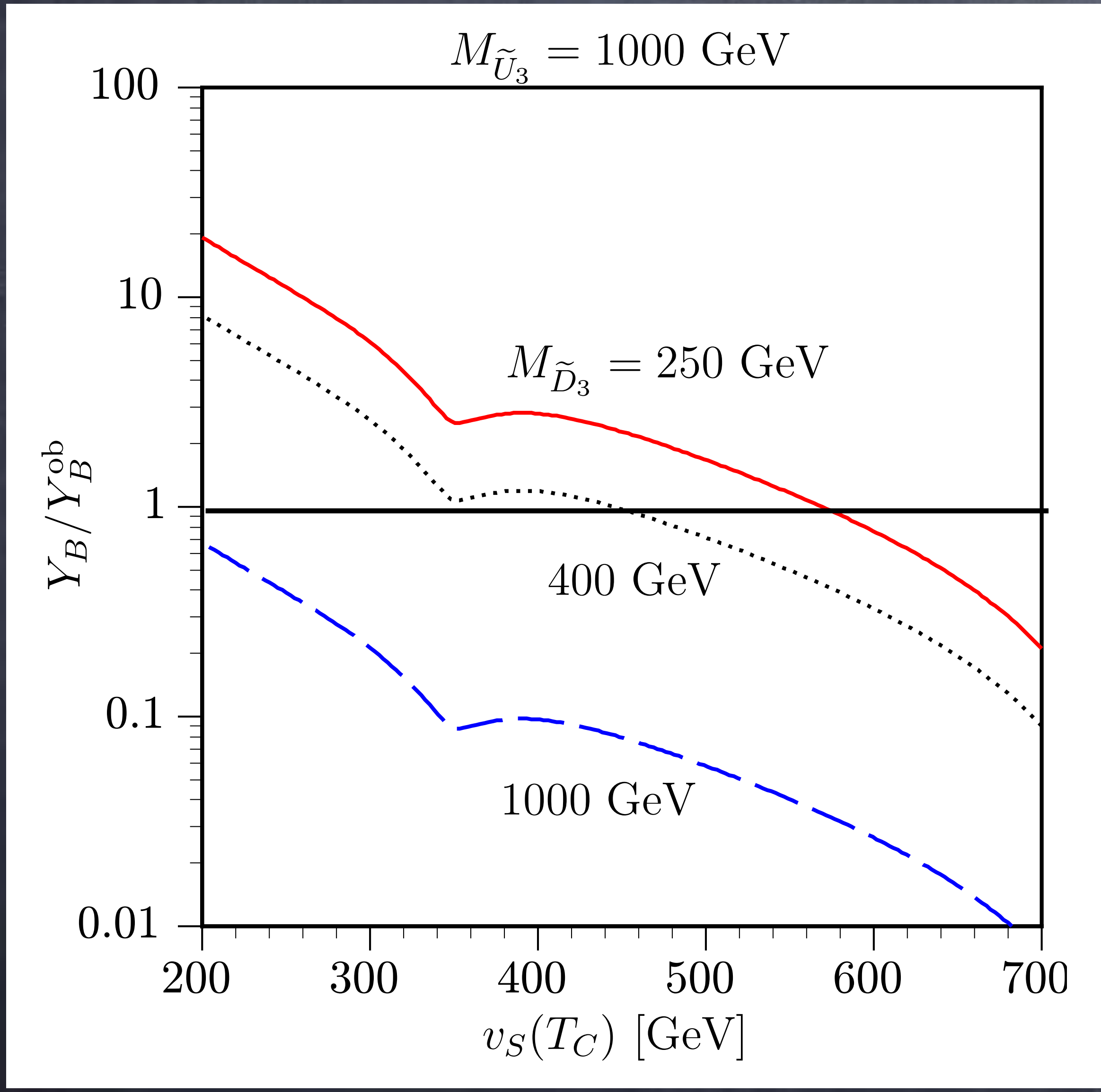

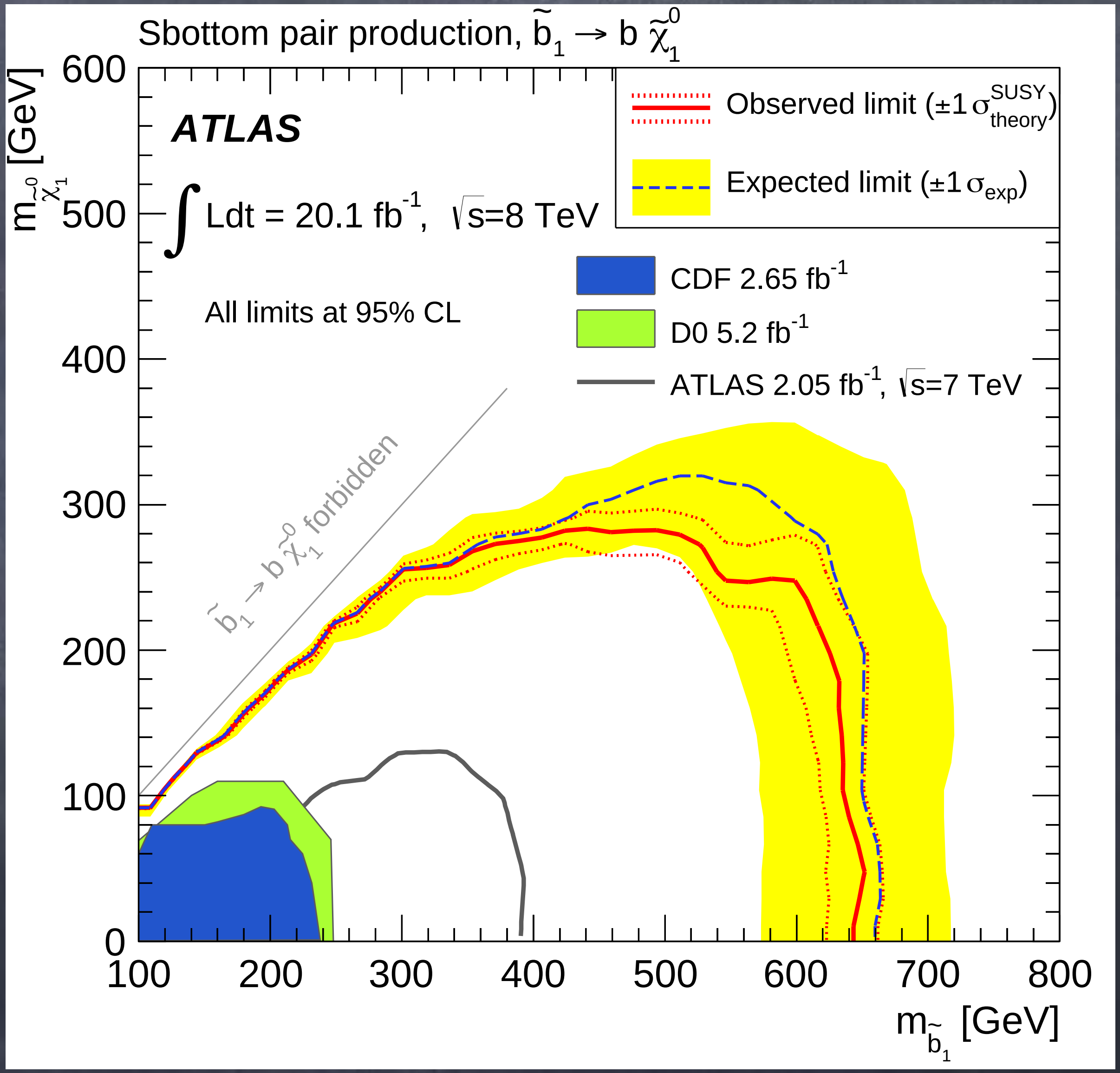

Singlino-driven EWBG in the NMSSM

[K. Cheung, TJ. Hou, JS. Lee, E.S., PLB710 (2012) 188]

- ❒ Strong 1st-order EWPT is driven by the doublet-singlet mixing effects.
- ❒ CP-violation relevant to the BAU comes from Higgsino-singlino int.

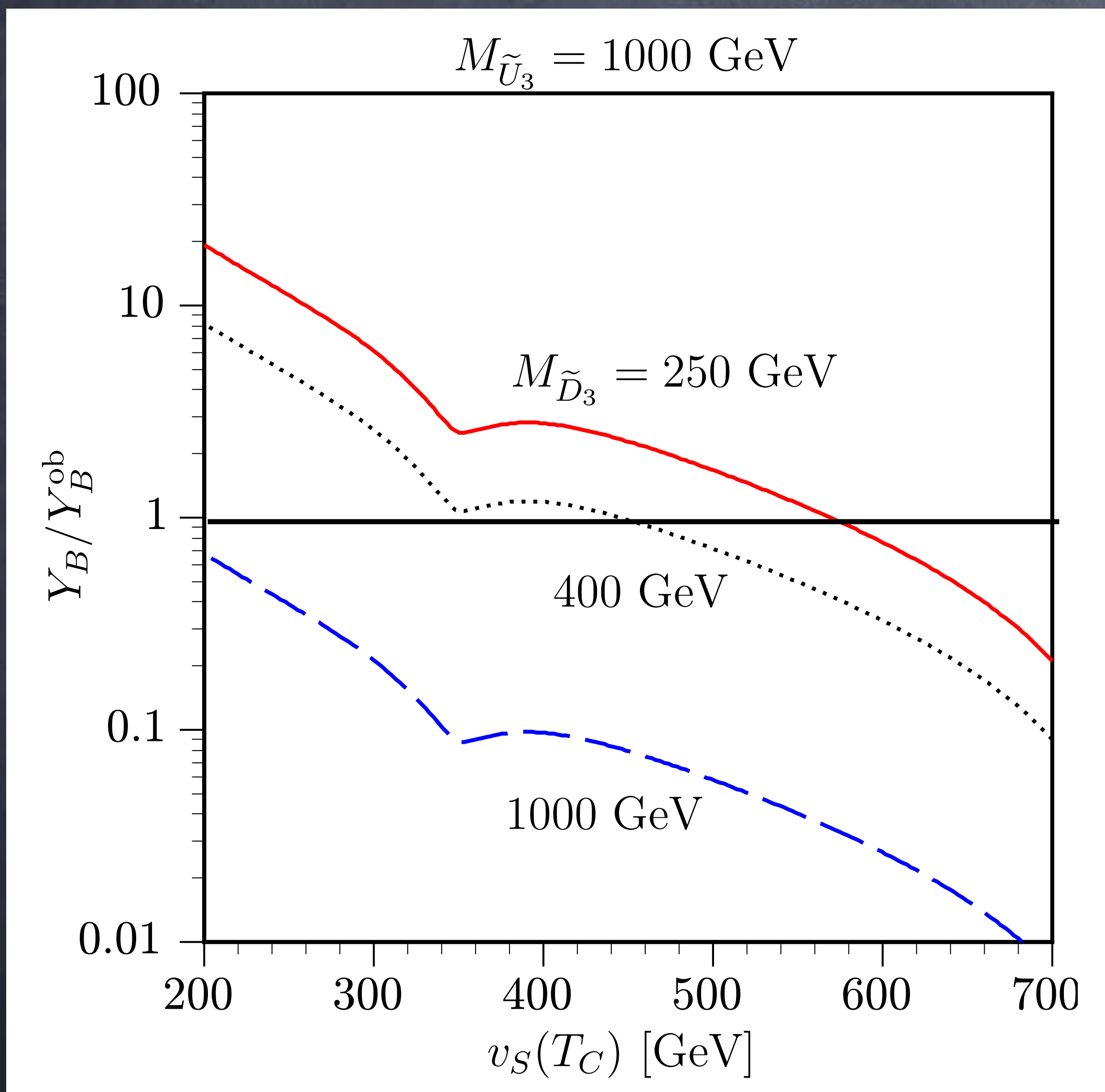

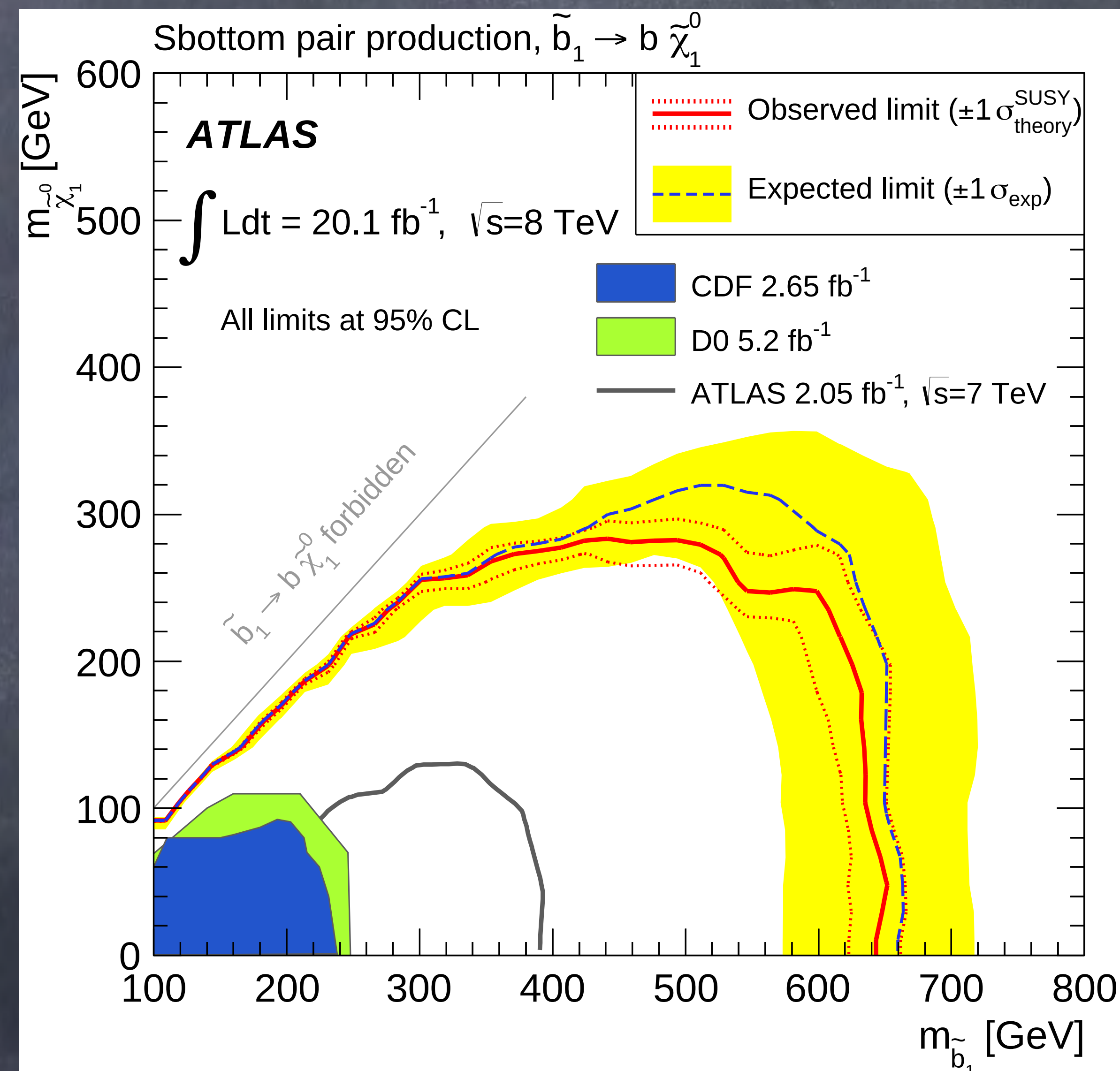

- ❒ This specific scenario is disfavored by sbottom searches.

Singlino-driven EWBG in the NMSSM

[K. Cheung, TJ. Hou, JS. Lee, E.S., PLB710 (2012) 188]

❒ Strong 1st-order EWPT is driven by the doublet-singlet mixing effects.

❒ CP-violation relevant to the BAU comes from Higgsino-singlino int.

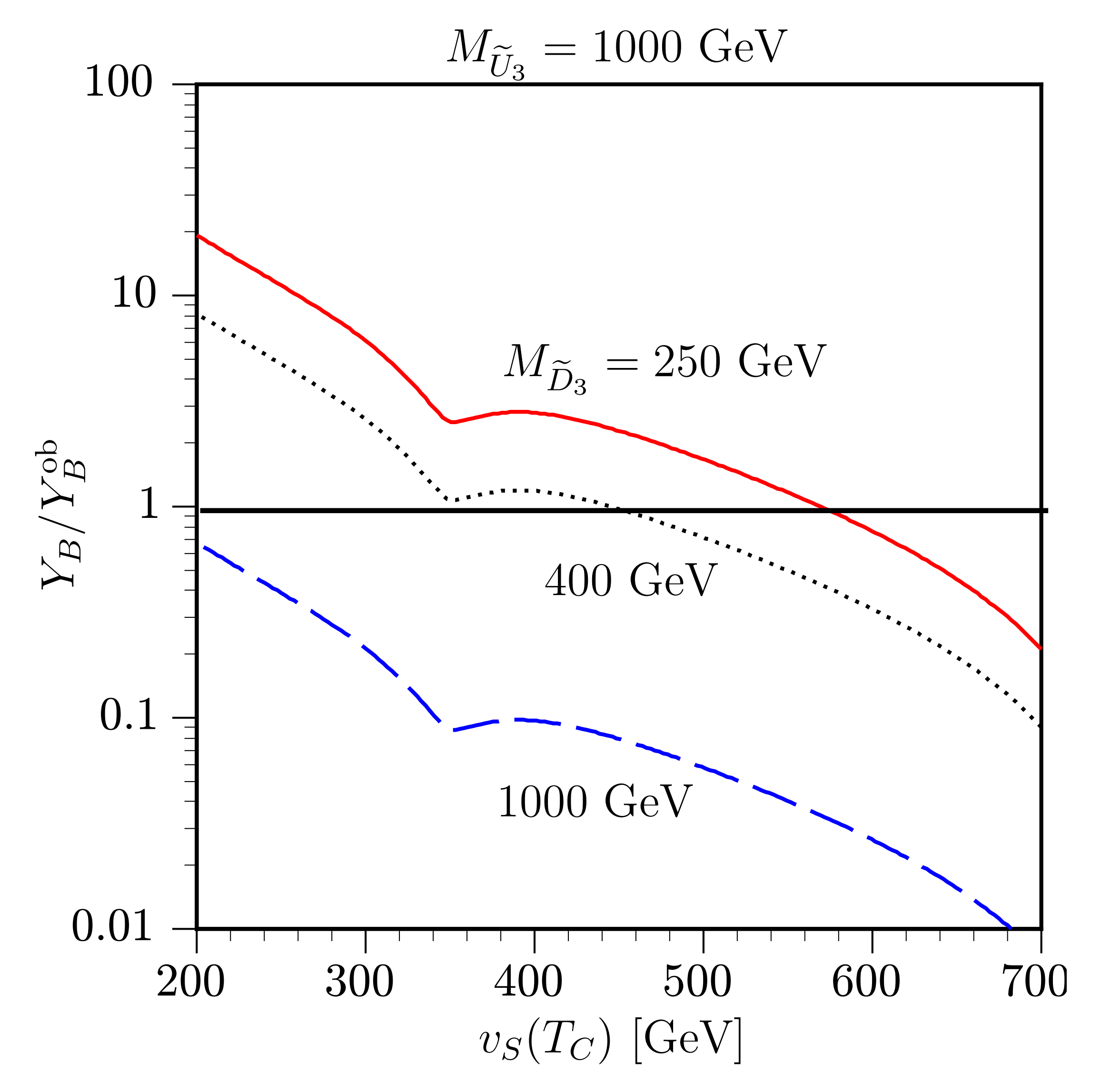

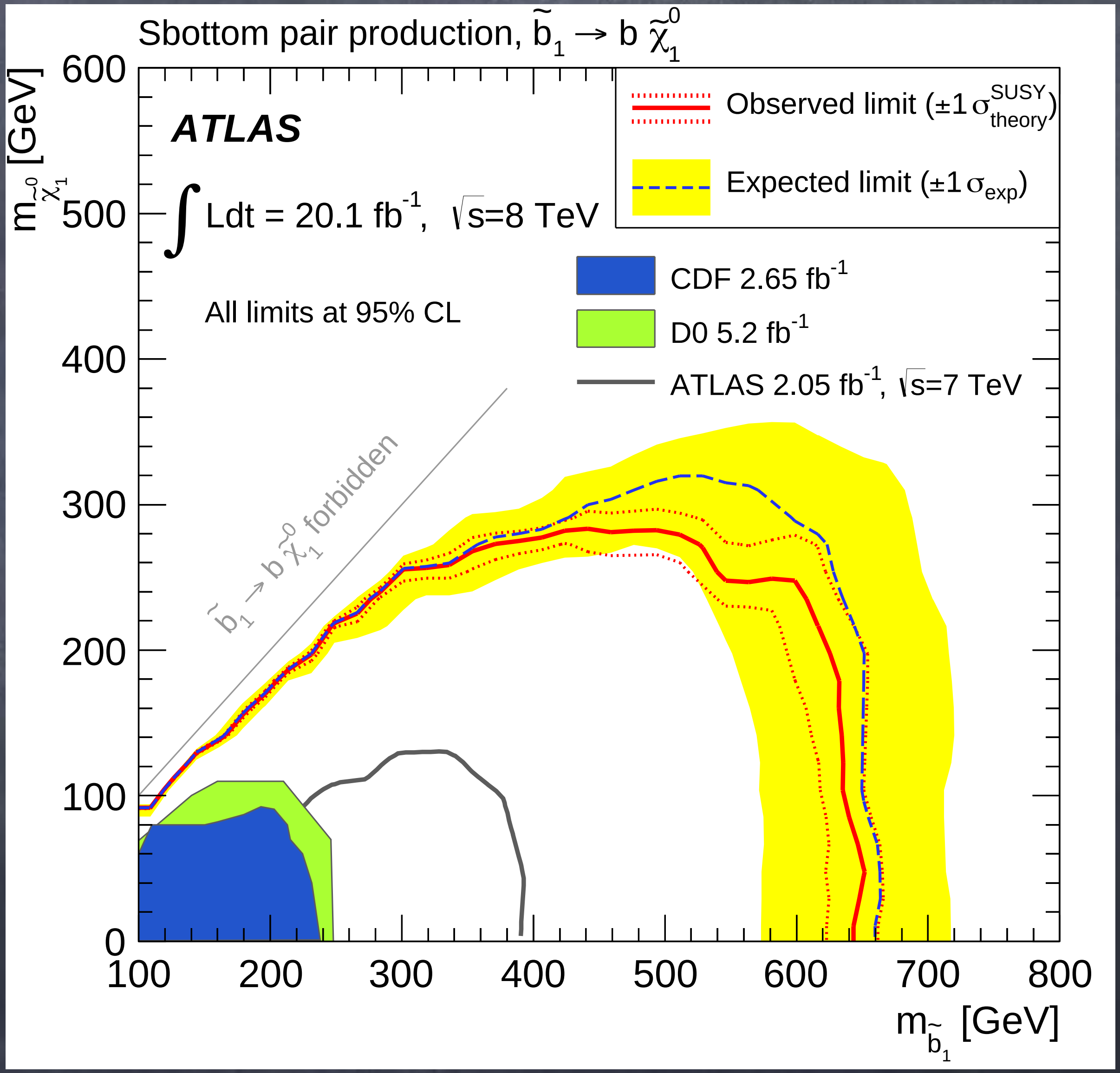

❒ This specific scenario is disfavored by sbottom searches.

❒ However, successful scenario still remain, e.g. bino-driven scenario.

Z′-ino-driven EWBG in the UMSSM

[E.S., PRD88, 055014 (2013)]

- ❒ Strong 1st-order EWPT is driven by the doublet-singlet mixing effects.
- ❒ CP-violation relevant to the BAU comes from Higgsino-Z′-ino int.

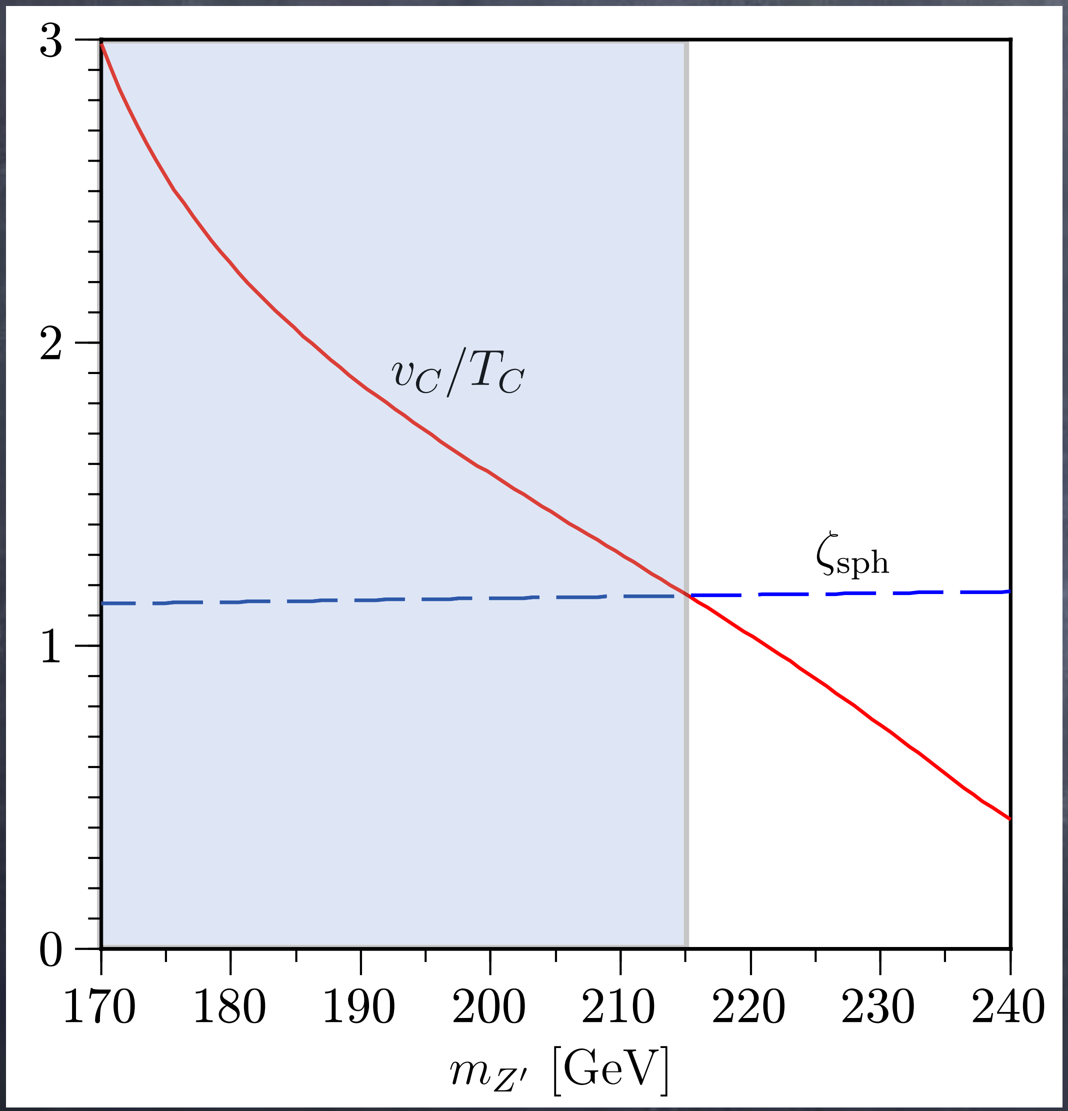

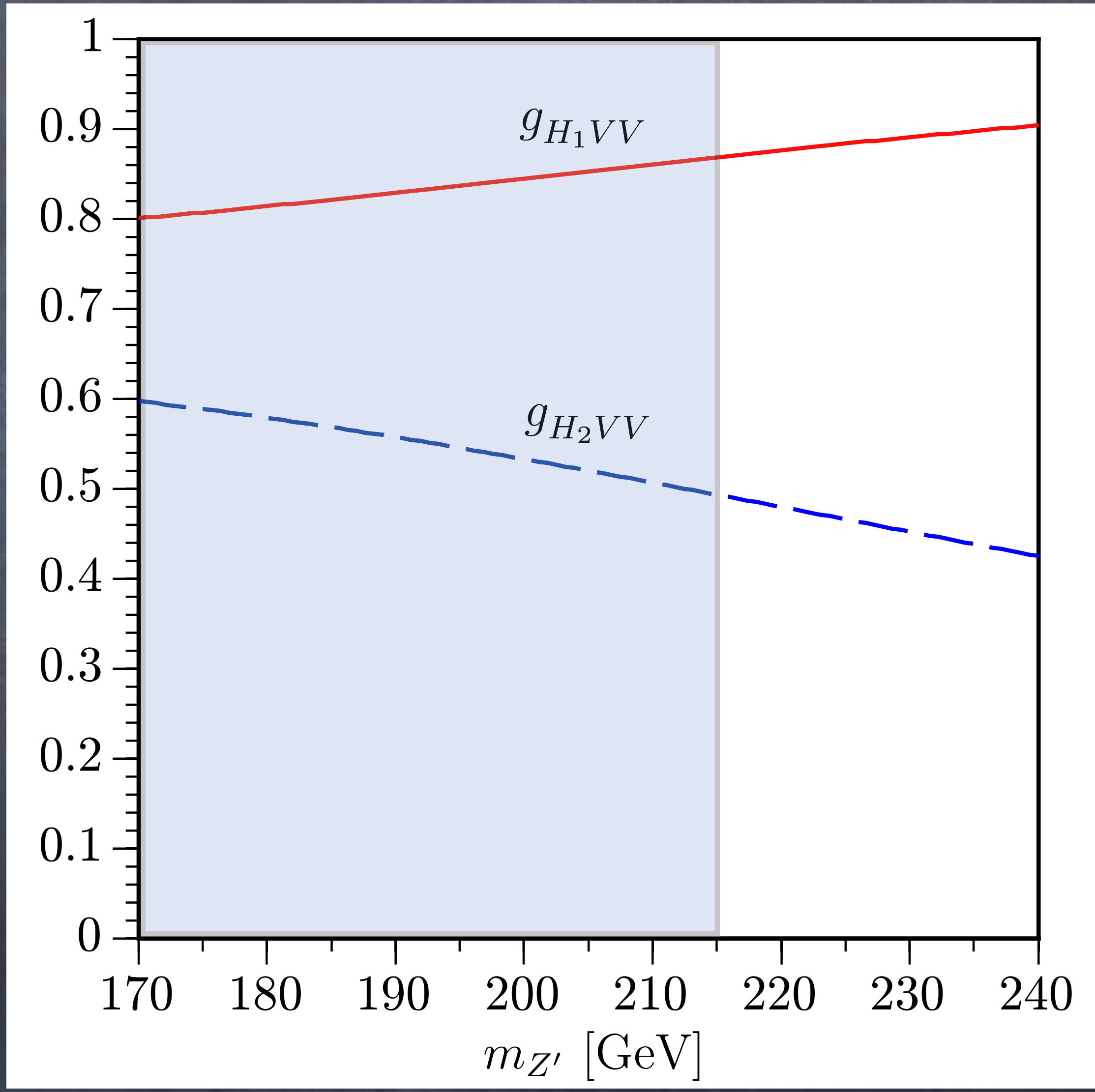

- ❒ BAU can be explained if the Higgsino and Z′-ino are nearly degenerate.
- ❒ Predictions: g_{H1VV}=(0.8-0.9) and light leptophobic Z′ (<215 GeV)

Z′-ino-driven EWBG in the UMSSM

[E.S., PRD88, 055014 (2013)]

❒ Strong 1st-order EWPT is driven by the doublet-singlet mixing effects.

❒ CP-violation relevant to the BAU comes from Higgsino-Z′-ino int.

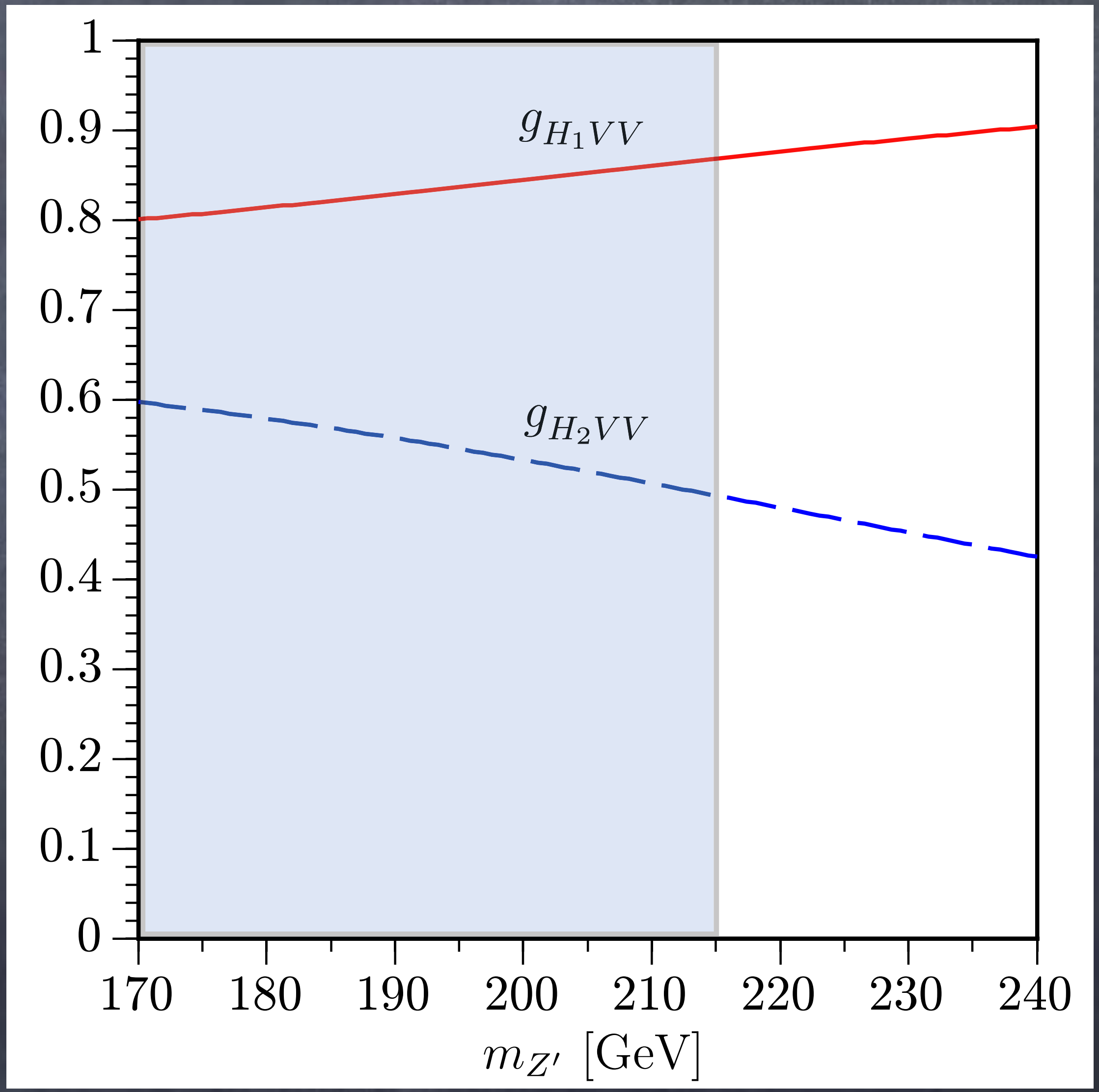

❒ BAU can be explained if the Higgsino and Z′-ino are nearly degenerate.

❒ Predictions: g_{H1VV}=(0.8-0.9) and light leptophobic Z′ (<215 GeV)

Z′-ino-driven EWBG in the UMSSM

[E.S., PRD88, 055014 (2013)]

- ❒ Strong 1st-order EWPT is driven by the doublet-singlet mixing effects.
- ❒ CP-violation relevant to the BAU comes from Higgsino-Z′-ino int.

- ❒ BAU can be explained if the Higgsino and Z′-ino are nearly degenerate.
- ❒ Predictions: g_{H1VV}=(0.8-0.9) and light leptophobic Z′ (<215 GeV)

Z′-ino-driven EWBG in the UMSSM

[E.S., PRD88, 055014 (2013)]

- ❐ Strong 1st-order EWPT is driven by the doublet-singlet mixing effects.
- ❐ CP-violation relevant to the BAU comes from Higgsino-Z′-ino int.

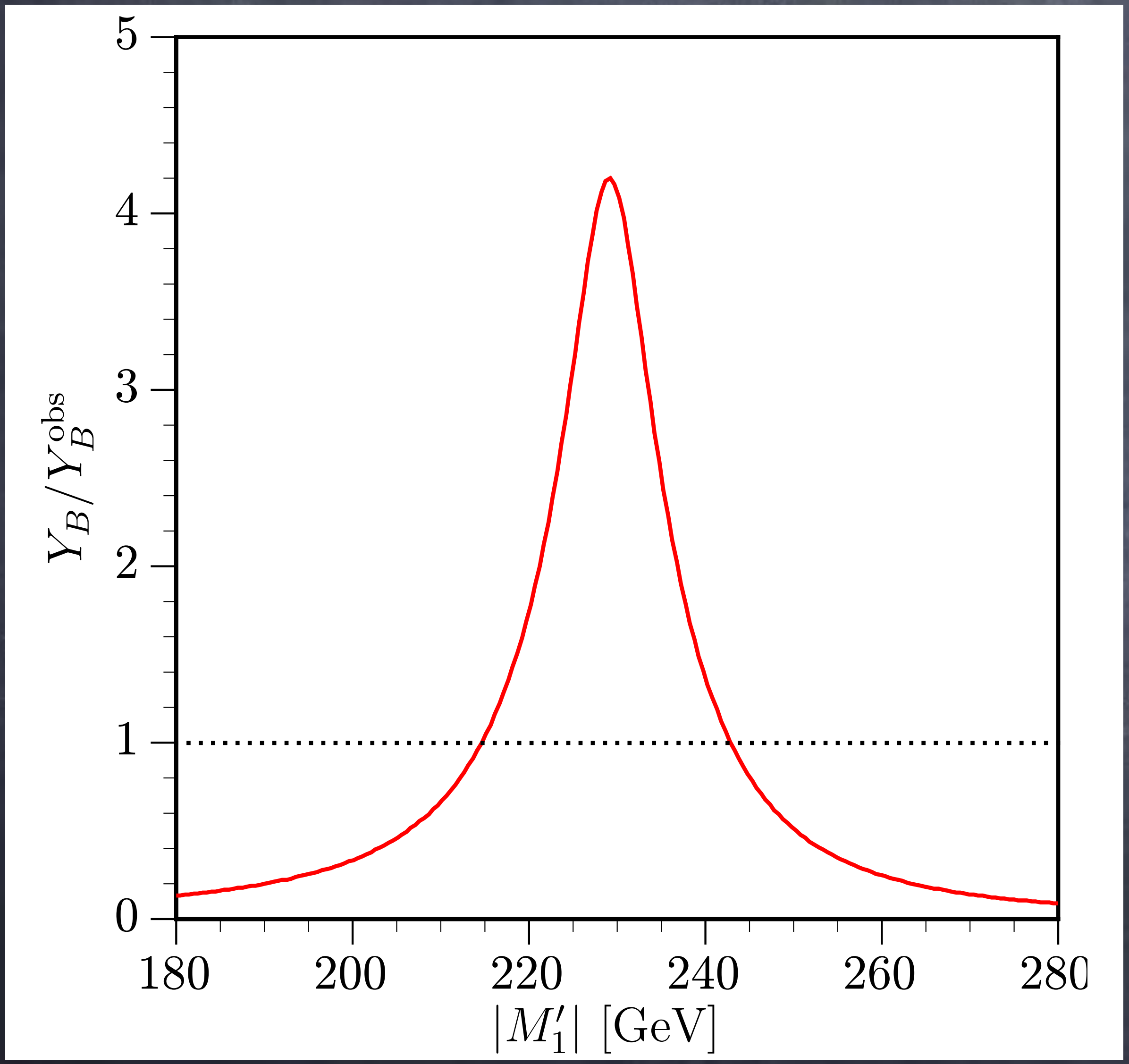

- ❐ BAU can be explained if the Higgsino and Z′-ino are nearly degenerate.
- ❐ Predictions: g_{H1VV}=(0.8–0.9) and light leptophobic Z′ (<215 GeV)

Z′-ino-driven EWBG in the UMSSM

[E.S., PRD88, 055014 (2013)]

❒ Strong 1st-order EWPT is driven by the doublet-singlet mixing effects.

❒ CP-violation relevant to the BAU comes from Higgsino-Z′-ino int.

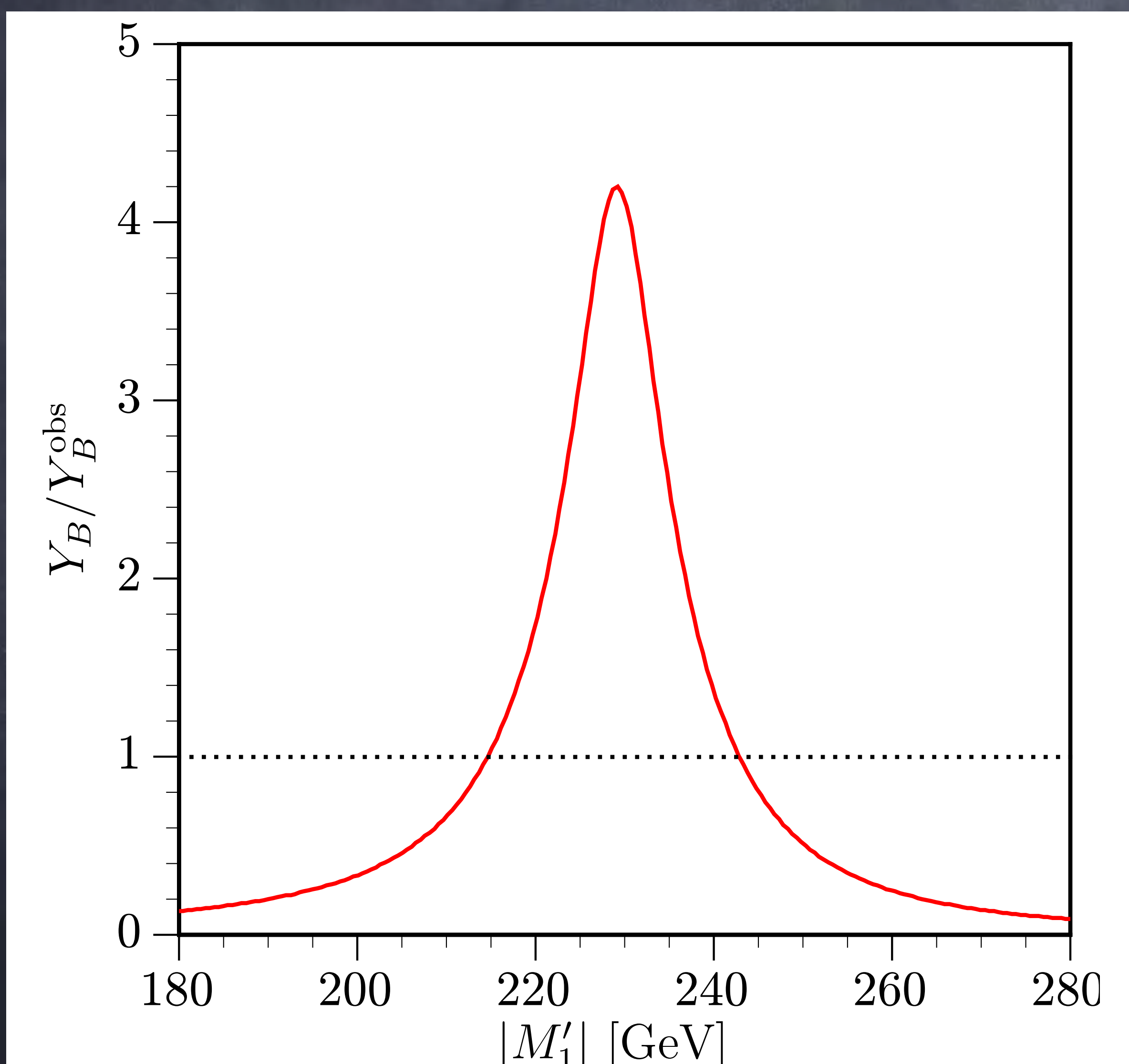

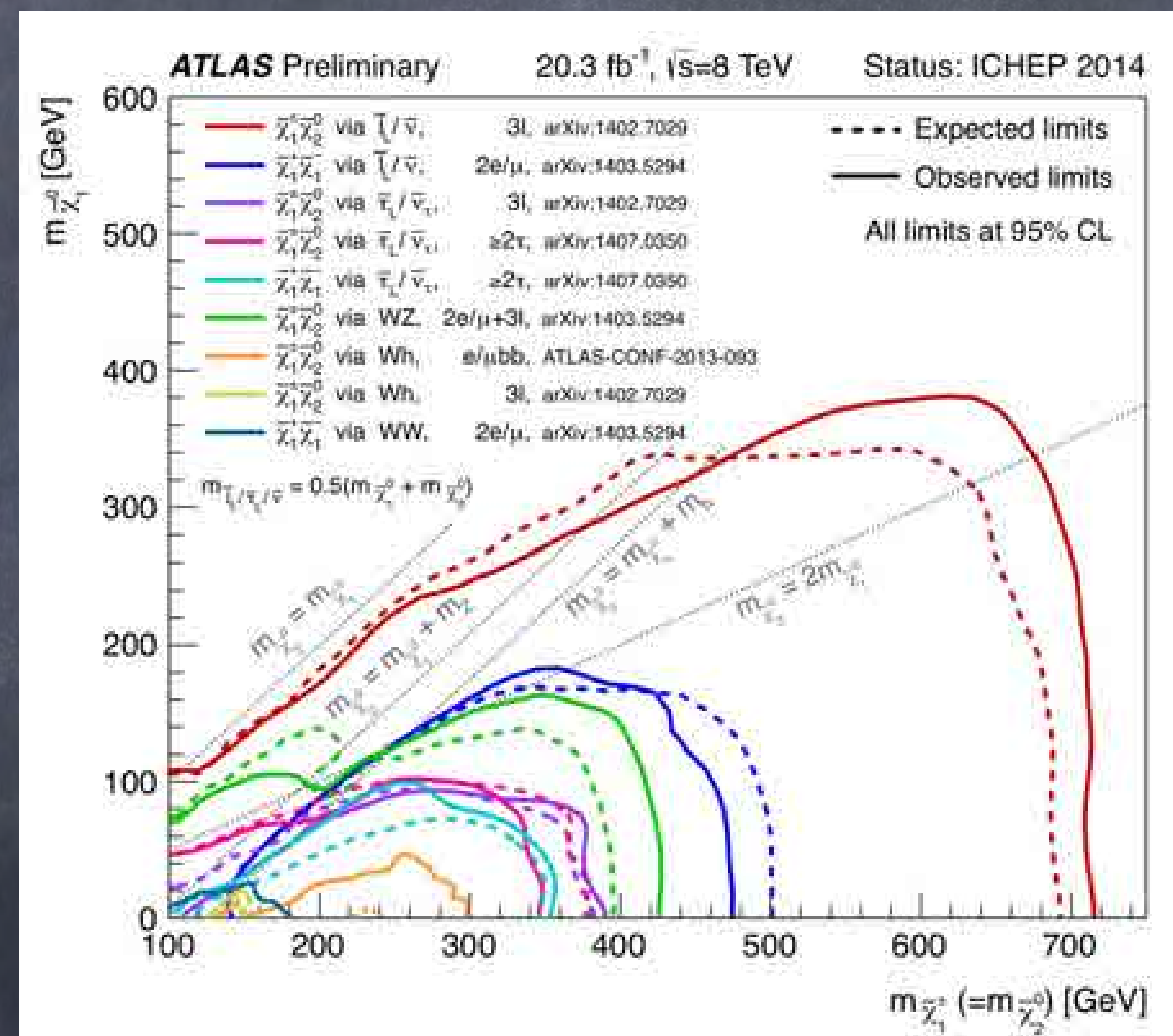

❒ BAU can be explained if the Higgsino and Z′-ino are nearly degenerate.

❒ Predictions: g_{H1VV}=(0.8–0.9) and light leptophobic Z′ (<215 GeV)

Experimental constraints on light leptophobic Z′

- Electroweak precision tests (see e.g. Umeda,Cho,Hagiwara, PRD58 (1998) 115008)

-> In our case, no constraint since Z-Z′ mixing is assumed to be small.

- All dijet-mass searches at Tevatron/LHC are limited to M_{jj}>200 GeV.

- Z′ boson (<200 GeV) is constrained by the UA2 experiment.

UA2 bounds on $m_{Z'}$

UA2 Collaborations,NPB400: (1993) 3

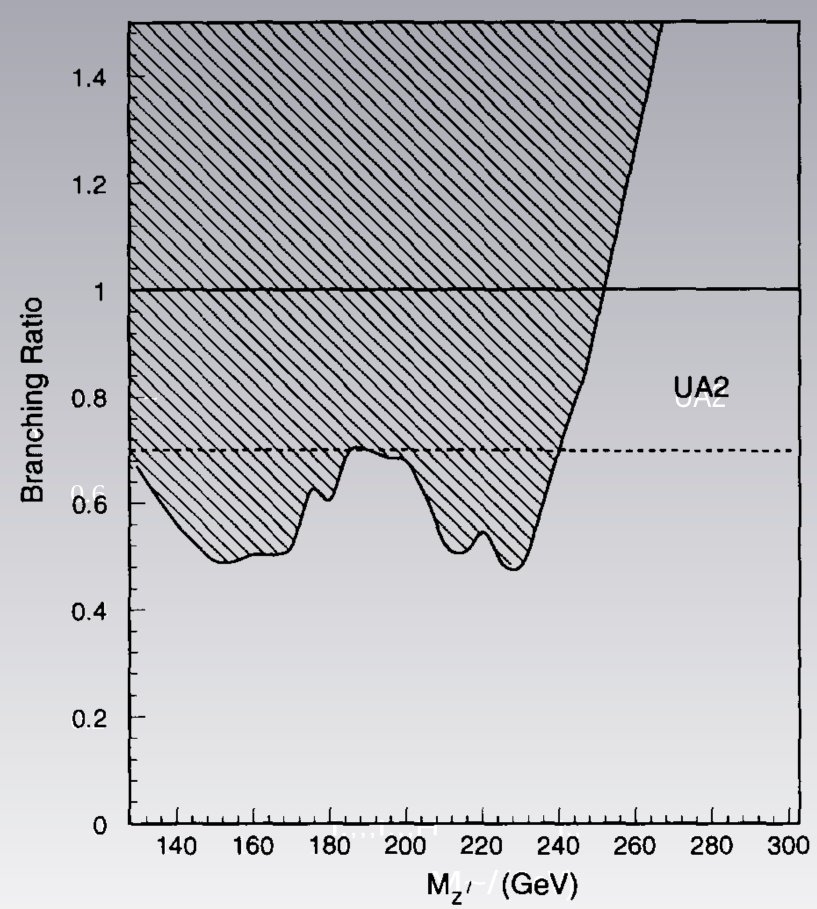

Fig. 5. Excluded region to 90% for $Z' \to \bar{q}q$, (excluded region is hatched). The branching ratio is given as a fraction of standard model branching ratio. The solid line shows a branching ratio of 1 for $Z' \to \bar{q}q$ whilst the dashed line shows a branching ratio of 0.7.

M. Buckley et al,PRD83:115013 (2011)

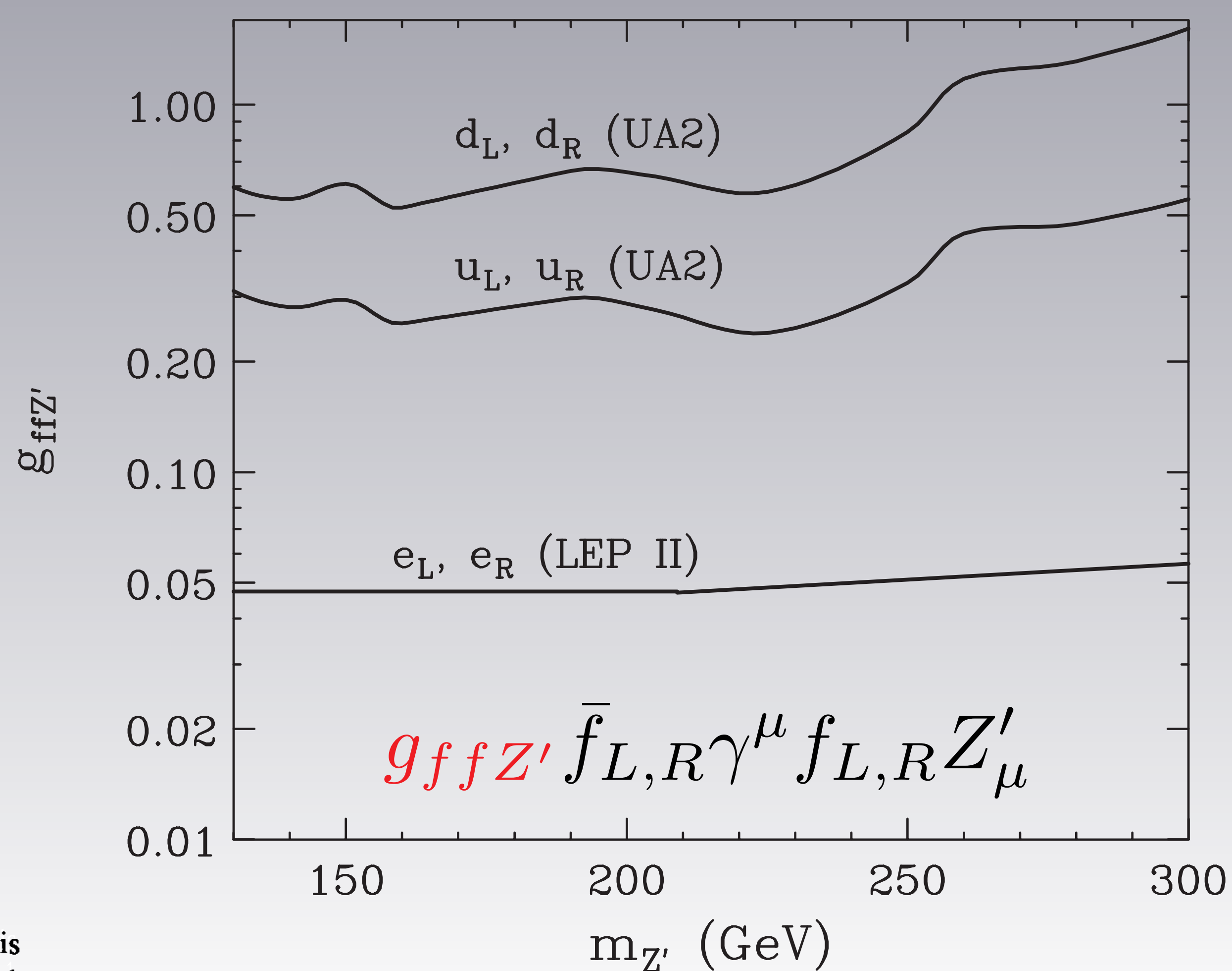

Sphaleron

σ φ α λ ε ρ ο s (sphaleros) "ready to fall"

[F.R.Klinkhamer and N.S.Manton, PRD30, 2212 (1984)]

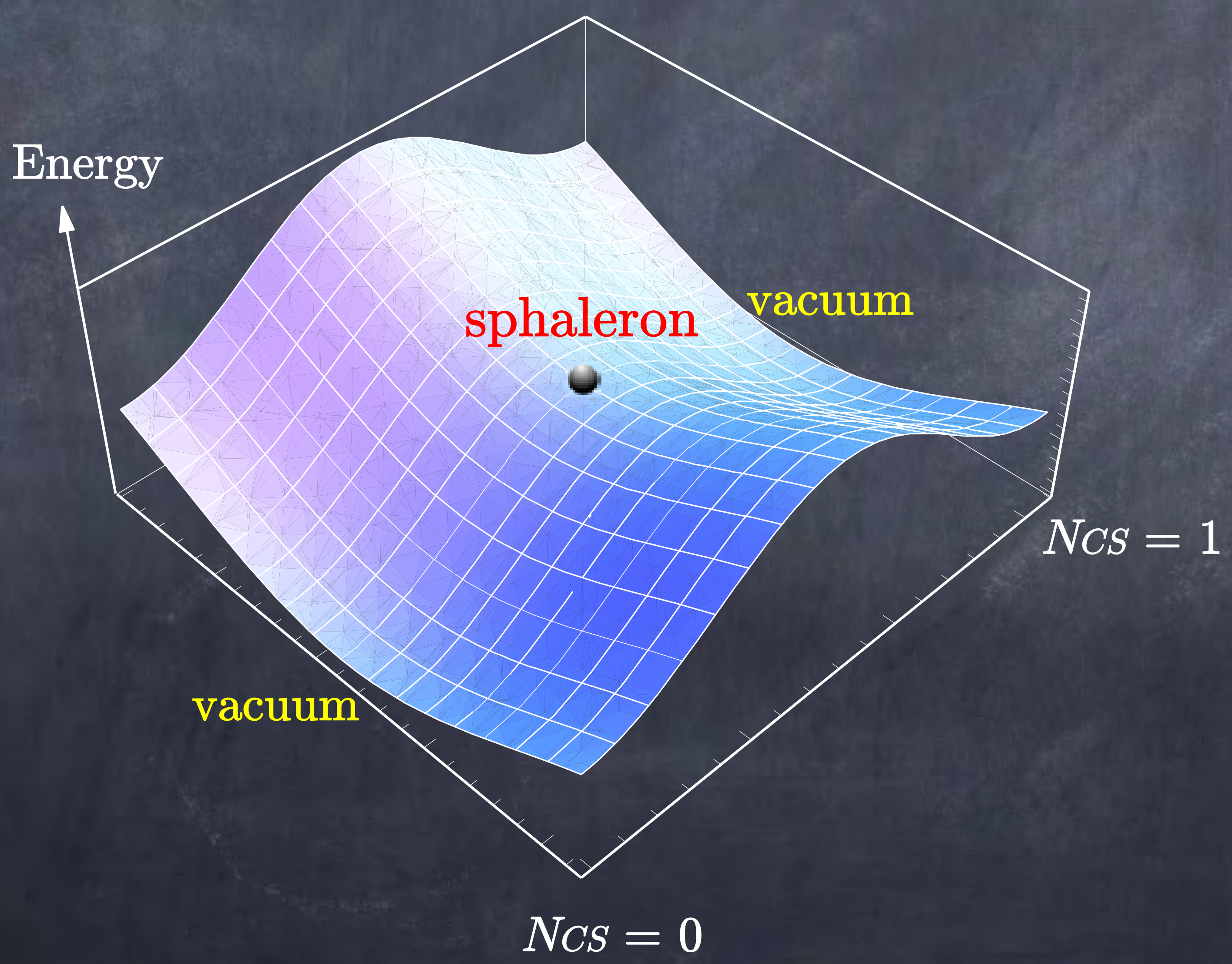

Sphaleron in the SU(2) gauge-Higgs system

$$\mathcal{L}_{\text{gauge+Higgs}} = -\frac{1}{4}F^a_{\mu\nu}F^{a\mu\nu} + (D_\mu\Phi)^\dagger D^\mu\Phi - V(\Phi)$$

$$\begin{aligned} F^a_{\mu\nu} &= \partial_\mu A^a_\nu - \partial_\nu A^a_\mu + g_2\epsilon^{abc}A^b_\mu A^c_\nu, \\ D_\mu\Phi &= \left(\partial_\mu - ig_2A^a_\mu\frac{\tau^a}{2}\right)\Phi, \quad V(\Phi) = \lambda\left(\Phi^\dagger\Phi - \frac{v^2}{2}\right)^2. \end{aligned}$$

We consider the static classical solution.

$$E = \int d^3\boldsymbol{x}\left[\frac{1}{4}F^a_{ij}F^a_{ij} + (D_i\Phi)^\dagger D_i\Phi + \lambda\left(\Phi^\dagger\Phi - \frac{v^2}{2}\right)^2\right], \quad A_0 = 0.$$

Since $\lim_{|\boldsymbol{x}|\to\infty} E =$ finite, A and Φ must have the form of the vacuum configurations at $|\boldsymbol{x}| = \infty$:

$$\begin{aligned} A^\infty_i(\boldsymbol{x}) &= -\frac{i}{g_2}\partial_i U(\theta,\phi)U^{-1}(\theta,\phi), \\ \Phi^\infty(\boldsymbol{x}) &= U(\theta,\phi)\begin{pmatrix} 0 \\ v/\sqrt{2} \end{pmatrix}, \end{aligned}$$

where $U(\theta,\phi)$ such that $S^2 \to SU(2) \simeq S^3$. $U(\theta = 0,\phi) = 1$.

Noncontractible loop

1 parameter familiy $U(\mu,\theta,\phi)$ $(\mu \in [0,\pi])$ with finite E.
$[S^1 \times S^2 \to S^3]$

where

$$\begin{aligned} U(\mu,\theta,\phi) &= U(\mu,\theta+\pi,\phi) = U(\mu,\theta,\phi+2\pi), \quad \text{for } {}^\forall\mu, \\ U(0,\theta,\phi) &= U(\pi,\theta,\phi) = 1, \quad U(\mu,0,\phi) = 1, \quad \text{vacuum} \end{aligned}$$

$(\mu,\theta,\phi) \in S^3$, $U(\mu,\theta,\phi)$ is noncontractible since $\pi_3(SU(2)) \simeq \mathbb{Z}$.

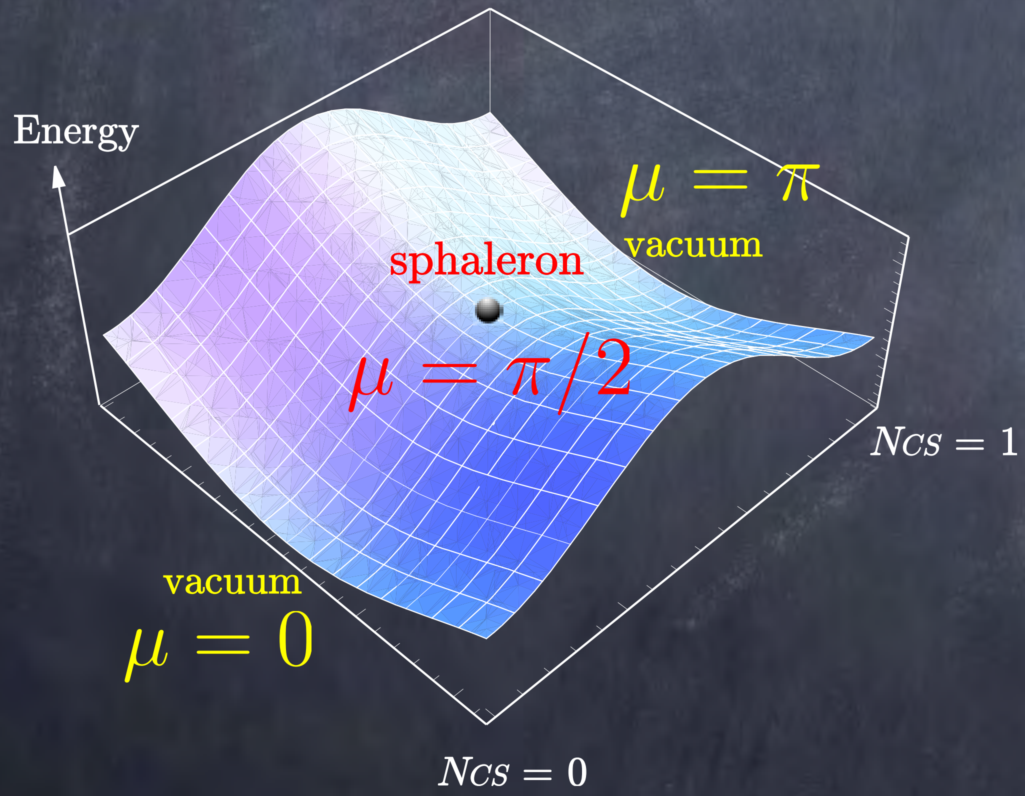

- saddle point = maximum energy along the least energy path -> μ =π/2
- vacuum -> μ =0,π.

$$U(\mu,\theta,\phi) = \begin{pmatrix} e^{i\mu}(\cos\mu - i\sin\mu\cos\theta) & e^{i\phi}\sin\mu\sin\theta \\ -e^{-i\phi}\sin\mu\sin\theta & e^{-i\mu}(\cos\mu + i\sin\mu\cos\theta) \end{pmatrix}.$$

Ansatz

Let us consider the configuration space spanned by the following:

$$\begin{aligned} A_i^\infty(\mu, \boldsymbol{x}) &= -\frac{i}{g_2}\partial_i U(\mu,\theta,\phi)U^{-1}(\mu,\theta,\phi), \\ \Phi^\infty(\mu, \boldsymbol{x}) &= U(\mu,\theta,\phi)\begin{pmatrix} 0 \\ v/\sqrt{2} \end{pmatrix} \end{aligned}$$

in the limit of $r = |\boldsymbol{x}| = \infty$. The most highest symmetry configurations in this space are

$$\boxed{\begin{aligned} A_i(\mu, r,\theta,\phi) &= -\frac{i}{g_2} f(r)\partial_i U(\mu,\theta,\phi)U^{-1}(\mu,\theta,\phi), \\ \Phi(\mu, r,\theta,\phi) &= \frac{v}{\sqrt{2}}\left[(1-h(r))\begin{pmatrix} 0 \\ e^{-i\mu}\cos\mu \end{pmatrix} + h(r)U(\mu,\theta,\phi)\begin{pmatrix} 0 \\ 1 \end{pmatrix}\right]. \end{aligned}}$$

$\mu = \pi/2 \;\Rightarrow$ saddle point configuration (spahaleron)

cf. $\mu = 0, \pi \quad \Rightarrow \quad$ vacuum configuration

Change the variable $r = \sqrt{\boldsymbol{x}^2}$ to ξ.

Energy functional

$$\begin{aligned} E_{\text{sph}} &= \frac{4\pi v}{g_2}\int_0^\infty d\xi \left[4\left(\frac{df}{d\xi}\right)^2 + \frac{8}{\xi^2}(f-f^2)^2 + \frac{\xi^2}{2}\left(\frac{dh}{d\xi}\right)^2 + h^2(1-f)^2 + \frac{\lambda}{4g_2^2}\xi^2(h^2-1)^2\right] \\ &\equiv \frac{4\pi v}{g_2}\mathcal{E}, \quad \text{where} \quad \xi = g_2 v r. \end{aligned}$$

Equations of motion for the sphaleron

$$\begin{aligned} \frac{d^2}{d\xi^2}f(\xi) &= \frac{2}{\xi^2}f(\xi)(1-f(\xi))(1-2f(\xi)) - \frac{1}{4}h^2(\xi)(1-f(\xi)), \\ \frac{d}{d\xi}\left(\xi^2\frac{dh(\xi)}{d\xi}\right) &= 2h(\xi)(1-f(\xi))^2 + \frac{\lambda}{g_2^2}(h^2(\xi)-1)h(\xi) \end{aligned}$$

with the boundary conditions

$$\lim_{\xi\to 0} f(\xi) = 0, \quad \lim_{\xi\to 0} h(\xi) = 0,$$
$$\lim_{\xi\to\infty} f(\xi) = 1, \quad \lim_{\xi\to\infty} h(\xi) = 1.$$

Higgs couplings measurements@ILC

ILC white paper, 1310.0763

Table 9.1. Summary of expected accuracies $\Delta g_i/g_i$ for model independent determinations of the Higgs boson couplings. The theory errors are $\Delta F_i/F_i = 0.1\%$. For the invisible branching ratio, the numbers quoted are 95% confidence upper limits.

	ILC(250)	ILC(500)	ILC(1000)	ILC(LumUp)
$\sqrt{s}$ (GeV)	250	250+500	250+500+1000	250+500+1000
L (fb^{-1})	250	250+500	250+500+1000	1150+1600+2500
$\gamma\gamma$	18 %	8.4 %	4.0 %	2.4 %
gg	6.4 %	2.3 %	1.6 %	0.9 %
WW	4.8 %	1.1 %	1.1 %	0.6 %
ZZ	1.3 %	1.0 %	1.0 %	0.5 %
$t\bar{t}$	–	14 %	3.1 %	1.9 %
$b\bar{b}$	5.3 %	1.6 %	1.3 %	0.7 %
$\tau^+\tau^-$	5.7 %	2.3 %	1.6 %	0.9 %
$c\bar{c}$	6.8 %	2.8 %	1.8 %	1.0 %
$\mu^+\mu^-$	91%	91%	16 %	10 %
$\Gamma_T(h)$	12 %	4.9 %	4.5 %	2.3 %
hhh	–	83 %	21 %	13 %
BR(invis.)	$<$ 0.9 %	$<$ 0.9 %	$<$ 0.9 %	$<$ 0.4 %

ILC can probe EWBG-favored region.

Measurement of λ_{hhh}

λ_{hhh} can be measured by double Higgs productions.

At linear collider:

Higgsstrahlung

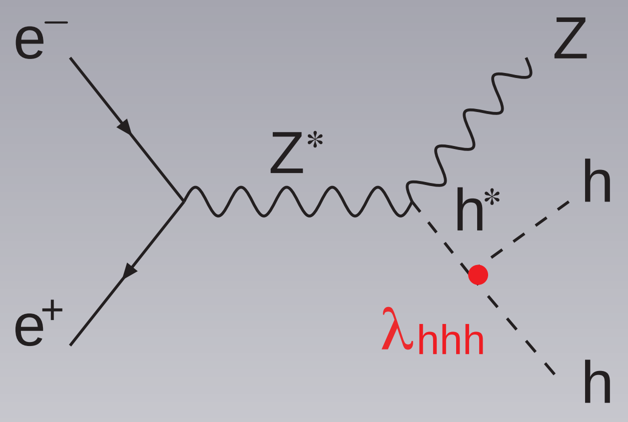

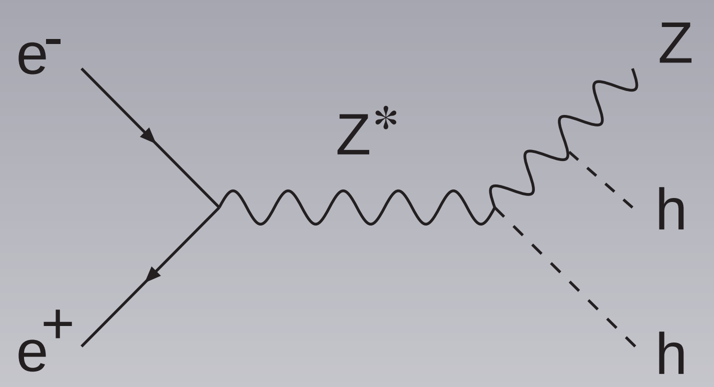

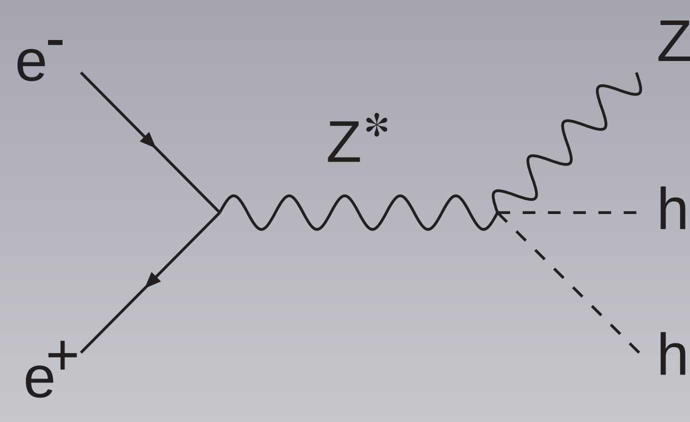

WW-fusion

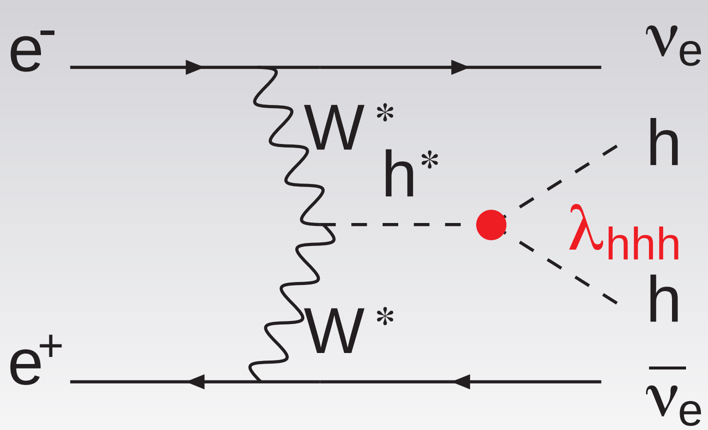

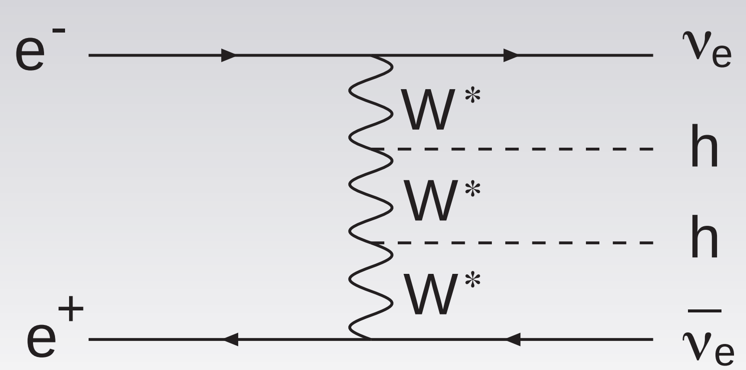

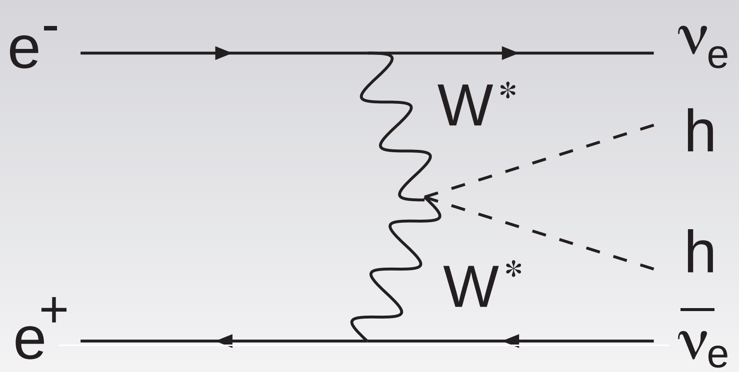

Production cross sections

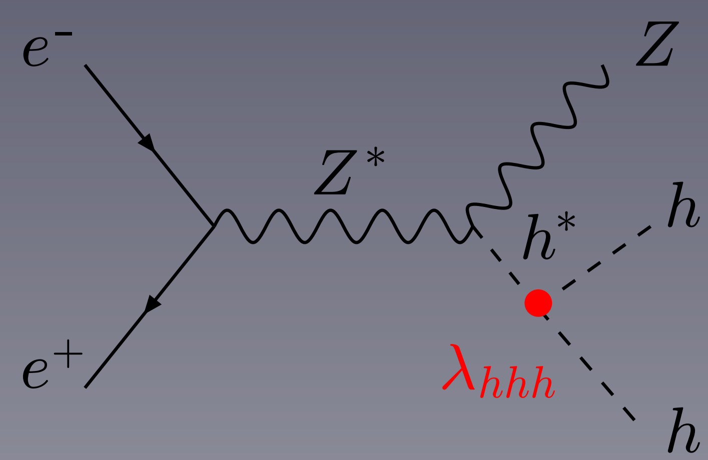

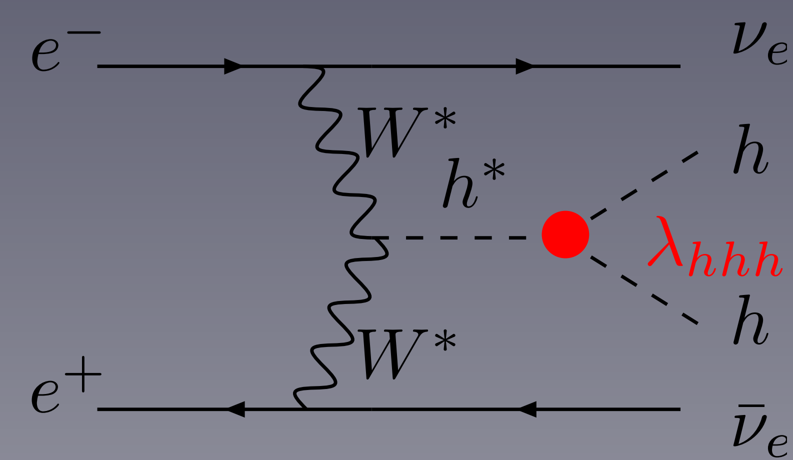

$$\lambda_{hhh} = \lambda_{hhh}^{\mathrm{SM}}(1 + \Delta\kappa),$$

[E.Asakawa, D.Harada, S.Kanemura, Y.Okada, K.Tsumura, PRD82(2010)115002]

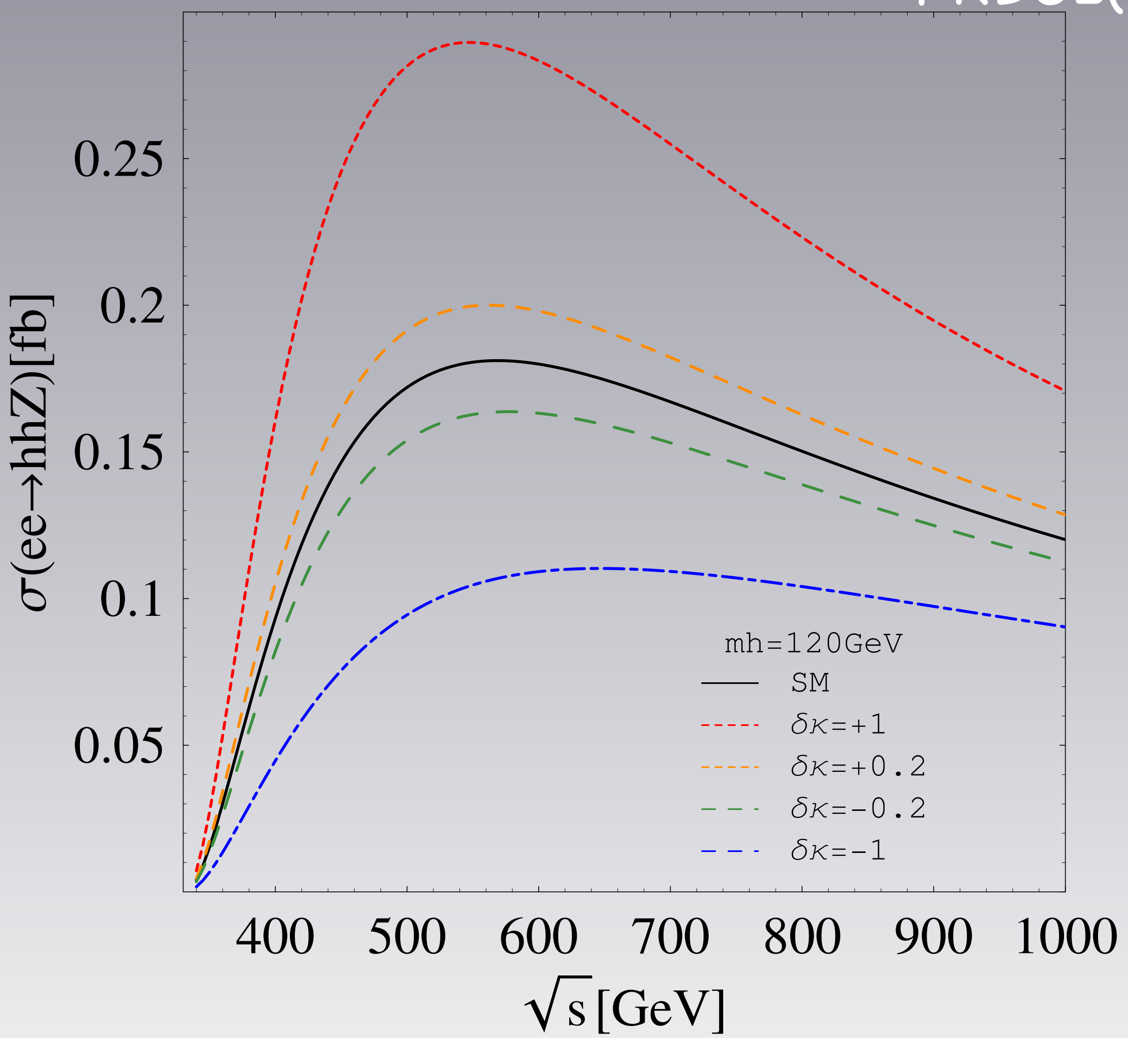

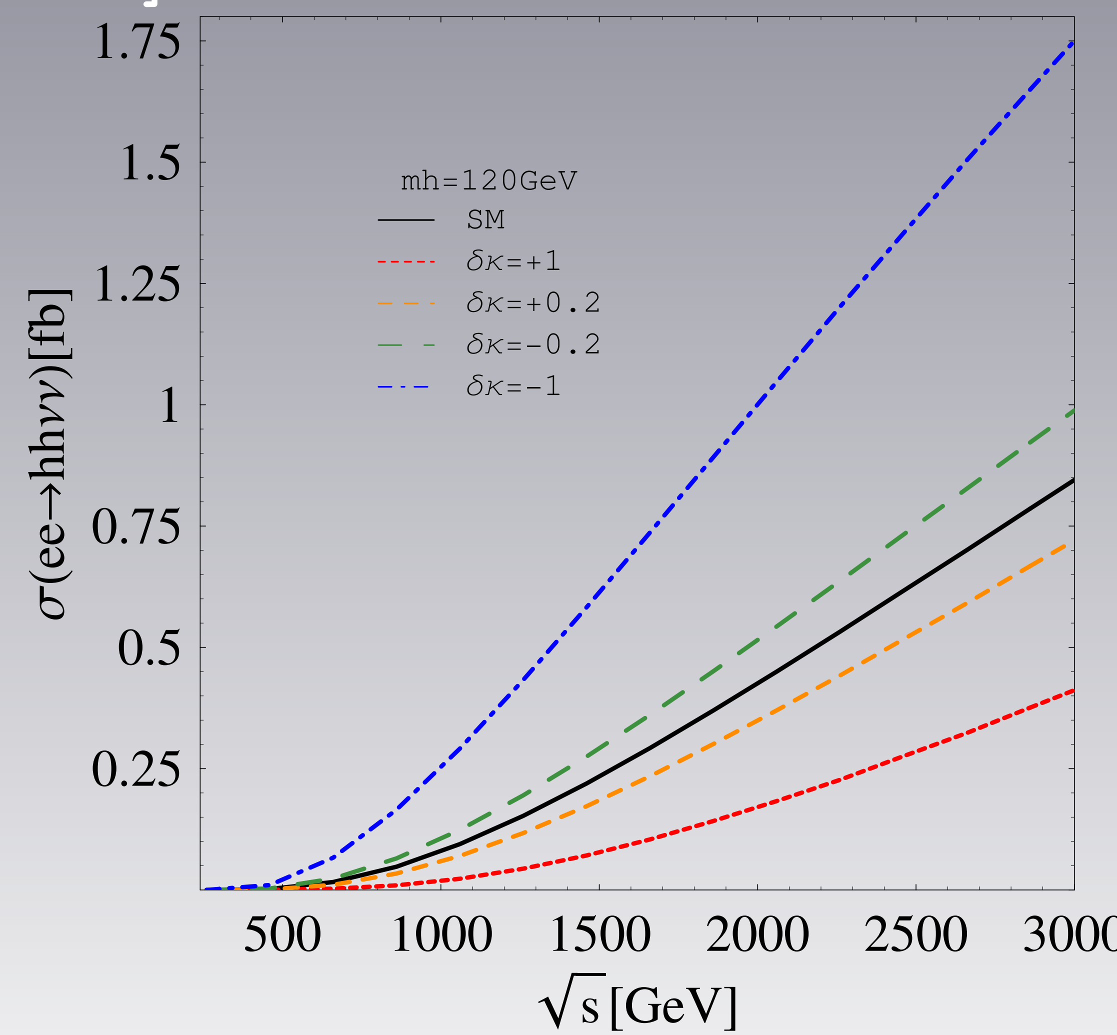

For √s≃1TeV, production cross section is O(0.1)fb

For √s>1TeV, WW-fusion is also important.